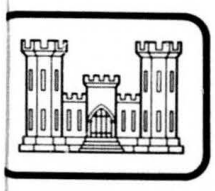

MISCELLANEOUS PAPER SL-80-4

CONCRETE AND ROCK TESTS, MAJOR REHABILITATION AND COMPLIANCE LOCKPORT LOCK, ILLINOIS WATERWAY CHICAGO DISTRICT

by

Richard L. Stowe, Steve A. Ragan, Roy L. Campbell
Barbara A. Pavlov, Henry T. Thornton, Jr., Ging S. Wong

Structures Laboratory
U. S. Army Engineer Waterways Experiment Station
P. O. Box 631, Vicksburg, Miss. 39180

April 1980

Final Report

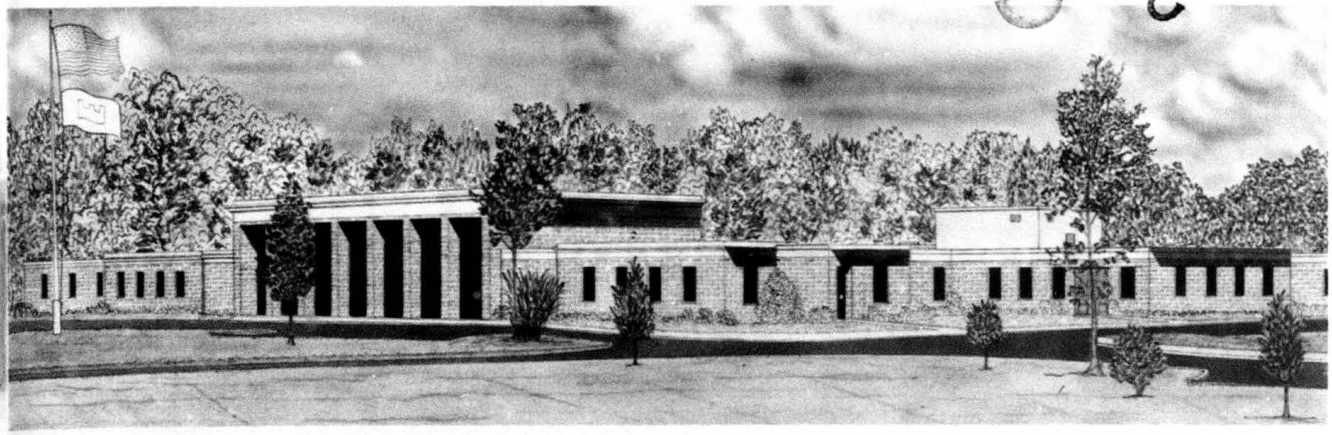

Prepared for U. S. Army Engineer District, Chicago
Chicago, Illinois 60604

Destroy this report when no longer needed. Do not return it to the originator.

The findings in this report are not to be construed as an official Department of the Army position unless so designated by other authorized documents.

The contents of this report are not to be used for advertising, publication, or promotional purposes. Citation of trade names does not constitute an official endorsement or approval of the use of such commercial products.

Unclassified

SECURITY CLASSIFICATION OF THIS PAGE (When Data Entered)

REPORT DOCUMENTATION PAGE	READ INSTRUCTIONS BEFORE COMPLETING FORM
1. REPORT NUMBER Miscellaneous Paper SL-80-4	2. GOVT ACCESSION NO. AD-A085 380	3. RECIPIENT'S CATALOG NUMBER
4. TITLE (and Subtitle) CONCRETE AND ROCK TESTS, MAJOR REHABILITATION AND COMPLIANCE, LOCKPORT LOCK, ILLINOIS WATERWAY, CHICAGO DISTRICT		5. TYPE OF REPORT & PERIOD COVERED Final Report
		6. PERFORMING ORG. REPORT NUMBER
7. AUTHOR(s) Richard L. Stowe, Steven A. Ragan, Roy L. Campbell, Barbara A. Pavlov, Henry T. Thornton, Jr., Ging S. Wong		8. CONTRACT OR GRANT NUMBER(s)
9. PERFORMING ORGANIZATION NAME AND ADDRESS U. S. Army Engineer Waterways Experiment Station Structures Laboratory P. O. Box 631, Vicksburg, Miss. 39180		10. PROGRAM ELEMENT, PROJECT, TASK AREA & WORK UNIT NUMBERS 16
11. CONTROLLING OFFICE NAME AND ADDRESS U. S. Army Engineer District, Chicago Chicago, Ill. 60604		12. REPORT DATE April 1980 13. NUMBER OF PAGES 131
14. MONITORING AGENCY NAME & ADDRESS(if different from Controlling Office) WES/MP/SL-80-4		15. SECURITY CLASS. (of this report) Unclassified 15a. DECLASSIFICATION/DOWNGRADING SCHEDULE

16. DISTRIBUTION STATEMENT (of this Report)

Approved for public release; distribution unlimited.

17. DISTRIBUTION STATEMENT (of the abstract entered in Block 20, if different from Report)

18. SUPPLEMENTARY NOTES

19. KEY WORDS (Continue on reverse side if necessary and identify by block number)

Concrete tests
Cracks
Illinois Waterway
Lock walls
Rock tests (Laboratory)
Sinkholes
Ultrasonic velocity

20. ABSTRACT (Continue on reverse side if necessary and identify by block number)

A crack survey, drilling, field and laboratory testing of concrete, and laboratory testing of foundation rock were carried out as part of a major rehabilitation and compliance program at Lockport Lock. The work was performed for purposes of determining if significant structural cracks exist at the lock and the extent and cause of concrete deterioration. Selected physical properties of the concrete and foundation rock were determined to verify previous properties.

(Continued)

DD FORM 1 JAN 73 1473 EDITION OF 1 NOV 65 IS OBSOLETE

Unclassified

SECURITY CLASSIFICATION OF THIS PAGE (When Data Entered)

411415

20. ABSTRACT (Continued).

A significant crack exists in the land lock wall. The crack increased in width during an instrumentation monitoring study performed subsequent to the major rehabilitation and compliance studies. Movement of one vertical monolith joint was monitored on the riverside lower approach wall.

New air-entrained concrete placed during resurfacing operations is in good condition. Old concrete is lightly to severely deteriorated. Freezing and thawing of nonair-entrained concrete is the major cause of the damaged concrete; alkali-silica reaction is the minor cause. Average depth of damaged concrete is from 0.2 to 1.3 ft in the lock chamber walls and just downstream of the lower gate bay, respectively. Severe damage exists at monolith joints, especially on the back side of the river wall. Beyond the damaged concrete zones, the concrete is strong (6000-psi plus compressive strength). The foundation rock was found not to be different than foundation rock previously recovered at the lock. Previous physical properties of foundation rock were verified. The major structural feature in the bedrock is stylolitic bedding with relief up to 1/2 in. Vertical jointing and fracturing exist throughout the bedrock. Zones of intensely fractured rock are present, with the largest zone existing just beneath the upper gate sill. The zone below this sill appears to be a shear zone associated with faulting. The possibility exists that a 30-ft upthrown block is present just downstream of the lock and a 70-ft plus structure is indicated in borings about 2 miles upstream of the lock. Solution activity is evident in the bedrock core, and sinkholes have been observed adjacent to the lock; a small section of a road collapsed into a sinkhole in 1978 during the conduct of this investigation.

PREFACE

The testing program reported on herein was conducted for the U. S. Army Engineer District, Chicago, as authorized by DA Form 2544, No. NCC IA 78-30 and NCC IA 78-35, dated 1 February 1978 and 23 February 1978, respectively.

Drilling was conducted by members of the staff of the Geotechnical Laboratory (GL) of the U. S. Army Engineer Waterways Experiment Station (WES) during the period February 1978-April 1978 and June 1978 under the direction of Mr. M. A. Vispi. Laboratory tests were performed at the Structures Laboratory (SL), WES, and the GL during the period August 1978-September 1978 under the direction of Messrs. Bryant Mather, Chief, SL, and J. M. Scanlon, Chief, Engineering Mechanics Division, SL. The crack survey was conducted by Mr. R. L. Campbell; the ultrasonic velocity survey was conducted by Mr. H. T. Thornton, Jr., both of the SL. Mr. G. S. Wong, SL, conducted the petrographic examination. Mr. R. L. Stowe was Project Leader and was assisted in performing laboratory work at the SL by Messrs. F. S. Stewart and J. B. Eskridge and Ms. B. A. Pavlov. This report was prepared by Messrs. Stowe, Ragan, Campbell, Thornton, Wong, and Ms. Pavlov.

Commanders and Directors of WES during the conduct of the investigation and the preparation and publication of this report were COL John L. Cannon, CE, and COL Nelson P. Conover, CE. Mr. F. R. Brown was Technical Director.

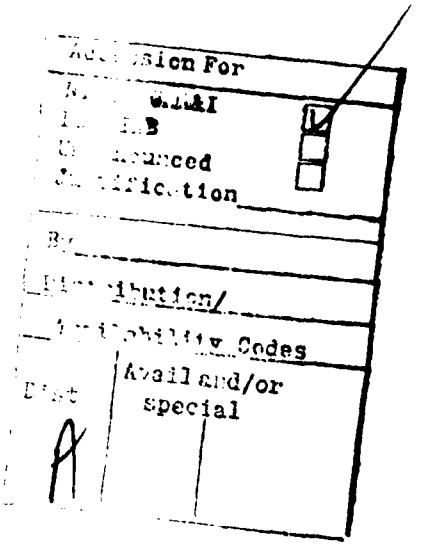

CONTENTS

CONTENTS (Continued)

* Copies of Appendixes D and E may be obtained from U. S. Army Engineer District, Chicago, 219 South Dearborn St., Chicago, Illinois 60604.

CONVERSION FACTORS, INCH-POUND TO METRIC (SI)
UNITS OF MEASUREMENT

Inch-pound units of measurement used in this report can be converted to metric (SI) units as follows:

Multiply	By	To Obtain
cubic feet	0.02831685	cubic metres
degrees (angle)	0.0174533	radians
feet	0.3048	metres
feet per second	0.3048	metres per second
miles (U.S. statute)	1.609344	kilometres
pounds (force) per square inch	0.006894757	megapascals
pounds (mass) per cubic foot	16.01846	kilograms per cubic metre
square feet	0.09290304	square metres
tons (force) per square foot	0.09511274	megapascals

CONCRETE AND ROCK TESTS, MAJOR REHABILITATION AND COMPLIANCE, LOCKPORT LOCK, ILLINOIS WATERWAY, CHICAGO DISTRICT

PART I: INTRODUCTION

Location of Study Area

1. The Lockport Lock is located about 2 miles* north of Joliet, Illinois, on the Chicago Sanitary and Ship Canal, a part of the Illinois Waterway. The lock is located at mile 291 on the Illinois Waterway just east of the Des Plaines River and just west of the town of Lockport. A general plan view of Lockport Lock is given in Plate 1.

Background

2. In January 1978 the Waterways Experiment Station (WES) was asked by the US Army Engineer District, Chicago (NCC for North Central Division, Chicago) to assist with a major rehabilitation and a compliance study at Lockport Lock. It was requested that a proposal be submitted for concrete and rock exploration and laboratory testing. The major rehabilitation study would involve resurfacing and stabilizing of lock walls and appurtenant structures. WES's major work effort was to ascertain the extent of concrete deterioration and selected physical properties of concrete and bedrock. The compliance study involved drilling and testing of limited concrete and bedrock core in accordance with specific recommendations given in Reference 1.

3. Copies of two reports, a geological foundation report and a reconnaissance report for major rehabilitation, both pertinent to the lock site, were received at WES for review and background information.[2,3] Certain Office, Chief of Engineers (OCE) and North Central Division (NCD) recommendations for drilling and testing of concrete and bedrock were included in the WES proposed work plan.[1] A WES representative traveled

* A table of factors for converting inch-pound to metric (SI) units of measurement is presented on page 4.

to the lock and conducted a brief condition survey prior to formulizing the work plan. Attempts were made to gather additional information on the concrete and foundation condition from the State of Illinois (former owners), the NCC, and the Joliet Project Office (representatives of the owner-operator, which is the U.S. Government), and the Illinois Geological Survey. No geological information was obtained dating back to the time of the actual excavation (boring information) of the lock. No concrete data was obtained from the construction period. References 4 and 5 were useful in preparing the proposed work plan.

4. After due consideration of the available information, a drilling and field and laboratory testing program was drawn up. The drilling involved putting down vertical and inclined borings, the vertical borings going through concrete and well into bedrock. The inclined borings were quite shallow. All borings were located to obtain core that was representative of the concrete and hopefully the bedrock. The field testing involved a significant crack survey incorporating ultrasonic velocity measurements and dyed-water tests. Several significant cracks were described in Reference 3 and observed during the brief condition survey. Recommended laboratory tests of concrete included selected characterization and engineering design property tests and a detailed petrographic examination to determine the extent of damaged concrete.

Objectives

5. The objectives of the major rehabilitation study were to:

   a. Conduct drilling for field and laboratory testing of concrete and laboratory testing of bedrock. The bedrock is to be tested if found to be significantly different than rock previously recovered from the foundation.

   b. Determine extent of significant cracking in the lower gate monoliths.

   c. Make an analysis of tests conducted, a summary of the concrete condition over the lock site, and an evaluation of the foundation using available geological information.

The objective of the compliance study was to conduct limited drilling and testing of concrete and bedrock cores. Physical properties obtained

from both studies are to be used by the District for structural stability analysis and design of a prestressed anchoraged system.

Scope

6. Drilling was accomplished using a WES drilling crew, plant, and supplies. The Chicago District Construction and Operations Division supplied the necessary floating plant assistance. WES geologists and the Chicago District geologist logged and preserved the core for possible testing. The core was transported to the WES for storage and testing as soon as drilling was completed for both studies.

7. A limited crack survey was made at the lock. It was accomplished by locating significant cracks and areas of deterioration where a change in the structural adequacy of the lock could occur. A detailed study of these areas was accomplished using downhole soniscope equipment and borehole dyed-water pressure tests. The ultrasonic velocity testing involved borehole to surface and surface to surface readings. The borehole dyed-water pressure tests were made using the column of water in the borehole.

8. The laboratory testing of concrete and bedrock was accomplished by conducting petrographic examinations, selected characterization property tests (unconfined compression, unit weight, and compressional wave velocity), and selected engineering design property tests (modulus of elasticity, Poisson's ratio, and direct shear, and rebar pullout tests). Limited direct shear tests were run on concrete to rock, filled partings, and natural joints because a large number of these tests had been previously conducted.[2]

PART II: DRILLING AND EXPLORATION

Previous Exploration

9. Attempts were made to obtain copies of any original borings made at the lock; such information was not received at the WES. It is not known if borings were put down prior or during construction; it is believed that borings would have been made for such a structure (39.5-ft lift lock).

10. Drilling was conducted by the NCC in 1970 for purposes of making a foundation appraisal from which to obtain design parameters for a structural stability analysis. Four borings were put down, two in backfill on the land side of the chamber and two near the back side of the river wall.[2] In 1972 two additional holes were drilled in the backfill (land side of chamber) for monitoring any water levels in the backfill.[2] During the NCC drilling in 1970 and 1972, about 149 ft of bedrock was drilled. Three of the deeper borings were taken about 25 ft below the base elevation of the lock.

11. During the period between December 1966 and February 1973, a total of 31 borings were put down beginning just south of the lock at the lock and generally, along the Deep Run Channel to just past the Ninth Street Bridge in the city of Lockport, Illinois. The purpose of the drilling was to obtain information and data about overburden, bedrock, construction materials, spoil, and groundwater problems. This information and data was for conceptual design, plan formulation, and preliminary cost estimates for the proposed duplicate locks at Lockport Lock. The average depth drilled into bedrock was 56 ft, with a range of depths of from 11 ft to 132 ft. The deeper borings are located at the Ninth Street Bridge.

Current Drilling

12. Drilling was accomplished during two different time periods. The first period was from 6 February 1978 to 8 April 1978. Due to the

increase in work load at the Joliet Project Office, crane support was not available to complete the inclined drilling on the back side of the river lock wall. The drill crew terminated dilling on 8 April and moved to the Brandon Road Lock. Drilling was begun at Brandon Road Lock in connection with the NCC major rehabilitation program. The drill crew moved back to the Lockport Lock on 6 June 1978 and completed drilling on 20 June 1978.

13. Drilling for the major rehabilitation and the compliance study consisted of 52 and 4 borings, respectively. The general location of the vertical borings s presented in Figure 1, while the inclined boring (horizontal to nearly horizontal) locations are shown in Figure 2. A summary of boring locations, direction of boring, number of borings/ approximate depth, and material drilled is given below:

Major Rehabilitation	Location	Direction	No. of Borings and Approximate Depth, ft	Material Drilled
Lock Structure	Lock chamber land wall	V*	1/99	Concrete & Rock
	Lock chamber land wall	H**	9/3	Concrete
	Lock chamber river wall	V	2/97	Concrete & Rock
	Lock chamber river wall, chamber side	H	5/3	Concrete
	Upper gate sill	V	1/30, 1/66	Concrete & Rock
	Gate bays	H	2/3	Concrete
	Lock chamber river wall, river side, ledge	V	3/3	Concrete & Rock
	Lock chamber river wall, river side	H	18/3	Concrete
	River wall D/S of D/S gate bay	H	2/3	Concrete
	D/S vertical face, monolith 57		2/9	Concrete
Approach Walls	Upper approach wall		3/3	Concrete
	Lower approach wall		3/3	Concrete

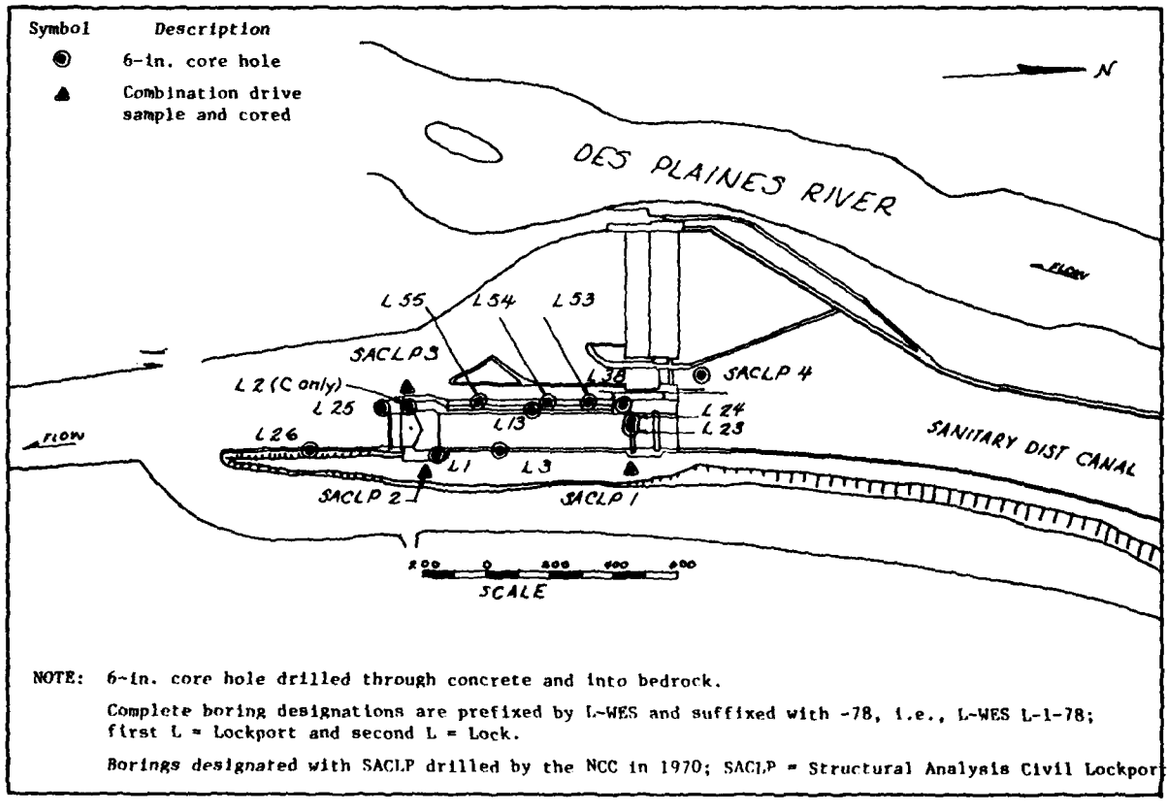

Figure 1. General boring location plan, vertical borings

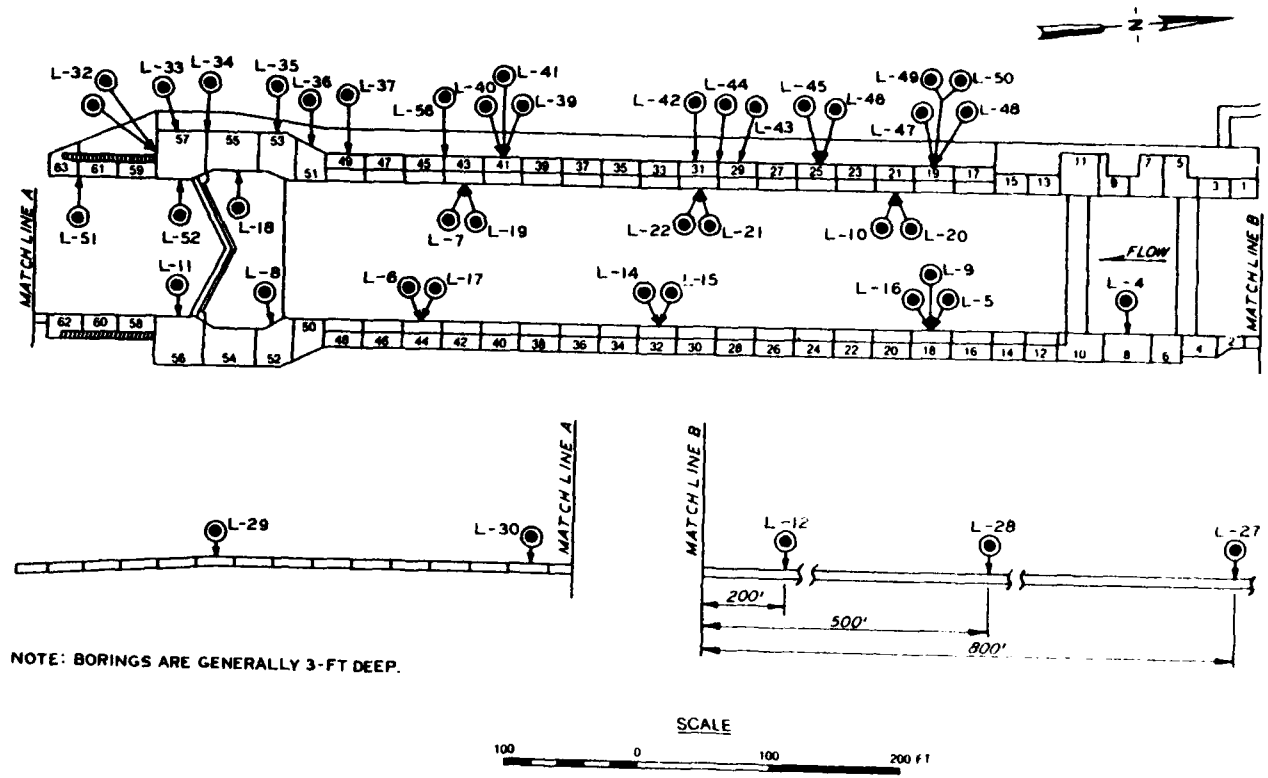

Figure 2. Angle boring location plan

Compliance	Location	Direction	No. of Borings and Approximate Depth, ft	Material Drilled
Lock Structure	Lock chamber land wall	V	1/99	Concrete & Rock
	Lock chamber river wall	V	1/47, 1/73	Concrete & Rock
	Lock chamber river wall, chamber side	H	1/5	Concrete

* Vertical
** Horizontal.

14. Total footage drilled was about 570 ft in concrete and about 220 ft in bedrock. Selected portions of the vertically drilled concrete core (top, middle, and bottom 5 ft), about 90 percent of the horizontally drilled concrete core, and about 95 percent of the bedrock were preserved for laboratory testing. The badly broken concrete and bedrock were not preserved in the field. Procedures for handling the field samples and preserving the core for testing were the same as described in Reference 6. Color photographs of all the core recovered are included in a notebook as Exhibit A to this report; the field core logs are presented in Exhibit B to this report. Both exhibits are on file at the NCC.

15. Core recovery for the concrete and bedrock was between 95 and 100 percent. Seven of the eight borings that penetrated bedrock had 100 percent water loss in the bedrock. This fact points up the highly fractured nature of the foundation at Lockport Lock. Only boring L-1 in monolith 52 of the land wall had water return while drilling in bedrock. The bedrock core from L-1 contained numerous healed vertical fractures as well as open vertical fractures. Nevertheless, the rock can be considered quite tight in contrast to the bedrock recovered from L-23 and L-24 in the upper gate sill where intensely fractured rock was recovered. Intensely fractured rock has fracture spacing < 4 in.

16. Drilling equipment consisted of an Acker Toredo Mark II skid-mounted rotary drill rig and a Concord portable drill rig. Six-inch inside diameter diamond core bits and a 10-ft long double tube barrel

was used to drill the concrete and bedrock core. A single core barrel was used with the Concord rig to drill the shallow holes (about 3-ft deep). Access to the drill holes inside the lock was by a marine floating plant, and for borings on top of the structure by crane. The floating plant and crane support was supplied by the Construction and Operations Division of the NCC through the Joliet Project Office. All drilled holes were backfilled to their full depth with concrete produced using a commercially available packaged dry combined mixture.

17. A 10-ft long core barrel was lost in boring L-23, which is located in the D/S-most upper gate sill. The boring was on the longitudinal center line of the lock. The barrel was stuck about 1 ft off the bottom of the boring. When the barrel stuck, the hole had been drilled through about 28 ft of concrete and 8 ft of bedrock. Core recovered just prior to the core barrel becoming stuck consisted of crushed dolomite. Fragments were angular, from 1 to 4 in. in size, and most were coated with a dark gray to black deposit. After numerous attempts to recover the barrel, it was concreted in the hole. Another hole was made in the sill 25 ft toward the river wall. This new boring (L-24) contained similar sized crushed rock to that encountered in boring L-23. Additional studies should be done to confirm or disprove that the same zone was found in L-23 and L-24.

18. The procedure for drilling through the crushed and fractured rock in boring L-24 was to drill several feet and grout. After the grout had set up, another several feet was drilled and the cycle repeated. This procedure was used to guard against sticking the core barrel in the crushed zones. After drilling to sounder rock (about 18 ft below the base of the concrete sill), dyed-water pressure tests were run at 5-ft increments from the bottom of the boring. The purpose of these tests was to see if the dye could be seen in the chamber while the chamber was at low pool. These pressure tests were inconclusive in that no dye was detected in the chamber, downstream of the lock nor just west of the lock at the Sanitary District of Chicago facility. The water take in the boring was extremely small compared to the volume of water in the chamber at low pool. The dye may have been present in the chamber but

obscured by the dark brown river water. No analysis of the water take in the borehole was made because of the procedure used in drilling the hole; i.e.. drill, grout, and redrill. In using this procedure, most all the fractures adjacent to the borewall would be filled or sealed off to some degree as the hole was grouted. The take that did occur was not representative of the take that would have occurred had the hole not been grouted during drilling.

19. A number of drilling operations were performed at and near Lockport Lock. The various projects from which information was obtained at the WES are included; the projects, the number of borings, and the boring series numbers are given in the following list.

Project (Agency)	Year	No. of Borings	Boring Series No.
Structural Stability Analysis (NCC)	1970	4	SACLP-1 through 4
Structural Stability Analysis (NCC), Lockport	1972	2	SACLP-5 & 6*
Lockport Duplicate Lock GSDM Study	1966 to 1973	31	CLP 500, CLP 600, & CLP 700 series
Compliance (WES)**	1978	3	LP WES L-1, 2, 25-78
Major Rehabilitation (WES)**	1978	6	LP WES L-3, 13, 23, 24, 26, & 38-78

* Not drilled into bedrock.
** Only vertical borings that penetrated bedrock considered.

20. Table 1 is a listing under each project of the above-listed borings. The following information is presented for each boring: the boring type, the location relative to the lock, the elevation of the top of boring, the elevation top of rock and the elevation bottom of the boring, and the date when the boring was started.

21. The location of the SACLP and WES designated borings has been presented in Figure 1. The CLP (Civil Borings Lockport) designated boring locations will be presented later in this report. Precise boring locations for the SACLP and WES borings are shown in key plan views on

log of boring sheets and geologic cross sections. Log of borings for the WES borings are shown (in a profile) in Plates 1 and 2. Log of borings and precise boring locations for the core recovered during the NCC structural stability analysis and the Duplicate Lock study can be found in References 2 and 7.

PART III: SIGNIFICANT CRACK SURVEY

General Comments

22. The crack survey located external expressions of internal cracks. Ultrasonic velocity measurements and borehole dye-water tests were used in an attempt to trace the internal portions of the significant cracks found. The procedures used and results obtained from the significant crack survey, ultrasonic velocity survey, and borehole dye-water tests will be presented separately. The significance of the findings from these three study efforts will be summarized under the last subheading in this part.

23. A limited crack survey was made as a part of the major rehabilitation program for Lockport Lock. The crack survey consisted of: (1) a general inspection of the exposed exterior concrete surfaces of the river and land walls and of the interior surfaces of their respective cable galleries; the intent of the inspection was to locate any significant structural cracks and areas of deterioration that denoted a potential change in the structural adequacy of the lock; and (2) a detailed inspection of these areas to accurately define their locations and, when possible, to determine the extent of damaged concrete. The cracking in the concrete of the resurfaced areas (top surface) of lock walls was considered not to be representative of the concrete it covered. Therefore, no attempt was made to map or correlate the extent of cracking in the resurfaced areas of the lock walls. In general, Reference 8 was used as a guide for performing the field work and preparing the crack survey portion of this report. The probable cause of concrete cracking is discussed where appropriate.

River Wall Inspection

Monolith 7

24. Medium to severe scaling due to frost action was noted in both cable gallery walls of river wall monolith 7 (Plate 1). This is shown in Figures A1 and A2 of Appendix A, showing the lock side face of

the gallery. As can be seen, the loss of mortar is to the extent that the aggregate is clearly exposed and stands out from the concrete. Also shown is a horizontal crack that is less than 2 mm (0.08 in.) in width. Crack width definition as presented in Reference 8 is: fine is < 1 mm (0.04 in.), medium is 1 to 2 mm, and wide is >2 mm (0.08 in.). The crack is located about mid-height at approximate elevation 579* along the lock side face of the cable gallery and extends from the corner where the gallery makes its turn to a point approximately 6 ft upstream. Top elevation of lock wall is 585. The extent of this crack appears to be limited in depth and significance at this time.

Monolith 11

25. The upstream face of the cable gallery in river wall monolith 11 has several cracks near the lock side corner where the gallery makes a 90° turn. These cracks are shown in Figure A3 of Appendix A. The cracks are 2 mm (0.08 in.) or less in width and extend from within the ceiling of the gallery to the floor. This type of cracking is typical for many older lock structures where the pipe gallery makes a 90° turn. At present, these cracks appear to be limited in depth and pose no significant threat to the integrity of the structure.

River wall monoliths 17 through 49

26. In general, the exterior concrete surface of river faces of river wall monoliths 17 through 49 have severe scaling and spalling due to frost action. The most significant areas of deterioration are at the monolith joints. An overall view of the river faces of monoliths 17 through 49 is shown in Figure A4 of Appendix A. The advanced deterioration of the concrete at the monolith joints is directly attributed to water seepage. The monolith joints having the greatest amount of damaged concrete are depicted in Figures A5 through A12 of Appendix A.

27. From a detailed investigation it was noted that for most joints the maximum loss of concrete was less than 6 in. in depth. However, for monolith joints 29-31 (Figure A11 of Appendix A) and 37-39 (Figure A12 of Appendix A), the maximum loss of concrete was approximately 12 in. in depth.

* All elevations (el) cited herein are in feet referred to mean sea level.

28. It was also noted that for the joints at which seepage flow was visible the water surface of the seepage at the river face was at approximate el 572. This indicated the ineffectiveness of the joint filler above el 572 to be such that only 5 ft of differential water head caused seepage flow. This represents a creep ratio of 2 at the river face.

29. At present, the deterioration at these monolith joints does not present a serious threat to the structural integrity of the lock. However, this could change if remedial measures are not implemented to correct the seepage problem at the joints and to protect the existing surfaces from further deterioration due to frost action.

Monoliths 51, 53, 55, and 57

30. In general, the exterior concrete surfaces of the river face of river wall monoliths 51, 53, 55, and 57 also have severe scaling and spalling due to frost action. An overall view of the river faces is shown in Figure A13 of Appendix A.

31. A horizontal corner crack between the ceiling and river side face of the cable gallery spans the entire length of the gallery in monolith 51, an approximate distance of 25 ft. The maximum width of this crack exceeds 2 mm (0.08 in.). The crack is depicted in part in Figure A14 of Appendix A. The crack continues into monolith 53 and crosses the ceiling as the gallery makes a 90^{o} turn. The crack then extends into the downstream face until it reaches the floor at the lock side corner of the gallery. The crack in the downstream face of the gallery is shown in part in Figure A15 of Appendix A.

32. The lock face was inspected to see if the crack in the gallery extended outward to the lock surface. No trace of the internal crack was observed in the lock face. The lock face of monoliths 51 and 53 in the area of concern are shown in Figure A16 of Appendix A.

33. At present, the crack in the cable gallery of monoliths 51 and 53 appears to be limited in depth and does not pose an immediate threat to the integrity of the structure. Similar cracking in the gallery of the land wall was traced to that lock wall face (monoliths 50 and 52).

34. It is assumed that the mechanism that caused the severe cracking in land wall monoliths 50 and 52 is the probable cause of cracking in river wall monoliths 51 and 53. It is, therefore, concluded that the cracking in monoliths 51 and 53 could reach the same severity as that of land wall monoliths 50 and 52 and, thereby, threaten the integrity of the river wall. Therefore, it is suggested that the remedy for insuring the structural integrity of land wall monoliths 50 and 52 be considered for river wall monoliths 51 and 53 as preventative maintenance. The mechanism mentioned above is believed to be thermal expansion. However, to test this hypothesis is beyond the scope of this survey.

35. Monolith 57 has three significant structural cracks. The maximum width of each crack exceeds 2 mm (0.08 in.). One of the cracks is located in the river face of the monolith. It extends from the resurfacing area (about 2 ft from the top of the wall) vertically down the river face to the horizontal surface at el 547. This is depicted in Figure A17 of Appendix A. The second significant crack is in the downstream face of monlith 57. It extends downward from the bottom river side corner of the stairway to the horizontal surface at el 547. This is depicted in Figure A18 of Appendix A. The third significant crack is in the lock face of monolith 57. It extends upward from the top of the emptying culvert to approximately el 554, a distance of 18 ft. This crack is shown in part in Figure A19 of Appendix A.

36. A detailed mapping of these cracks was made, and the results are presented in Figure 3. The extent of cracking in monolith 57 could not be determined from the crack survey. Ultrasonic velocity measurements and borehole pressure tests were used to obtain additional information. The results of these efforts and an analysis of the cracking in monolith 57 are presented elsewhere in this part.

Land Wall Inspection

Land wall monoliths 32 through 46

37. A horizontal crack in the lock face of land wall monoliths 32 through 46 spans the entire length of these monoliths (an approximate

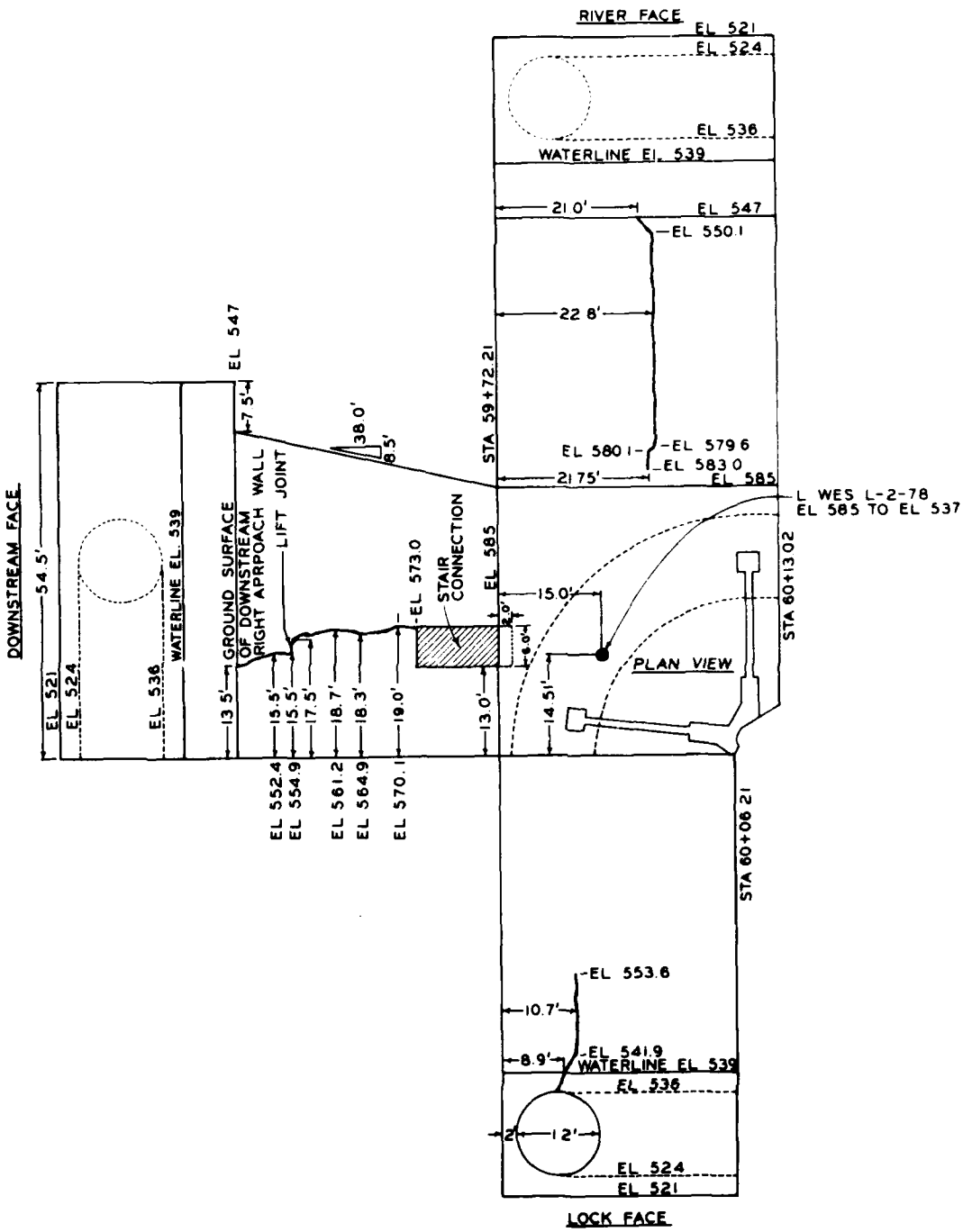

Figure 3. Results of crack survey, river wall, monolith 57, Lockport Lock.

distance of 240 ft). The crack appears to follow a lift joint at approximately el 576. Top elevation of lock wall is 585. The maximum width of the crack is less than 2 mm (0.08 in.). The crack is depicted in part in Figure A20 of Appendix A.

38. A horizontal corner crack between the ceiling and lock side face of the cable gallery spans the entire length of land wall monoliths 34 through 46 (an approximate distance of 210 ft). The maximum width of the crack is generally less than 1 mm (0.04 in.).

Monoliths 48, 50, and 52

39. The horizontal crack in the lock face of land wall monoliths 32 through 46 continues into monoliths 48, 50, and 52. In monolith 48 the crack deviates downward and reaches its lowest point (approximate el 566) at the gate recess of monolith 52. The crack in the lock face of monoliths 48, 50, and 52 is shown in Figure A21 of Appendix A. The maximum width of the crack is greater than 2 mm (0.08 in.). A detailed mapping of this crack was made and results presented in Figure 4. Drill water was observed coming from the crack during the drilling of boring L-WES L-1-78; the boring is located about 15 ft from the face of the lock wall.

40. The cable gallery has approximately 8 in. of water above its floor when the lock is filled. Elevation of floor of gallery is 576, and upper pool elevation is 576.8 I.G.L.D. (1955). As the pool in the lock chamber was being lowered, water was observed flowing out of the crack near its lowest point at the gate recess of monolith 52. Shortly after the water level had reached lower pool in the chamber an inspection of the gallery showed that it contained no water.

41. It was concluded that the water in the gallery was being drained through a crack plane that exists between the gallery floor and the crack in the lock face. The crack in the gallery floor could not be clearly defined as to length and maximum width. A large quantity of silt was deposited on the floor.

42. The horizontal corner crack between the ceiling and lock side face of the cable gallery in land wall monoliths 34 through 46 continues into monoliths 48 and 50. The crack spans the entire length of monoliths

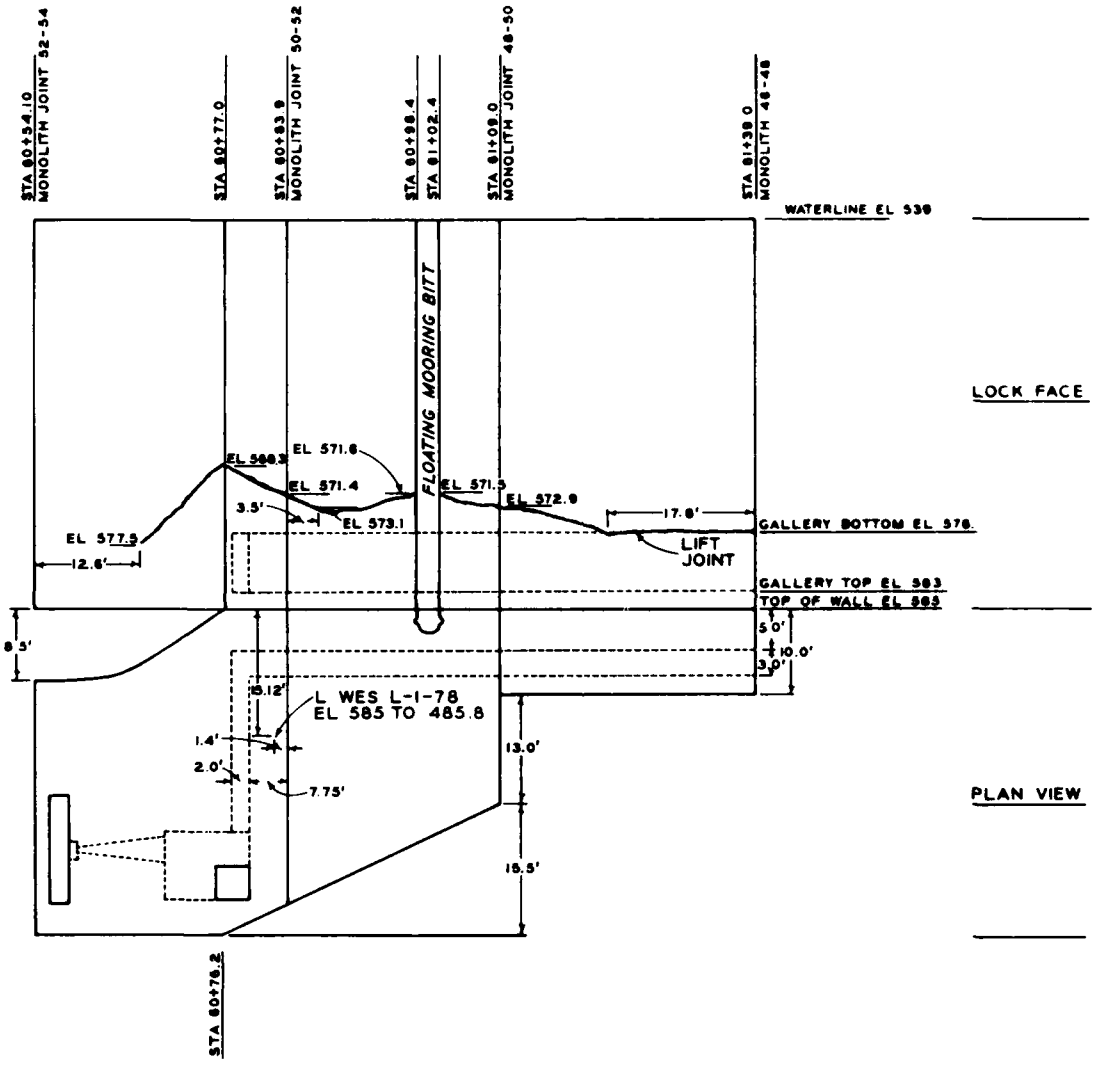

Figure 4. Results of crack survey, land wall monoliths 48, 50, and 52, Lockport Lock

48 and 50 (an approximate distance of 55 ft) and has a maximum width of 2 mm (0.08 in.) or less. Another horizontal corner crack exists between the ceiling and the land side face of the cable gallery. It spans the entire length of the gallery that is parallel to the lock in monoliths 48, 50, and 52 (an approximate distance of 65 ft). In monolith 52 the crack crosses the ceiling landward of the corner where the gallery makes its 90° turn. The crack continues into the downstream face until it reaches the floor of the gallery. The crack then extends into the floor surface upstream for approximately 1 ft. The maximum width of the crack is greater than 12.1 mm (0.5 in.). This occurs near the land side corner where the gallery makes its 90° turn. The crack is depicted in part in Figure A22 of Appendix A. The location of the cracks noted in monoliths 48, 50, and 52 is illustrated in Figure 5. Ultrasonic velocity measurements were used in determining the possible extent of the significant cracking in monolith 52.

Ultrasonic Velocity Measurements

43. Ultrasonic velocity measurements were made on portions of the river wall and land wall at Lockport Lock. The measurements were made in an effort to determine the general condition and quality of the concrete and to access the extent and severity of cracks that are visible in some monoliths. The test equipment and procedure used in this investigation are described in test method CRD-C 51-72.[9] The three areas of interest were river wall monoliths 17 through 49 (odd numbers only), river wall monolith 57, and land wall monolith 52.

River wall monoliths 17 through 49

44. There were no specific problems cited for investigation in river wall monoliths 17 through 49. Velocity measurements were made through the 10-ft sections of each of the seventeen 30-ft-long monoliths at points approximately 10 ft from each end of the monolith. These two data points are designated data point 1 (upstream point) and data point 2 (downstream point) on Table 2. Table 2 also gives the monolith number and the velocities and signal strength obtained at each data point.

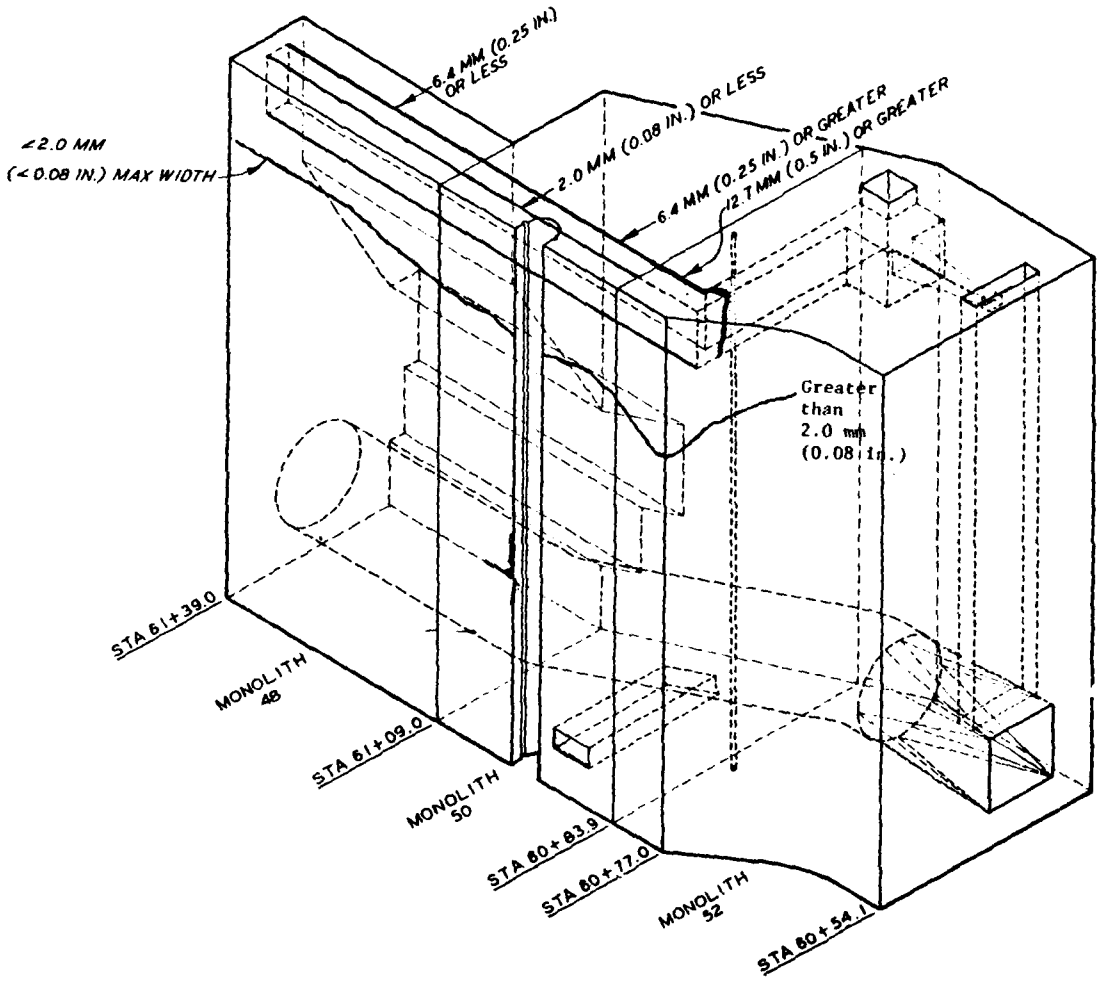

Figure 5. Lockport Lock land wall monoliths 48, 50, and 52

One measurement was made 2 ft down from the top of the wall at each data point. On monoliths 23, 35, and 45, two additional measurements were made at data point 2, i.e., 11 ft and 15 ft below the top of the wall. The measurements made 2 ft below the top of the wall traversed the 10-ft section just above the pipe gallery, and the measurements made 11 ft and 15 ft below the top of the wall transversed the 10-ft section below the pipe gallery.

45. Velocity measurements made through good quality, continuous concrete will normally produce high velocities accompanied by good signal strengths. Poor quality or deteriorated concrete will usually decrease velocity and signal strength. Concrete of otherwise good quality, but containing cracks, may produce high or low velocities, depending upon the nature and number of cracks, but will almost always diminish signal strength. Eight of the velocities obtained from measurements through monoliths 17 through 49 had accompanying signal strengths that indicated continuous transient paths. These velocities ranged between 13,210 fps and 15,040 fps, and were obtained at:

Monolith No.	Data Point and Velocity, fps
17	2 (13,570)
29	1 (14,620)
	2 (13,570)
31	1 (14,685)
37	1 (14,430)
	2 (15,040)
45	1 (13,210)
	2 (15,040)

The signal strengths of the other measurements were weaker, and at some locations the signal was completely attenuated. The possible causes for these weak signals are surface or internal deterioration and cracking. The river side of the river wall has experienced extensive surface deterioration. All monoliths exhibit loss of surface concrete in some areas, and much of the surface concrete that is still present is separated from the wall, forming a hollow shell. Although an attempt was made to make all velocity measurements on a solid surface, there is no way to be

certain that this was accomplished. It was noted that in monoliths 31, 37, 41, and 49 there was a crack about 2 ft down from the top of the wall on the river side that ran longitudinally along the monolith. Crack survey documentation locates a longitudinal crack in the roof of the river wall pipe gallery in monoliths 49 and 51. If a crack has formed in this section of each monolith, some of the velocity measurements could have been influenced by it.

46. The eight velocities accompanied by good signal strengths indicate that the concrete in the river wall monoliths (17 through 49) is of good to excellent quality if free from surface deterioration and cracking. The other measurements indicate that the concrete in the areas tested has experienced surface deterioration or internal cracking, or both. The extensive surface deterioration which can be observed on the river side of the river wall strongly suggests that this is the probable cause of the low velocities and weak signals. There is a possibility that some cracking has occurred between the gallery roof and the river side of the wall in some monoliths.

River wall monolith 57

47. Vertical cracks are visible on each of the three exposed vertical faces of monolith 57. Velocity measurements were made through sections of this monolith (excluding the river face which was hollow) in an attempt to determine the depth these cracks extend into the concrete and if these cracks meet within the monolith. To facilitate these measurements a 7-3/4-in. diameter vertical hole (boring L-WES L-2-78) was drilled in the monolith. By lowering an omnidirectional borehole transducer into the water-filled hole, it was possible to transmit signals to various points on the vertical faces of the monolith. Four locations were selected along the horizontal edges of two vertical faces (see Figure 6) where four vertical series of points (eight points per series) for measurements were established. Borings L-31 and L-32 are shown on the downstream face; information from these borings was used in interpreting crack depth. These four locations are designated data points 1 through 4 and were located so that velocity data obtained at these points would yield information about the cracks, or their absence,

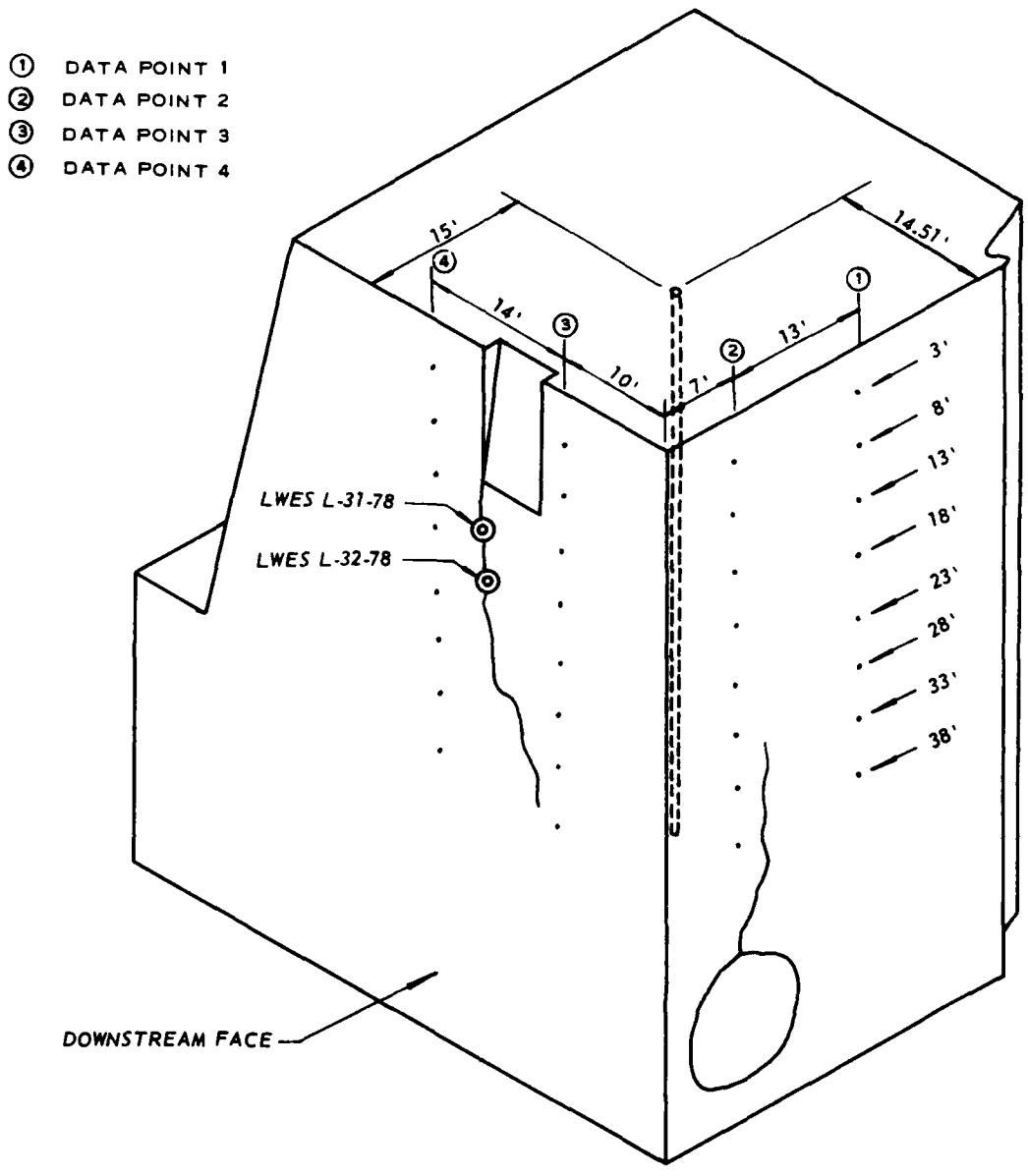

Figure 6. Borehole and data point locations, monolith 57

within the monolith. As the surface transducer was held on the face of the monolith at each depth from the top, i.e., 3 ft from top (Figure 6), 8 ft from top, 13 ft from top, etc., the borehole transducer was lowered to the same respective depth in the water-filled hole. Measurements were made at each data point using this procedure.

48. Table 3 gives the results of velocity measurements made in monolith 57. The vertical series of measurements made from the borehole to data point 1 (Figure 6) produced velocities typical of those usually obtained from structures of this type and age, i.e., lower velocities near the top, higher velocities at lower elevations. The two anomalous velocities obtained at 33 and 38 ft below the top of the monolith suggest that the visible crack above the culvert opening (Figure 6) extends into monolith 57 and follows the curvature of the culvert to a depth sufficient to influece signal propagation at these two locations (see Figure 7). The velocities obtained from the vertical series of measurements at data point 2 also showed the typical increase with increasing depth. The 8100-fps velocity obtained through the concrete at the 3-ft depth is considerably lower than what might be expected as a result of normal near-the-surface deterioration. This low velocity combined with the lower velocities and weak signal strengths obtained down through the 18-ft depth indicates the presence of cracking or some form of distress in the upper 18 to 20 ft. The velocities obtained from data point 3 exhibit this same pattern down through 13 ft and suggest that cracking or some form of distress is present in the upper 20 ft of this general area of the monolith. Results of velocity measurements made at data point 4 suggest that the visible crack on the downstream face of monolith 57 extends into the concrete to a depth sufficient to affect lower velocities down through 28 to 33 ft from the top of the monolith (see Figure 7). The higher velocities and stronger signals at and below 33 ft indicate that the crack is tighter or does not extend as deep into the monolith at depths below 28 ft. Figure 8 presents a graphic interpretation (showing minimum depths of cracks) of the velocity data and of information from L-31 and L-32 obtained in monolith 57.

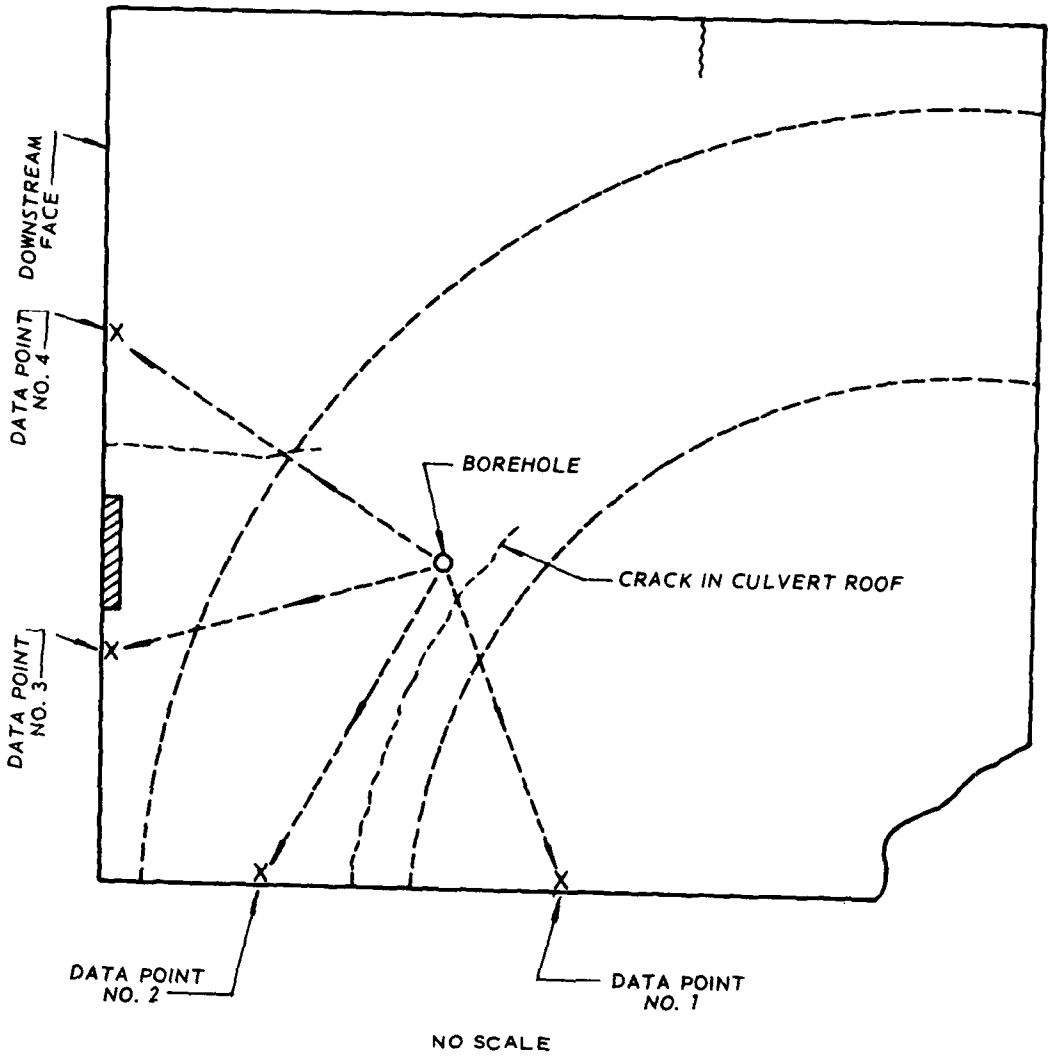

Figure 7. Plan view, top surface, monolith 57

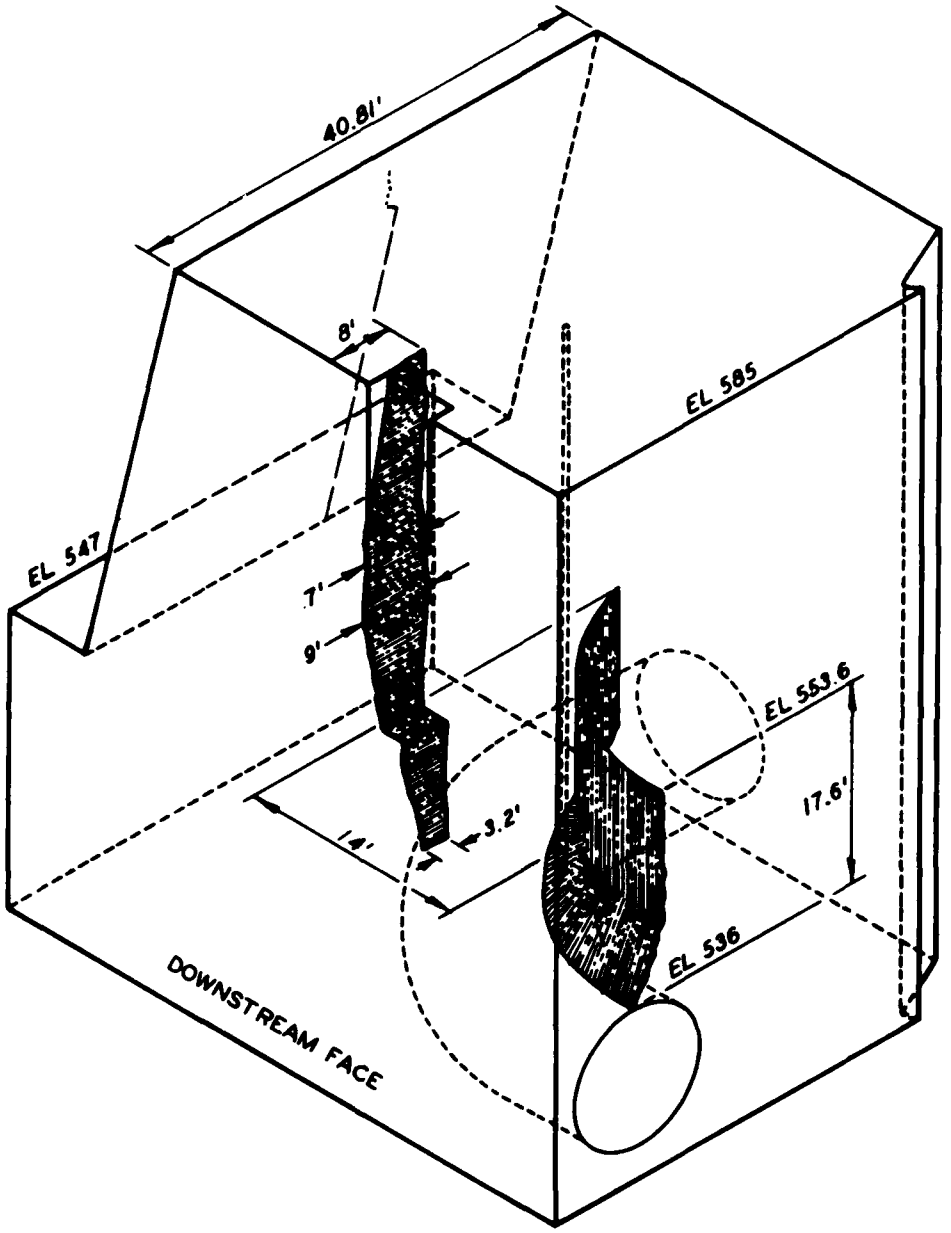

Figure 8. Graphic interpretation of velocity data, monolith 57, river wall

Land wall monolith 52

49. Velocity measurements were made in land wall monolith 52 in an attempt to learn more about the horizontal crack visible on the face of the lock chamber. The borehole transducer was used to check the continuity of the concrete between the borehole and the chamber wall. Figure 5 shows the relationship between the borehole, the gallery, and the visible crack. The fact that the gallery passed between the borehole and the chamber wall in the vicinity of the crack restricted the amount of information that could be gained from velocity data. In an effort to supplement borehole data, a point of transmission was established inside the gallery where measurements were made with the surface transducers from the gallery wall out to the chamber wall in the vicinity of the horizontal crack. Figures 9 and 10 show the locations of data points and transmission paths of velocity measurements in monolith 52. Table 4 presents all velocity data obtained from measurements in monolith 52 including borehole to chamber wall, borehole to gate recess, and gallery to gate recess.

Borehole Dyed-Water Test

50. The ultrasonic velocity data clearly indicated that the crack above the emptying culvert and the crack in the downstream face of monolith 57 extended well into the monolith. A dyed-water test was performed using boring L-2 in an attempt to further trace the cracks. Simply, the test involved filling up the borehole with dyed water and observing where it exited on the three free surfaces of monolith 57.

51. The test was run with the chamber at high pool. The water elevation in the boring before tests was 539, which is 2.0 ft above the bottom of the boring. Elevation 539 is the low pool elevation. With chamber water at high pool (el 576) and with no greater height of water in boring L-2 than low pool elevation, it is concluded that the borehole did not have a channel to the chamber. It took about 165 gal to bring the height of water in L-2 to the top of the monolith; take during the test was approximately 8 gpm. Water was detected flowing from cracks and small monolith joints as given below:

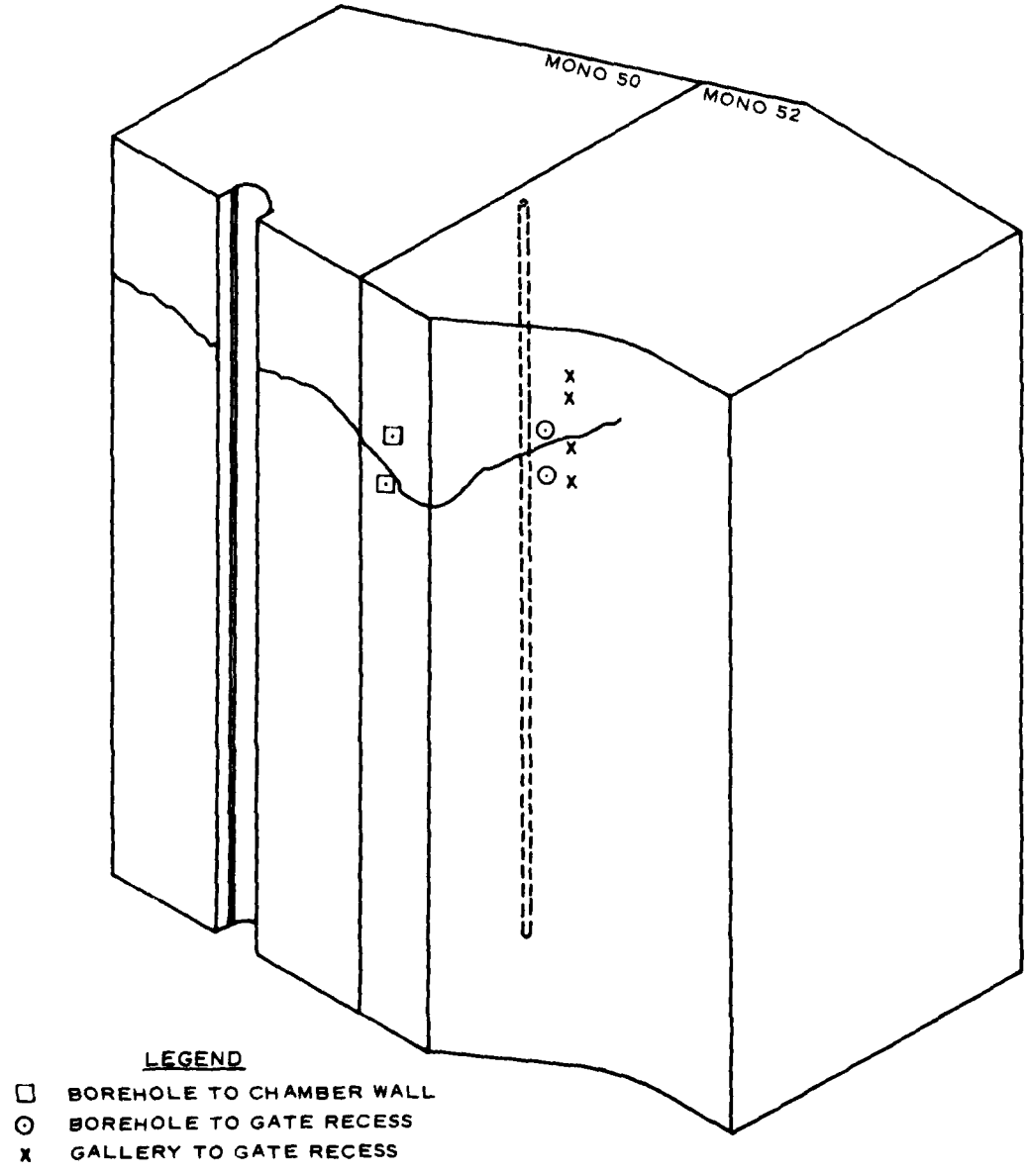

Figure 9. Borehole and data point locations, monolith 52

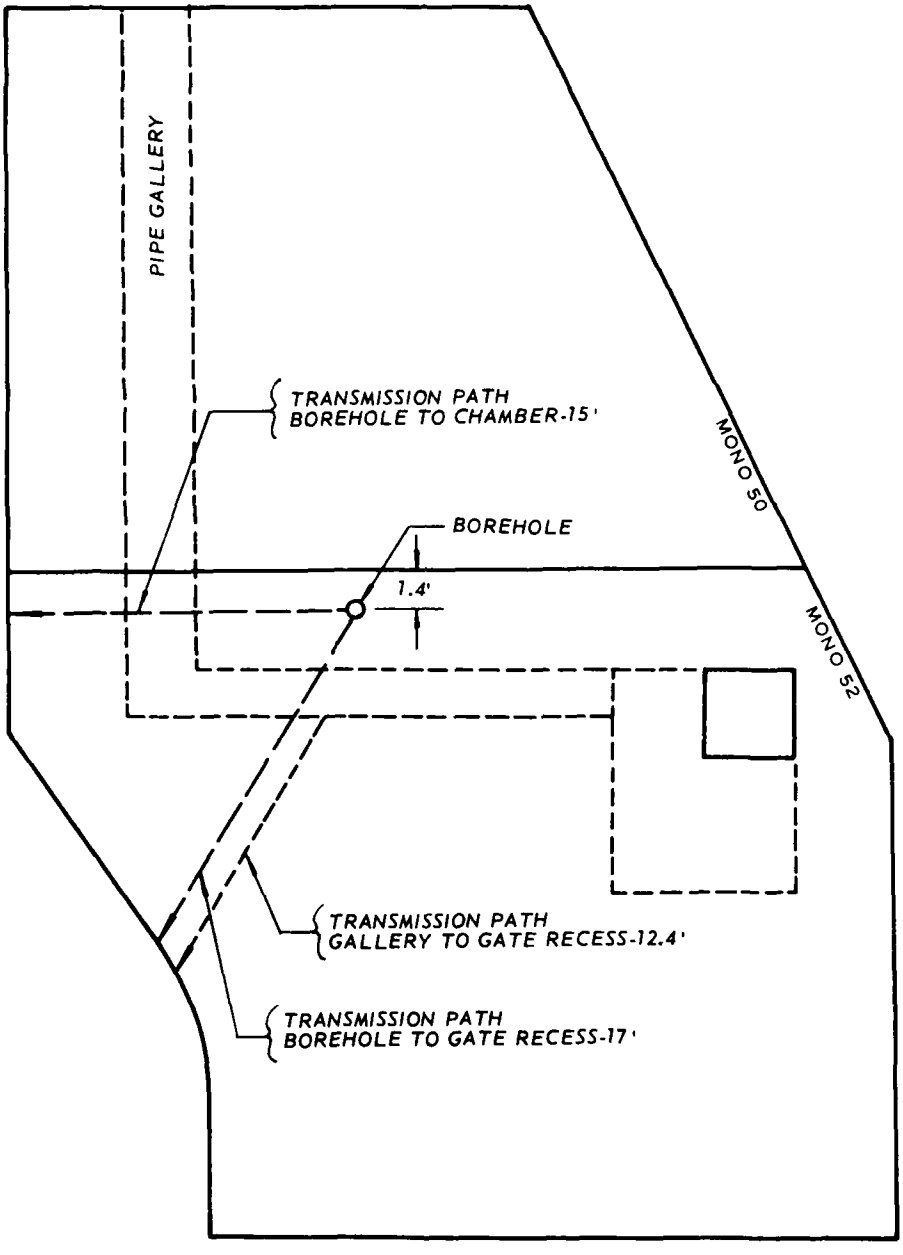

Figure 10. Plan view of transmission paths, monolith 52

Time	Location of Crack or Joint
4:00 p.m.	Test begun.
4:01 p.m.	Colored water flowed out of the crack that intersects the crown of the emptying culvert. Flow began at elevation 539.5 ft. Elevation of low pool is 539. Flow from this crack remained steady for duration of test.
4:25 p.m.	Colored water trickled out of vertical construction joint between monoliths 55 and 57 on back side (river side) of lock wall. Trickle was coming out 12 ft above the ledge.
4:27 p.m.	Colored water trickled out of vertical construction joint between monoliths 55 and 57 on back side of lock wall. Trickle was coming out 2 ft above low pool elevation 539.
4:45 p.m.	Lock chamber taken to low pool.
5:25 p.m.	Colored water trickled out of the vertical crack located about in the middle of monolith 57 on back side. Water was coming out at a point located 17 ft from the top of the wall.
6:00 p.m.	Test terminated due to no further evidence of dyed water exiting from monolith 57. No water was detected coming from the vertical crack on the downstream face of monolith 57.

Extent of Significant Cracks

River wall, monolith 57

52. The crack above the emptying culvert is interpreted to exist along the full length of the culvert to the vertical construction joint between monoliths 55 and 57. Estimated height of crack above the culvert is 18 ft. It is believed that the dyed water traveled from the boring along the crack atop the culvert and then along the vertical construction joint at monoliths 55 and 57. Figure 11 shows probable extent of cracking into monolith 57 from the chamber side and downstream faces. The mechanism causing the crack is not postulated.

53. The crack in the downstream face of monolith 57 extends at least 8 ft into the monolith near the top of the wall and 9 ft about half way down the face. The crack does not intersect boring L-2. The crack appears tight in the downstream face but was observed to be open after about 1 ft within the monolith. Its surfaces, as detected by drilling of L-31 and L-32, contained black stains and crusty white reaction products. The mechanism causing the crack is not known.

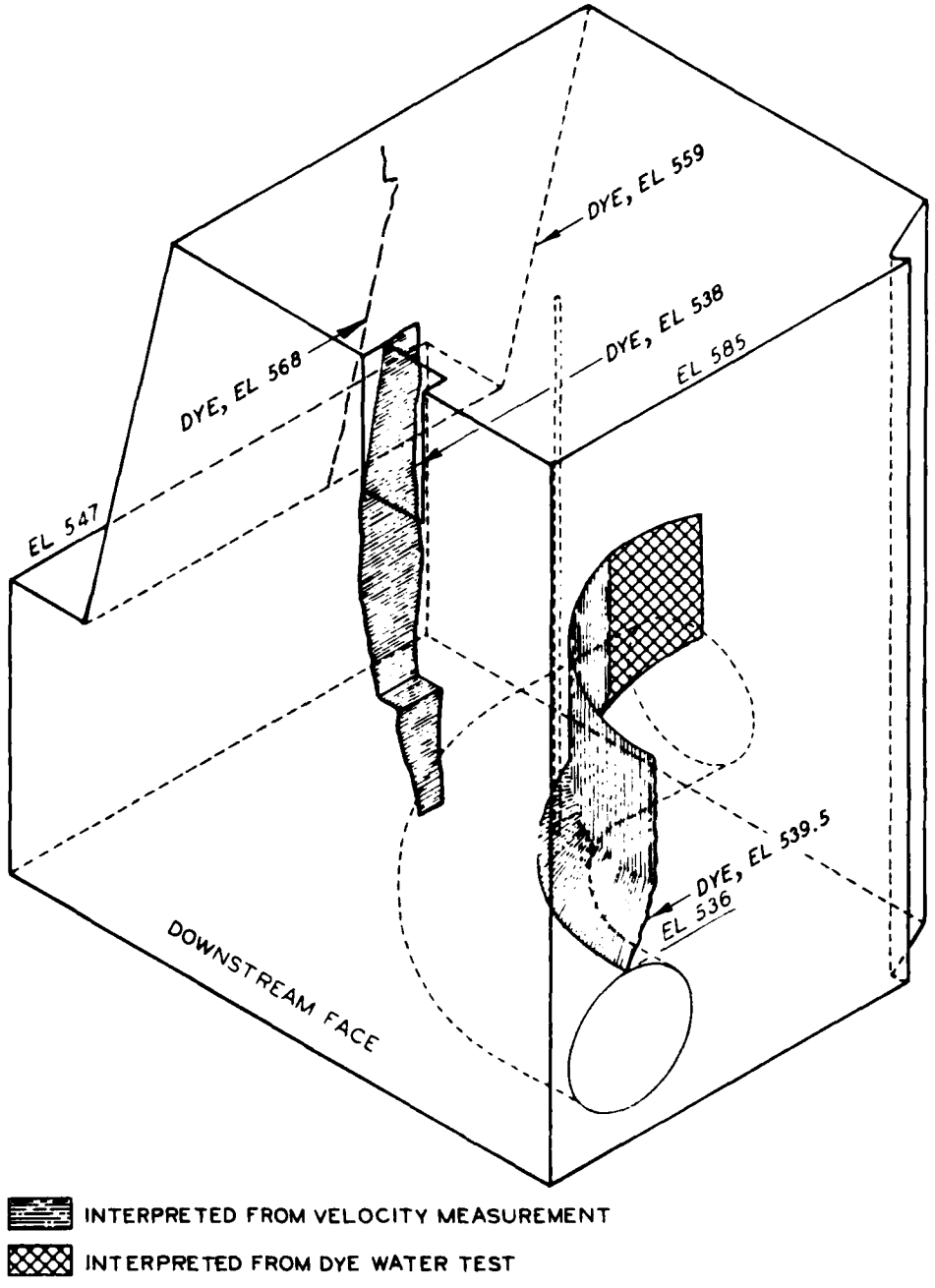

Figure 11. Probable extent of cracking into monolith 57 from the chamber side and downstream faces

54. Attempts were made to trace the crack in the back side of monolith 57. Due to the deteriorated condition of the surface concrete on the back side, meaningful velocity measurements were not obtained. The crack did have dyed water trickling from it and therefore, is connected to borehole L-2 by cracks in the concrete or by horizontal construction joints. The extent of this crack is not known.

Land wall, monoliths 48, 50, and 52

55. Figures 12 and 13 present graphic interpretations of structural cracks based on data obtained in the crack survey, velocity survey, and boring L-1. Figure 14 presents sections showing cracks at the corner of the cable gallery. The horizontal crack in the chamber side of the land wall is connected to the floor corner crack of the cable gallery in monoliths 48, 50, and 52. A land-side roof corner crack extends upward and is covered by a recently placed concrete overlay. In monolith 52 a wedge-shaped mass of concrete with an irregular base inclined about 45° exists with limits as shown in Figure 14. A similar wedge of concrete exists in monoliths 50 and 48, but the irregular base makes a transition from a 45° inclined base to a nearly zero incline base in monolith 48. Again the roof crack is present.

56. Structural engineers at WES were consulted concerning the significance of the structural cracks found in monoliths 48, 50, and 52 of the land wall and monoliths 51, 53, and 57 of the river wall. It was concluded that none of the structural cracks studied appear to pose any immediate problems. If an anchorage system is used at the lock during the major rehabilitation work, then adequately arranged post-tensioned tendons could be considered for monolith 57. The wedge-shaped concrete mass in monolith 52 should be tied together with post-tensioned tendons. It is believed that tendons should be installed perpendicular to the base of the wedge. Similar treatment could be used in monoliths 51 and 53 as preventative maintenance.

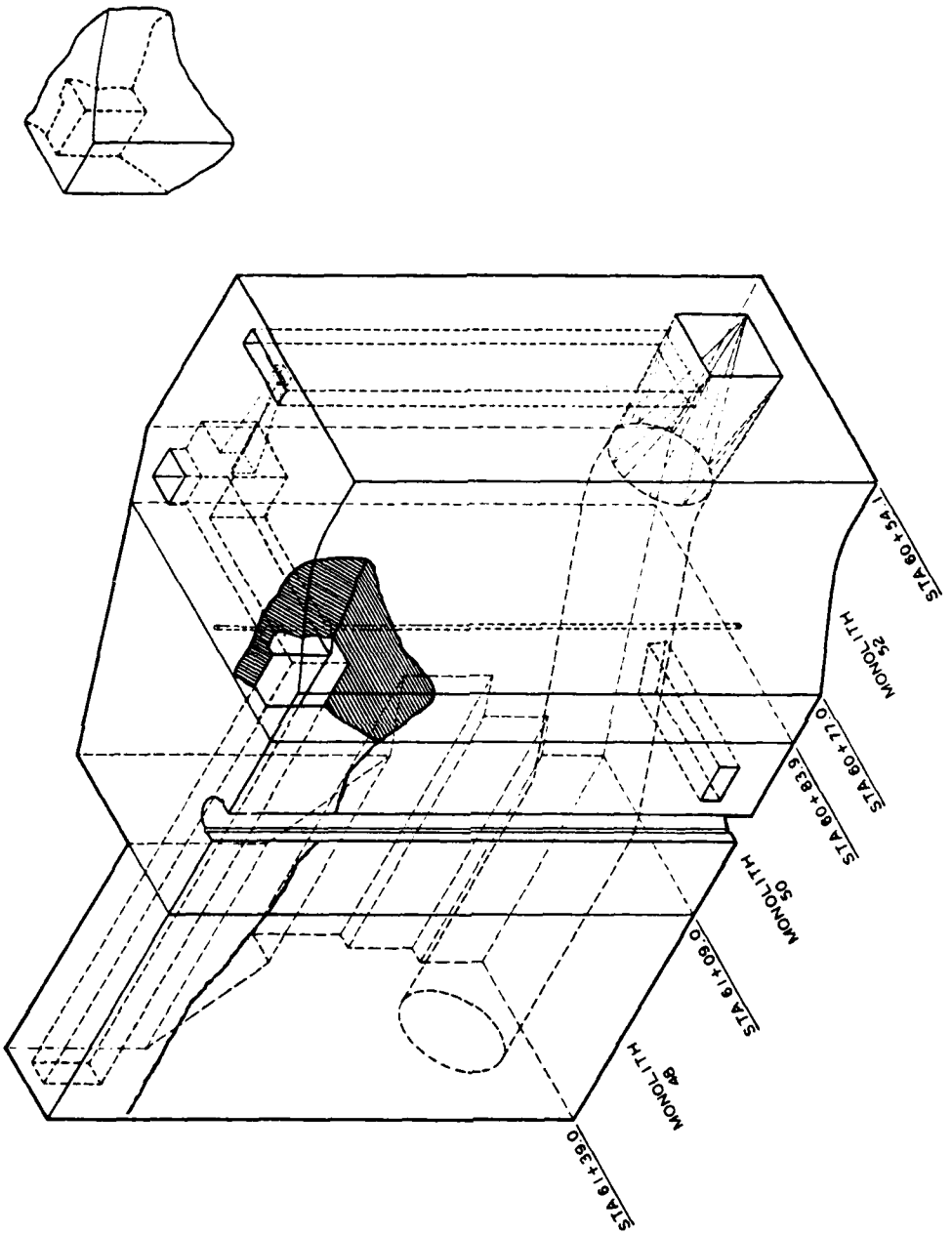

Figure 12. Interpretation of velocity data, land wall monoliths 48, 50, and 52

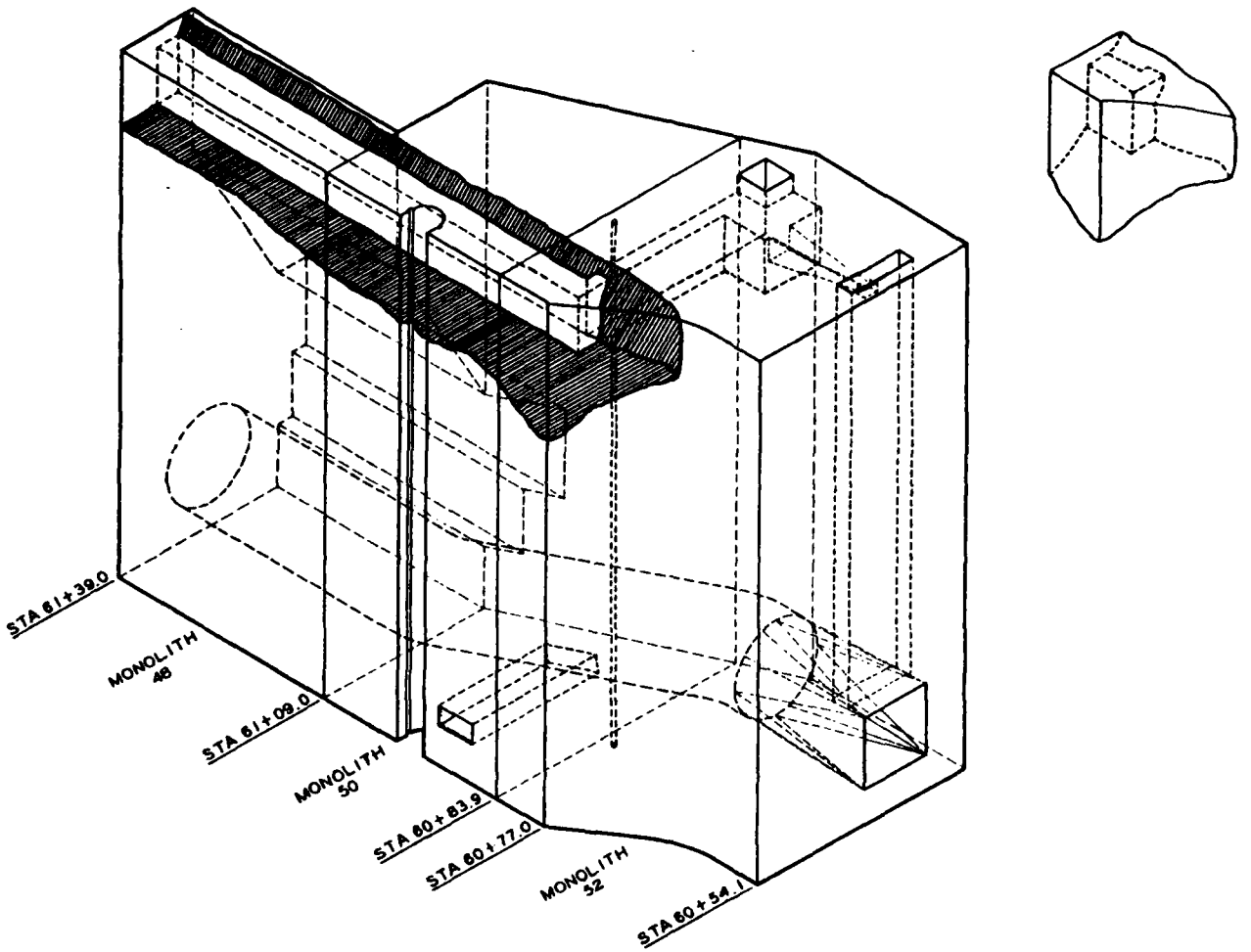

Figure 13. Interpretation of crack survey and velocity data, land wall monoliths 48, 50, and 52

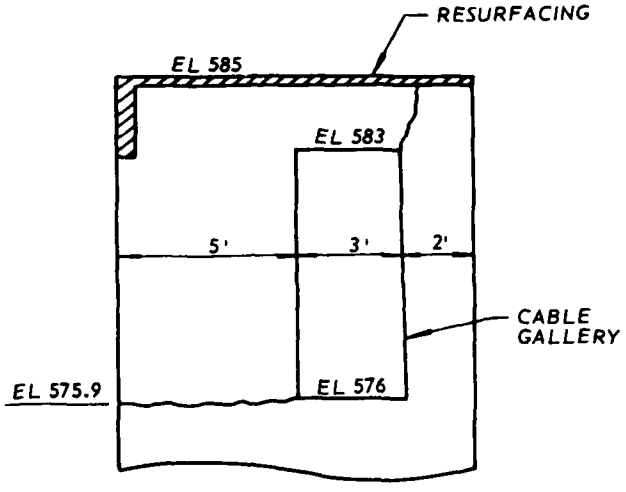

STATION 61+30.0

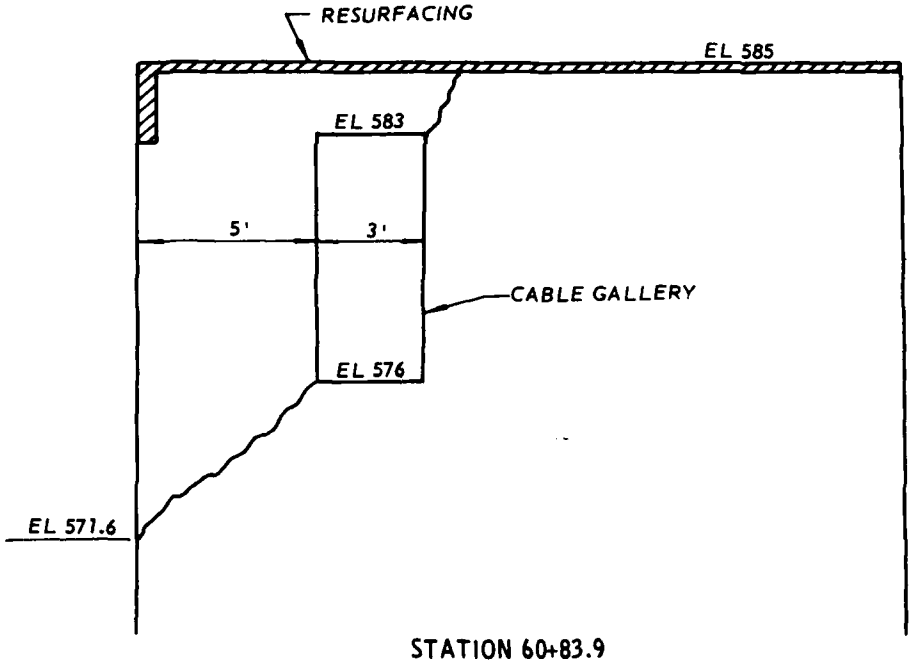

STATION 60+83.9

Figure 14. Sections showing crack location interpreted from crack and velocity survey data, land lock wall

Instrumentation Monitoring Program

57. An instrumentation monitoring program was conducted at Lockport Lock by WES personnel after the major rehabilitation and compliance work was completed.[10] A brief description of the instrumentation used follows; summary of findings will be presented in the Part VII of this report. The objective of the study was to monitor and record any movement of the lower forebay monolith 63, river side lock wall, and cracks in the gallery through monolith 50, land side lock wall. Extensometers and tilt meters were installed in lower forebay area to detect movement of monolith 63 relative to monolith 57. Extensometers were placed across existing cracks in a gallery through monolith 50. The instruments were monitored for a period of 7 months.

PART IV: GEOLOGICAL CHARACTERISTICS

Bedrock Stratigraphy

58. The bedrock beneath Lockport Lock belongs to the Joliet Formation of the Niagaran Series of the Silurian System. The Joliet Formation has each of its three members represented at Lockport. The Brandon Bridge Member is identified by its strong shaley partings. The top of the shaley partings is the base of the Markgraf Member, a silty argillaceous dolomite containing chert nodules. The Markgraf is approximately 30-ft thick as interpreted by the Illinois Geological Survey from borings just north of the Ninth Street Bridge. The borings were drilled by the NCC. At the top of the Markgraf is the Romeo Member, a vuggy, relatively pure dolomite. The dolomite contained in all three members is fine-grained, light gray to light tan, and crinoidal. Clay and shale-filled bedding planes and clay-filled fractures are found throughout the Joliet. The rock is highly to intensely jointed. Bedding planes are stylolitic in nature; the planes may be open, cemented or healed, clay- or shale-filled or incipient. The stylolitic bedding planes have interlocking asperity heights about 1/2 in. There are no distinctive individual layers within the Members that are traceable across the lock.

Geologic Cross Sections

59. Two geologic cross sections were drawn; sections A-A' and B-B' (Plates 3 and 4, respectively). Section A-A' includes holes L-25, SAC-3, L-13, L-38, and SAC-4 which were drilled into or adjacent to the river wall of the lock. Section B-B' includes holes SAC-1, L-23, L-24, and L-38 and cuts through the upper gate sill. The SAC holes were included in the cross sections for comparison of the structure and geology with the new borings.

60. Contact of concrete and rock was tight in every case except L-1 and L-3 where concrete came in contact with fractured or crumbly rock. Approximately 227 ft of rock was recovered from the eight borings,

all of which was dolomite. The dolomite contains green and gray shale and clay partings. The thickness of these fillings is rarely greater than 1/8 in. Many of the bedding planes are stylolitic. Breaks occur along the bedding planes. Spacing of these bedding plane breaks ranges from one break every 0.6 ft in L-24 to every 2.5 ft in L-13. Many of the bedding plane breaks and fractures in the dolomite are stained, indicating an opening to the passage of water. The clay is found filling a few of the vertical joints and fractures. Clay thickness ranges up to 1 in. Toward the base of several of the holes in the Brandon Road Bridge Member, shale-filled bedding planes are closely spaced (<0.02 ft). Within the dolomite chert occurs in thin 1- to 2-in. beds or in spherical, ellipsoidal, or irregularly shaped nodules that are generally in layers parallel to bedding but in some cases sporadically distributed. The chert is compact, fine-grained, and colored white to gray.

Bedrock Structural Characteristics

61. The bedrock structural characteristics relevant to foundation are presented in Plates 5, 6, and 7. Bedrock under Lockport Lock contains green and gray clay- and shale-filled horizontal bedding planes (generally paper-thin). The dolomite is medium (beds 4 in. to 1 ft thick) to thinly (beds < 4 in. thick) bedded, bedding planes becoming closely spaced (< 1/4 in.) toward the bottom of the cores (in the Brandon Bridge Member). Bedding planes are stylolitic. Bedding plane breaks occur more frequently in the upper portions of the core. In several areas the dolomite is porous and sometimes friable, most notably in the top 10 ft of boring L-25.

62. There appear to be pathways open to direct flow of water through the dolomite. These pathways show up as black stains on open bedding planes, vertical joints, and fragmented rock. The water is freely flowing through the bedrock is illustrated by the fact that drillers lost water along the entire length of every bedrock core drilled into Lockport Lock. Ten percent of the 227 ft of dolomite drilled under Lockport was intensely fractured. Besides the horizontal bedding planes,

the most recognizable structural characteristic found in the bedrock beneath Lockport Lock is the joint system commonly found in the Joliet Foundation. Vertical joints and vertical fractures relating to the joints were found in all cores. The joints occur in two sets, each set containing numerous roughly parallel joints, nearly at right angles to one another. The joint system described in Illinois geological literature for the Lockport area trends N40-50°W and N50-60°E. However, no directional measurements were taken on the joints found in the Lockport cores.

63. The joints under Lockport are probably shear joints. Shear joints are smoother and straighter than tension joints. Joint faces found in the Lockport cores are relatively smooth and flat. Shear joints also tend to be more closely spaced or more intensely developed in certain belts or zones with less intensely developed rock between these. A good example of this is found in these cores. Boring L-24 is an intensely jointed core drilled through the upper gate sill. Most all joints are closely spaced (< 0.1 ft) and open. R.Q.D. values for the entire core are 0 percent. Where the rock is not jointed, it is intensely fractured. The fractured rock occurs in an 18-ft-deep zone in L-24 beginning just beneath the sill; the zone contains angular pieces of rock from 1 to 4 in. in length. The top 2.5 ft of rock is in pieces averaging 1- to 2-in. maximum size. Portions of this same zone were thought to be found in L-23, which is 25 ft east of L-24 and in L-38, which is 25 ft west of L-24 and about 25 ft downstream. Additional studies should be done to confirm that fractured zone is interconnected between these three borings. Pieces of the core from L-23 were slickensided. Slickensides were found on and parallel to near vertical fractured surfaces and some were oriented at about 45° to the core axis. The area appears to be a shear zone associated with faulting. The shear zone was not encountered in the previous borings although two borings were drilled adjacent to the lock walls (one in water and one in backfill) in the vicinity of the sill. If the shear zone is narrow and oriented along the N50° to 60°E bearing joints, it could have gone undetected; see Plate 1.

64. It is unlikely that the fractured rock beneath the sill is the result of blasting during excavation or due to drilling action. Drilling action probably caused some breakage of the core. Some intact pieces would fall apart as it was extracted from the core barrel. Upon examination of these sections of cores, it was evident that the core was intensely fractured before being drilled. In some cases the pieces could be fitted back together, and most all surfaces were heavily stained. The remaining seven borings do not possess this degree of jointing, although some jointing is present in each. L-24 also has clay coatings on many of its joint faces and contains the largest number of stained openings in the cores drilled at Lockport.

65. Beds in the Joliet dolomite lack much distinction; therefore, faults are not easily recognized. Small vertical displacements were noted in several cores (at el 505 in L-1 and two faults in L-3 (1.2 in., 1/2 in. displacements)), but the offset in each case was measureable only because the fault plane cut through and dislocated a chert nodule or bedding plane. This indicates that there may be faults along joints in the rock which go undetected because they do not pass through some distinguishing portion of the rock. There has also been horizontal movement in the Joliet dolomite ("Geology and Mineral Resources of the Joliet Quadrangle"). This movement probably occurred along bedding planes. The only other method of detecting faults that was found useful in this case was the occurrence of slickensides. Slickensides were found on one vertical joint and on numerous pieces in the intensely fractured bottom 2 ft of core in L-23 which was drilled through the upper gate sill.

66. The Illinois State Geological Survey defines the base of the Markgraf Member as the highest strong shaley parting in the Joliet dolomite. If this is the same strong shaley parting that is found in the lower part of the cores, then there is a 30-ft difference in elevation of the base of the Markgraf between borings L-1 and L-26 (see Plate 8). Further drilling is needed to determine whether or not this represents a fault. Information obtained from previous cores made at Lockport by the Chicago District in 1967-73 indicates the strong possibility of an upthrown block at the downstream end of the lock. There is as much as

a 30-ft difference in elevations of a marker bed (surface of the Brandon Bridge Member) in a section delineated by L-26 (WES hole), CLP-506, and CLP-605. The trend of this block appears to be ~E-W and seems to cut across the lower approach wall. Borings on either side of this line all fall into the range of elevation of 483 to 490 ft, while along this line the elevations are 517 ft, 509.7 ft, and 501.5 ft, respectively; see Plate 8. A relatively high incidence of cracking of concrete in the lower gate blocks and the possible movement of the end of the ledge (monolith 63) could be associated with settlement or lateral movement of bedrock adjacent to an upthrown block. Boring SACLP-3 indicates that grout was recovered about 2 ft below top of rock; angular and rounded rubble was found with the grout. The grout was probably injected into the broken rock at the time of construction. Nevertheless, the angular and rounded pieces could indicate a shear zone associated with an upthrown block. The strong shale partings were not found in the borings near the upper gate. If the Markgraf-Brandon Bridge contact is near the same elevation as detected near the lower gate, then the upstream borings needed to be drilled 10 to 15 ft deeper to intersect the contact.

67. Evidence of tectonic activity in the vicinity of the lock was observed about 2 miles upstream and adjacent to the Chicago Sanitary and Ship Canal. The area is just upstream of the Ninth Street Bridge in the city of Lockport. The Chicago District drilled four borings in this area as part of their duplicate locks investigation. The Illinois State Geological Survey had obtained boring logs and core from several of the borings. A preliminary geologic cross section obtained from the Survey (see Appendix C) shows a 36-ft offset of the top of the Brandon Bridge Member between borings No. 702 and No. 701. A significant structure appears to exist between borings No. 704 and No. 700 (+70.0 ft). As the Survey indicates, another 20 to 25 ft in boring No. 700 would be required to obtain absolute proof or dismissal of this interpretation.

68. Possible localized weak zones in the bedrock beneath Lockport Lock include the parallel vertical joint sets, the clay- and shale-filled bedding planes, the porous friable dolomite found in some local areas,

the intensely fractured dolomite found at the top of several cores, and the stained solution channels. The closely spaced parallel intersecting vertical joints found in the dolomite can be considered one zone of weakness. Where these joints intersect and break the rock up into small units, they present much less resistance to movement than a massive body would. Occasional joints were filled with up to 1 in. of plastic clay. Since only five vertical joints were filled over short distances, they are not considered significant in terms of stability. Faults with displacements of up to 1.2 in. were noted along these joints.

69. The clay- and shale-filled bedding planes represent an area of weakness in the bedrock. The majority of bedding planes are stylolitic in nature and therefore, there is less chance of slippage due to their tightly interlocked nature. The frequency of occurrence of filled bedding planes increases toward the bottom of the cores; however, the frequency of breaks along filled bedding planes increases toward the tops of the cores. The weaker areas are, therefore, considered to be the filled breaks occurring toward the tops of the cores. From available information, these bedding planes are not considered continuous across the foundation of the lock. Several cores contained highly fractured zones in their upper portions (L-3, L-23, L-38, and especially, L-24). The fractured rock is clay-coated in some cases and contains slickensides in others.

70. Another zone of potential weakness is the porous and occasionally friable dolomite found in the cores. This rock is open to the passage of water and subsequently, to even further weakening by solution (L-25 in ledge downstream of end of river lock wall). These zones are believed to be local in extent and if they are local, they are not considered significant in terms of stability.

71. This weakening can occur in the other areas open to the flow of water, indicated by black staining on the dolomite. These areas include joint and fault faces, bedding plane breaks, areas of highly fractured dolomite, and cavities in the dolomite. The flow of water through these openings allows further solution and widening of the openings. The study of the accumulative effect of solution activity in

the bedrock is beyond this investigation; however, recommendations are made in Part VII to study this potential problem.

PART V: TEST SPECIMENS AND TEST PROCEDURES

Cores Received

72. Concrete and rock core from 56 borings were received at the WES. Pertinent information concerning the core received for both the major rehabilitation and compliance studies is presented in Table 5. Upon receiving the core boxes, test specimens were selected and stored in a concrete moist curing room until time for testing. All remaining core was stored in the laboratory.

Selection of Test Specimens

73. A detailed visual examination of all the core was made to assist in the selection of representative test specimens of concrete and foundation rock. The examination was further used to verify and improve the field drilling logs. Concrete test specimens were selected from the top, middle, and bottom portions of six of the eight deep vertical borings. Test specimen depths shown in the tables of test results represent the mid-section of the test specimen. Six-in. diameter by 12-in. long concrete and rock cores were used for testing, the exception being the specimens for direct shear testing, which had lengths of about 6 in. Characterization properties for concrete and rock; effective (wet) unit weight (γ_m), compressional wave velocity (V_p), and compressive strength (UC), and engineering design properties; Young's modulus (E), and Poisson's ratio (ν) were determined.

74. For the engineering design tests (E, ν, and the direct shear tests), an attempt was made to obtain test specimens to be representative of the rock close to the base of the concrete structure. The test assignment locations can be obtained from appropriate tables of test results. Specimens for the reinforcing bar pullout tests were selected from a depth of about 20 ft below the base of the lock walls.

75. There were four types of dolomite specimens tested in direct shear: concrete cast to rock, filled partings, natural joints, and

bedding planes. A limited number of tests were conducted because the previous direct shear test results, given in Reference 2, indicated reasonable shear strength parameters for the foundation rock at Lockport Lock.

Test Procedures

76. The characterization properties tests and the engineering design properties tests were conducted in accordance with the appropriate test methods tabulated below:

Property	Test Method
Characterization	
Effective Unit Weight (As Received), γ_m	RTM 109*
Dry Unit Weight, γ_d	RTM 109
Water Content, w	RTM 106
Compressional Wave Velocity, Vp	RTM 110 (ASTM D 2845)**
Compressive Strength, UC	RTM 111 (ASTM D 2938)
Direct Tensile, T_D	RTM 112
Engineering Design	
Elastic Modulus, E	RTM 201 (ASTM D 2148)
Direct Shear Strength	RTM 203

* Proposed Rock Test Method, Corps of Engineers, in review prior to publication.

77. The concrete-on-rock specimens were prepared for direct shear testing in accordance with procedures described in Reference 6. A petrographic examination was conducted on concrete cores that represented the best and the worst physical conditions. The test procedure used is given in Appendix B, along with detailed results of the examination.

78. The reinforcing bar pullout resistance test is sketched in Figure 15. A 6-in. diameter by 12-in. long dolomite core was placed upright in a 12-in. high by 30-in. diameter mold. A concrete mixture having the average compressive strength approaching that of the rock (9680 psi at 7 days) was placed into the mold, embedding the core to its full length. The concrete portion served two purposes. First, it

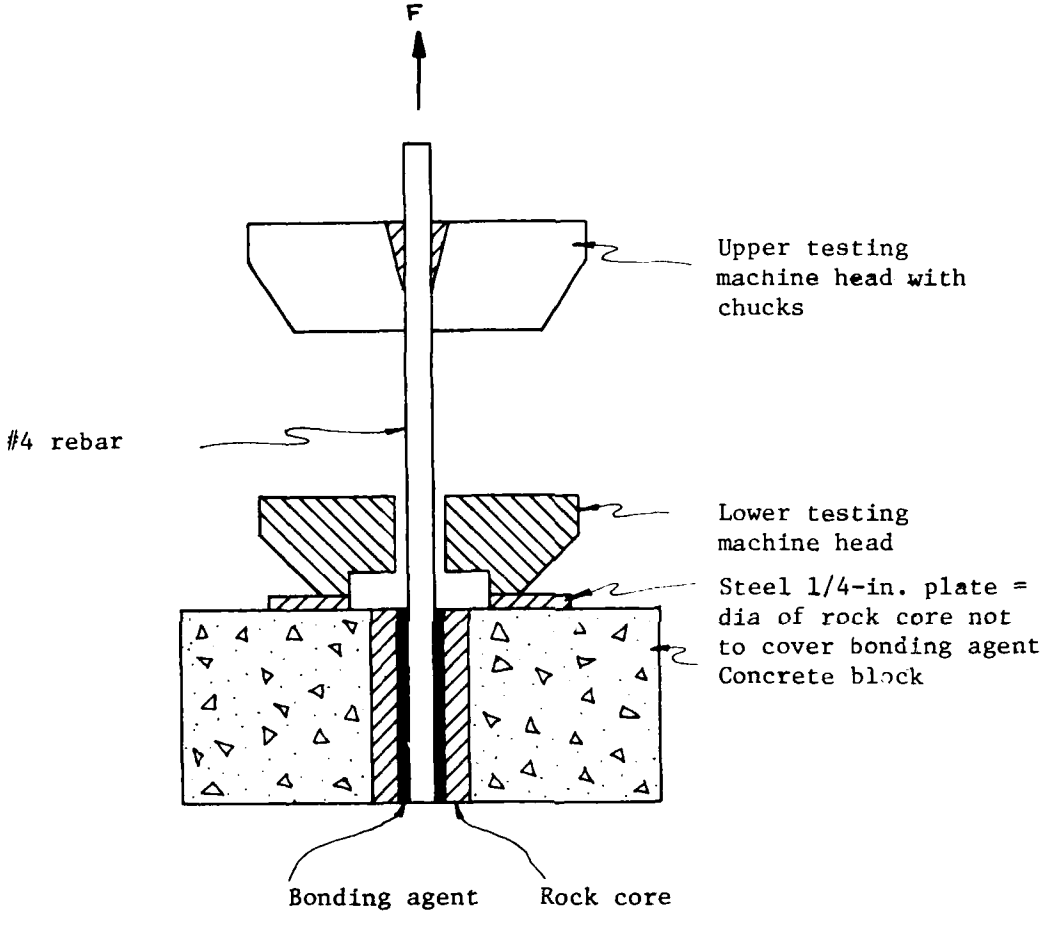

Figure 15. Section showing test configuration for the reinforcing bar pullout tests

acted as a resistance block allowing the bar to be pulled, and second, it served as a host material in case the core instead of the bar was pulled out.

79. After the concrete had cured, a 1-in. diameter hole was drilled in the center of the dolomite core. A diamond thin-wall bit was used, resulting in a smooth-walled borehole. A No. 4 bar was grouted the full depth of the core using a commercially available packaged dry combined grout mixture for anchoring bolts and dowels. Grout strength at test time was about 6500 psi. After the grout attained desired strength, the bars were pulled using the setup depicted in Figure 15. Total weight of the suspended specimen was taken into account in calculating the bond stress.

PART VI: TEST RESULTS AND ANALYSIS

Results of Petrographic Examination

80. The results of the petrographic examination of concrete cores are presented in detail in Appendix B. A brief summary is presented in the following paragraphs.

81. The concrete was not air-entrained. The concrete was damaged by frost-action, principally due to the lack of an adequate air-void system. For the five cores examined in detail, freezing and thawing damage was evident to a maximum depth of 0.6 ft in boring L-11; L-11 was drilled into gate block monolith 56, land wall. Maximum depth of frost damage is 2.1 ft adjacent to the structural crack above the emptying culvert in monolith 57 of the river wall.

82. Alkali-silica gel lining the surfaces of old cracks, coating aggregates, and filling voids was present in four of the five cores examined. The alkali-silica gel was detected in the greater majority of the concrete cores recovered at Lockport Lock; it was found near to free surfaces as well as 60 ft within the lock walls. Cracking beneath frost-damaged concrete and parallel to the core axis is attributed to the alkali-silica reaction. The majority of this type of cracking extended to shallow depths of about 8 ft; it is most prominent in the angle borings occurring in 10 of the 44 borings. The same type of cracking occurred at Starved Rock Lock and Dam.[11] Some chert particles in the gravel contained chalcedony, a constituent known to be reactive with alkalies. Other reactive particles may be present but if so, were not detected.

Characterization Properties of Bedrock

83. The results of the characterization properties tests are presented in Table 6. A limited number of tests were run to verify the tests that were reported in Reference 2. In general, the agreement between the two sets of data is excellent, as shown in the following tabulatino of average values.

Property	Current Study	Previous Study, Reference 2
Unit Weight, γm, lb/ft^3	168.0	167.3
Unit Weight, γd, lb/ft^3	164.3	165.1
Compressional Wave Velocity, Vp, fps	19,007	18,770
Compressive Strength, UC, psi	13,820	17,370
Elastic Modulus, E_{t50}, psi x 10^6	8.94	9.19

E_{t50}, tangent modulus at 50 percent compressive strength

Unit weight

84. Effective unit weight averaged 168 lb/ft^3. The value indicates a competent well compacted rock with few voids or low porosity or both. This is true for intact specimens; however, local areas in the foundation are highly fractured and porous. Unit weights for the rock in these areas would be reduced somewhat; a reasonable estimate is given in Reference 12 for highly fractured rock (blasted 155 lb/ft^3). The unit weight of blasted dolomite would be slightly lower considering the differences in absolute specific gravities of the two rocks.

Compressional wave velocity

85. The velocities of intact cores were measured to verify previous velocities,[2] the previous data being collected to compare to in situ values should the need arise to obtain them. The current and previous data compare well.

Compressive strength

86. The compressive strength values show a large difference which could be attributed to a number of variables. The diameter of specimens tested in Reference 2 was 4 in. while those tested during this study were 6 in. It is known that the larger a core is the more likely it is to contain a greater number of natural discontinuities that normally contribute to lower strengths. With the high frequency of filled, healed, and open fractures observed in the bedrock samples, decreased strength of larger test specimens is to be expected. The population of test specimens could also have contributed to the strength difference seen in the two sets of data. The average strength reported in Reference 2 and this study was obtained from 22 and 6 specimens, respectively.

Elastic modulus

87. Plots of stress-strain relations are presented in Plate 9. The stress response is indicative of very little closure of microfractures or bedding planes. The curves are generally straight up to failure, which indicates very little consolidation. Modulus values were calculated as tangent values at 50 percent of peak stress. The average E_{t50} is 8.94×10^6 psi, which compares well with a previous[2] value of 9.19×10^6 psi.

Reinforcing Bar Pullout Resistance

88. The bond strength calculated from the pullout tests of reinforcing steel bars is presented in Table 6. The average bond strength for the dolomite is 117 tsf. This strength represents the bond developed between the grout used to embed the bar in the dolomite and the grout itself. Three specimens were made; one failed due to bar separation.

Peak and Ultimate Shear Strength

89. Two types of direct shear tests were conducted during this study to ascertain peak strength and sliding friction properties of intact and discontinuous specimens, respectively. Peak strengths were obtained for concrete cast to dolomite; and sliding friciton strengths were measured for specimens containing filled partings, bedding planes, and natural joints. Both the partings and bedding planes were stylolitic in nature. Cross-bed shear tests were not conducted because previous tests had adequately defined this value.[6] The direct shear test results and the calculated strength parameters are presented in Table 7. Plates 10 through 13 are plots of shear stress-normal stress values that are presented in Table 7. Table 8 contains surface descriptions of sheared specimens. The descriptions allowed for a comparison of the shear strength parameters obtained previously[2] and during this study. Similarities in relief, surface area contact, surface coatings, and gouge or rock flour indicate that similar specimens were tested during the previous[2]and present study.

90. The word "ultimate" is used in this report in conjunction with the direct shear tests results; i.e., ultimate shear stress and ultimate shear strength. For purposes of this report the term "ultimate shear stress" is defined as the stress level reached at 0.4 in. of shearing displacement. The 0.4 in. is the single stroke travel of the shear device in use. The direct shear tests were run using two setups; i.e., the specimen was taken to peak load, repositioned, and sheared an additional 0.4 in.

Concrete-on-rock

91. Three tests were conducted along the interface of the concrete and dolomite, the concrete being cast directly onto the natural bedding surfaces. The bedding surfaces of the test specimens had relief of 1/4 to 1/2 in. On a 6-in. diameter specimen there were about six peaks over the surface. For two specimens, failure occurred at the interface with several peaks being sheared at their base; one specimen failed within the concrete. The cast surface was considered to be interlocked with 100 percent contact between the cocrete and rock. The specimens tested with a normal stress (σ_n) of 2 tsf had a relief of 1/2 in. The shear stress (τ) was higher than the τ for the specimen tested with the next highest σ_n. In calculating the shear strength for the concrete-cast-to-rock, the τ at σ_n=2 tsf was omitted. The peak cohesion (c) and angle of internal friction (ϕ) is 18 tsf and 67°, while the ultimate cohesion (c_u) and friction angle (ϕ_u) is 0 and 62°, respectively. The contact of the concrete and bedrock should be considered tight (no loose contact except in L-1 and L-3 where fractured rock was encountered) and interlocked. A shear strength of c=18 tsf and ϕ=67° is recommended for design. Similar test results were obtained for similar dolomite at Brandon Road Dam.[6] A coefficient of sliding friction (smooth concrete on dolomite) was not measured during this study. The value reported in Reference 6 (c=0 and ϕ=26°) is recommended for design, if needed; this previous value was obtained on the same geologic formation (Brandon Bridge Member) as exists at the Lockport Lock.

Filled parting

92. Upon inspection of the filled parting and bedding plane surfaces, noticeable differences were apparent. The conditions of both surfaces are tabulated below for ease of comparison.

Condition	Filled Parting	Surfaces Bedding Plane
Relief	2 of 3 specimens, 1/4 in.	1/2 in.
Surface contact	About 20%	About 70%
Surface coating	Green clay	Green clay
Solution activity	High	Low

The relief was considered rough (1/4 in.) to very rough (1/2 in.) with both surfaces interlocked where contact existed. The filled parting specimens did not withstand as high a shearing load as did the bedding-plane specimens. The likely reason is not the clay coating, rather the lack of contact between the two surfaces. The clay coating did not affect shearing resistance until after the projections were sheared off, the load then being transferred to the broader and flatter irregularities. Surface contact was the largest contrasting condition between the filled partings and bedding planes. The surface coating consisted of green clay with a thickness of less than 1/64 in. The clay generally coated the surfaces not in contact. Solution activity was much more prominent in specimens with filled parting surfaces than in specimens with bedding planes.

93. Both parting and bedding surfaces occur throughout the bedrock with the filled partings (open due to solution activity) occurring more frequently in the upper portions of the foundation. Neither discontinuous surface is considered continuous within the foundation. Scatter of the direct shear data was quite small. The average c and ϕ for the specimens with filled partings is 9.2 tsf and 48°, respectively. The previously reported values[2] are 1.3 tsf and 50°, and 0.43 tsf and 45° reported in Reference 6, for specimens with similar surface conditions. The previously reported residual friction angle (ϕ_r) is 35° with a c_r=0; these values are considered reasonable residual values for design purposes.[2]

Bedding planes

94. The condition of these surfaces were covered in the previous paragraphs. Scatter of the direct shear results was quite large and is attibuted to the roughness (relief about 1/2 in.) of bedding planes. Test data indicated (Table 7) that two specimens (L-26, el 519.7, and L-25, el 511.8) had projections sheared off under a σ_n=2 tsf, the load then being transferred to the broader and flatter irregularities for the remainder of the multistage tests. An example can be seen in Table 7 for specimen L-26, el 519.7, where τ=61.1 tsf for σ_n=2 tsf and subsequent τ's of 18.1 and 23.3 tsf for σ_n's of 4 and 8 tsf. The two other specimens appeared to have continuous shearing of asperities or intact rock throughout the three normal load applications.

95. The test results indicated that two types of failure occurred. Bedding planes either rode over undulating surfaces after shearing commenced (low profile projections) or stylolitic projections and intact rock sheared during the entire test. Shear strength values for sheared projections yield values for c and ϕ of 49 tsf and 61.5°, respectively. For those portions of the shear tests where specimen contact was on the broader and flatter irregularities, values of c and ϕ of 19.5 tsf and 40.3°, repsectively, were calculated. The ϕ=40.3° for the broad and flat irregularities correlates with the recommended residual value (ϕ_r=35°) along bedding planes as given in Reference 2.

Natural joint

96. Two naturally jointed specimens were tested. One specimen contained a rough relief having interlocking projections 1/4-in. high; the other had relief of about 1/32 in. The majority of the joints at Lockport Lock are estimated to have relief between 1/32 and 1/4 in. The c and ϕ for the high relief (1/4 in.) and the lower relief (1/32 in.) is c=36 tsf, ϕ=68.4°, and c=12.4 tsf, respectively. The specimen with the low relief has a ϕ value about equal to the precut dolomite (ϕ_r=22°). No joints with clay filling could be obtained for shear testing due to the fractured condition of segments of jointed core.

Summary of direct shear results

97. The previous investigators (University of Illinois, Reference 2) conducted an excellent direct shear testing program. No new materials

or natural features were detected during the present study that were not tested during the University of Illinois test program; our direct shear data then verifies that data presented in Reference 2. They presented representative shear strength parameters for interlocking stylolitic surfaces, residual values for these surfaces, vertical joints, and presented lower bound values for rock-on-rock surfaces (sawed and lapped surfaces); see Plates 6 and 7 in Reference 2). The authors concur with the following quote from Reference 2 as a summary statement regarding the controlling shear strength to be used in computing stability.

> It should be pointed out that stylolitic surfaces of this rock are only roughly planar and because of this irregular pattern they normally would not constitute a well defined planar shear surface of considerable extent necessary for any large scale type failure. Upon consideration of all information and additionally because of the absence of previously failed seams, partings or other shear surfaces that would indicate past movement, it is thought that peak shearing resistances would control and these are recommended for use when computing stability. However because of the importance of this determination, it is recommended that computations also be made employing residual values and that a further study be made of possible failure planes during the continuing investigation, thus, keeping this important matter open for additional study. Recommended shear values to be used are as follows:

	ϕ	c
Peak	50 degrees	18.5 psi
Residual	35 degrees	0 psi

Backfill

98. No backfill was recovered during this study. See Reference 2 for design values of backfill material.

General Comments for Concrete

99. The following general comments pertain to the condition of the concrete over the entire lock. Individual structural elements within the lock will be discussed separately. The results of the concrete characterization and engineering design tests are presented in Table 9. Stress-strain relations for concrete cores are presented in Plates 14-18. These

data will be referred to as appropriate. Results of the detailed petrographic examination are presented in Appendix B. General descriptions of the concrete from 56 borings are presented in Plates 19-21; and a description of the concrete cores examined in detail is presented in Plates B1-B5 of Appendix B. The field drilling logs for all borings are presented in Appendix E, which is on file at the NCC office. Concrete that appeared to be air entrained was encountered near the surface of vertical borings drilled into the lock walls. None of the concrete from the horizontal borings was air entrained. The nonair-entrained concrete was considered old, and the air-entrained concrete was considered new. The new concrete normally consisted of coarse aggregates smaller than 1 in. in nominal maximum size and was cemented with a gray paste. The old concrete consisted of gravel aggregate with a nominal maximum size of approximately 3 in. and was cemented with a light brown paste. The aggregate consists essentially of dolomite with some chert and igneous rock particles. The concrete sampled generally appeared well consolidated, although minor amounts of localized honeycombing were detected. The void areas should not directly affect the structural integrity of the lock; however, they may act as potential water storage cavities, and thereby accelerate damage due to freezing and thawing.

100. Examination of the core shows that nearly all of the near surface old concrete exhibits cracks subparallel to the surface of the concrete and to depths ranging from 0.1 ft to 2.1 ft. The navigation lock and approach walls contain frost-damaged concrete. Cracks at right angles to the free surface (formed surfaces) of the core were observed within some of the frost-damaged zones. Similar cracking occurred outside frost-damaged zones. Alkali-silica gel was present in some voids of all of the cores and along the joint and crack surfaces.

101. The longitudinal cracks normal to the free surface are characteristic of alkali-silica reaction in hydraulic structures and some bridges and represent the expansion of the less restrained exterior part of the concrete in the structure. The expansive force and the restraint combined govern the extent and frequency of the cracks normal to the surface.[11] The concrete in the dam and, to a small extent, in

the lock at Starved Rock has undergone similar deterioration due to alkali-silica reaction.

Lock Chamber Land Wall

Depth of deterioration

102. Eight horizontal borings were drilled into the lock chamber land wall, four near high pool elevation (about 10 ft from top of wall) and four at low pool elevation. Frost damage was evident to some extent in all of the cores with the deepest damage occuring in those from near the top of the wall. The average depth of frost damage in the chamber land wall is 0.4 ft with a maximum depth of 0.8 ft. Traces of alkali-silica gel were found deposited in air voids on the cored surface of each core. The total depth of deterioration as measured from the original face of the lock wall is the sum of the eroded depth and of the present frost-damaged concrete. The deepest damaged concrete is near the top of the wall.

103. One vertical boring (L-3) was drilled into the top of the land wall with approximately 0.2 ft of new concrete evident in the top of the core. Frost damage prior to placing the new concrete had deteriorated the underlying old concrete from 0.2 to 1.5 ft. Numerous air voids suggest that the concrete was poorly consolidated from 47.1 to 52.6 ft. Alkali-silica reaction gel was noted in voids on the cored surface and in voids on mechanical break surface along the entire core.

Average physical properties

104. Horizontal borings. The average physical properties of the concrete from the horizontal holes in the lock chamber land wall were:

Test	Near Surface Concrete	Bottom of Core Specimens	Percentage Difference
Effective Unit Wt, pcf	151.9	152.6	-0.5
Comp Wave Velocity, fps	15,486	15,021	+3.1
Compressive Strength, psi	6,460	6,700	-3.6
Modulus of Elasticity, x 10^{-6} psi	5.33	5.33	0.0
Poisson's Ratio	0.21	0.26	-19.2

The concrete is sound beyond the outer damaged concrete. The percentage differences indicate minor changes between the near and bottom of core concrete.

105. Vertical borings. The physical properties of the concrete from all of the vertical borings are tabulated in Table 9. Test specimens were obtained from the near surface, middle, and bottom of the structures within the lock. The properties of the specimens obtained from boring L-3 indicate that the concrete is sound; however, the near surface specimen was acquired below the frost damage. Consequently, the near surface physical properties are not necessarily characteristic of the concrete in the deteriorated area.

Lock Chamber River Wall, Upstream of Lower Gate Bay

Depth of deterioration

106. Frost damage was present in five of the six horizontal borings drilled into the lock wall; boring locations were similar to locations on land wall. The average depth of deteriorated concrete in this side of the wall is 0.1 ft; the maximum depth is 0.3 ft in hole L-21 near high pool elevation (see Plate 21 for depth of deteriorated concrete). Alkali-silica gel was present in small amounts on all concrete surfaces exposed by mechanical and natural breaks. Cored surfaces of the concrete revealed similar gel.

107. One vertical boring (L-13) was drilled at mid-length of the river wall (monolith 33). The core revealed 0.2 ft of new concrete characterized by a light brown paste, 3/4-in. nominal maximum size aggregate, and air entrainment. No apparent frost damage was detected in the concrete; however, small alkali-silica gel deposits were noted on the cored surface of the entire core.

108. One angular boring (L-38 in monolith 13) was drilled into the old boat lock in an effort to trace a zone of intensely fractured bedrock. No new concrete was detected in the core. Frost damage was apparent in the concrete to a depth of approximately 3.0 ft. Zones of horizontal cracks and fractured pieces were prevalent from el 565.2 to

558.4 ft, and staining was noted on the surfaces of horizontal construction joints from el 557.8 ft to the bottom of the concrete at el 520.4 ft, indicating penetration of river water into the concrete.

Average physical properties

109. The average physical properties of the concrete from the horizontal borings in the upstream side of the lock chamber river wall are presented below:

Test	Near Surface Concrete	Bottom of Core Specimens	Percentage Difference
Effective Unit Wt, pcf	150.9	152.1	-0.8
Comp Wave Velocity, fps	15,300	15,465	-1.1
Compressive Strength, psi	6,830	6,960	-1.9
Modulus of Elasticity, x 10^{-6} psi	4.43	5.41	-18.1
Poisson's Ratio	0.22	0.27	-18.5

Generally, the near surface concrete in the top of the lock wall has slightly lower physical properties than the near surface concrete at the low pool elevation. The bottom of core specimens exhibit higher physical properties than the near surface concrete. The modulus of elasticity and Poisson's ratio of the near surface concrete are approximately 81 percent of the bottom concrete. The concrete from the lock chamber land wall has a similar percentage difference with respect to Poisson's ratio. However, the values are reasonable and should be taken into account, should a stress analysis be made of the lock chamber walls.

110. The physical properties of the three test specimens obtained from the vertically drilled core (L-13) are slightly lower than those properties of the concrete removed from hole L-3 in the lock chamber land wall. The properties of both the specimens from both cores reveal, however, that sound concrete is prevalent beyond the frost-damaged areas. No core was saved from boring L-38.

Lock Chamber River Wall, Downstream of Lower Gate Bay

111. This section of the river wall is discussed separately because the concrete is deteriorated beyond the extent of that in the wall upstream of the gate.

Depth of deterioration

112. Two horizontal borings were drilled into the veritcal face of the wall downstream of the gate bay. The average depth of deteriorated concrete in the vertical face is 1.3 ft; the maximum depth is 2.1 ft in boring L-52 which is along the structural crack over the emptying culvert. The damaged concrete in the same boring is described in this report under Monolith 57.* Alkali-silica gel was noted in air voids on the surfaces and fractures in borings L-51 and L-52.

113. One vertical boring (L-25) was drilled into the downstream ledge of the river wall. New concrete, characterized by 3/4-in. maximum size crushed limestone aggegate, was noted to a depth of 0.4 ft. No frost damage was apparent in the new concrete, although the underlying old concrete contained frost damage from 0.4 to 1.9 ft. A longitudinal crack extending from 0.7 to 7.0 ft, paralleled by a crack from 4.2 to 6.5 ft, was observed in the core. The crack surfaces exhibited traces of alkali-silica gel, as did cored surface air voids. A large number of sizable voids were encountered in the concrete from the boring at 4.2 to 7.0 ft, indicating poor consolidation. Boring L-25 was drilled through monolith 63, which is currently instrumented for possible movement.

Average physical properties

114. One bottom of core specimen was tested from the concrete of boring L-51. The physical properties of the specimen indicate sound concrete. No near surface concrete was tested from boring L-51 or L-52. However, the amount of deterioration visually discernible from the surface to 1.0 ft in both cores suggests that the physical properties of the concrete within this area are somewhat lower than those of the bottom of core specimen.

---

* See p 67.

115. A near surface, middle, and bottom of core specimen was obtained from the vertical core. The physical properties of each specimen suggest sound concrete is present throughout the wall. The near surface specimen, however, was taken below the depth of frost damage and longitudinal cracking due to the extent of deterioration. Therefore, the properties of the near surface specimen are not necessarily indicative of those which actually characterize the upper 7.8 ft of the concrete.

Lock Chamber River Wall, River Side

Depth of deterioration

116. The average depth of deteriorated concrete throughout this side of the wall is 0.83 ft; the maximum depth is 2.8 ft in boring L-56. Frost damage was evident to some extent in the concrete from each of the horizontal borings except L-43. Loose aggregate along with subparallel fractures perpendicular to the core axis characterize the frost-damaged concrete. This side of the river wall has experienced a much greater degree of weathering and frost damage than the chamber side, as evidenced by the erosion and scaling of the surface concrete. The lower baffled section of the wall has sustained the greatest amount of deterioration. Alkali-silica gel was present within the entrapped air voids along the cored surfaces of the cores and on crack surfaces within the cores. The concrete from boring L-43 exhibited a longitudinal crack the length of the core which may have occurred as a result of the alkali-silica reaction. Black staining, possibly organic in origin, coated the longitudinal crack surfaces of core L-43 and the construction joint surfaces of concrete from borings L-44 and L-56. This staining is indicative of moisture migration along these features and into the concrete.

117. Three vertical borings were drilled into the ledge adjacent to the river wall. No new concrete was encountered in these borings. The average depth of frost damage in the ledge is 2.3 ft; the maximum depth is 2.9 ft in boring L-53. Alkali-silica gel coated the crack surfaces and void spaces of the highly deteriorated cores.

Average physical properties

118. The average physical properties of the concrete from the 16 horizontal holes in the river wall, river side, are presented below:

Test	Near Surface Concrete	Bottom of Core Specimens	Percentage Difference
Effective Unit Wt, pcf	151.7	151.8	-0.1
Comp Wave Velocity, fps	14,748	15,820	-6.8
Compressive Strength, psi	6,030	6,130	-1.6
Modulus of Elasticity, x 10^6 psi	4.34	5.05	-14.1
Poisson's Ratio	0.19	0.23	-17.4

The near surface concrete generally has higher physical properties than the bottom of core specimens, and the concrete near the top of the wall has slightly higher properties than that within the lower baffled portion of the wall. The test specimens representing the near surface concrete did not contain large amounts of the frost-damaged concrete. The strength of the same cores may not represent the actual strength of the damaged concrete, since cracks in the specimen perpendicular to the axis of applied load often times have little effect on the compressive strength.

119. Physical properties were determined for one specimen obtained from the near surface concrete of vertical boring L-54. The compressive strength of the specimen is indicative of sound concrete; however, no velocity or modulus of elasticity values are available to verify this supposition. Visual examination of the cores reveals generally unsound, deteriorated concrete within the ledge.

Upper Gate Sill

120. Two vertical borings were drilled into the concrete sill, which extends from monolith 10 to monolith 11, in order to investigate the condition of the foundation bedrock.

Depth of deterioration

121. The gate sill is not subjected to frequent freezing and thawing as are other structures within the lock; and consequently, no

frost damage was detected in the concrete taken from the sill. Alkali-silica gel was present on the construction joints and in voids on mechanical break surfaces.

Average physical properties

122. Test specimens were obtained from the near surface, middle, and bottom of core concrete of boring L-24. The physical properties of each specimen indicate that the concrete is sound throughout the depth of the sill.

Lower Gate Bay

Depth of deterioration

123. The average depth of deterioration in the vertical faces of the gate recesses is 0.1 ft, with a maximum of 0.3 ft. The two horizontal borings drilled into the gate recesses were below the resurfaced area, and therefore, no new concrete was encountered in the cores. Alkali-silica gel was noted on a vertically fractured surface at 2.4 ft of core L-8.

124. One vertical boring (L-1) was drilled into the lower gate bay block on the land wall side. Approximately 0.4 ft of new concrete with 1-in. maximum size coarse aggregate was encountered in the boring. Although the new concrete appeared undamaged, the underlying, non-air entrained concrete exhibited frost damage from 0.4 to 1.5 ft; this interval of concrete was damaged prior to placing the overlay. Longitudinal cracks were noted within the core at 12.4 to 13.7 ft, 15.5 to 19.1 ft, and 22.3 to 24.6 ft. No relative vertical displacement of one surface to the other had occurred; therefore, the cracks are probable results of local tensile failures; see Part III for detailed explanation on tensile failures. Light gray to light brown staining of the cracks indicate apparent infiltration of river water. The water may have migrated into the cracks via a vertical construction joint adjacent to the boring or through the cable gallery.

Average physical properties

125. The average physical properties of the concrete from the two horizontal holes in the lower gate bay are presented below:

Test	Near Surface Concrete	Bottom of Core Specimens	Percentage Difference
Effective Unit Wt, pcf	152.4	152.3	+0.1
Comp Wave Velocity, fps	15,095	14,404	+4.8
Compressive Strength, psi	6,740	5,310	+27.9
Modulus of Elasticity, x 10^6 psi	5.28	5.33	-0.9
Poisson's Ratio	0.27	0.20	+35.0

126. The near surface concrete generally has higher physical properties than the bottom of core specimens. However, the entire length of both cores exhibit sound concrete beyond the outer few inches.

127. The physical properties of the two specimens obtained from the top and middle portions of core L-1 are in close keeping with top and middle concrete average physical properties from other vertical borings at the lock. The bottom of core specimen from hole L-1 exhibits somewhat lower physical properties than the average bottom of core values from other vertical borings at the lock. The velocity of the specimen is only 5 percent lower than the average for bottom of core specimens; the compressive strength is 33 percent lower. The compressive strength for bottom of core specimen in L-1 is 4180 psi, which is the lowest value for strength obtained during the testing. Examination of the cylinder after testing showed no unusual break pattern, nor did the cylinder contain excessive voids or alkali-silica reaction products. The strength is accepted as a valid value.

Monolith 57

128. This component of the river wall is analyzed separately with respect to depth of deterioration and physical properties of the concrete in order to complement the crack and soniscope survey studies conducted on the monolith. The extent of frost damage, physical

properties of the concrete, and the crack and soniscope surveys investigation should be considered collectively in determining the degree and type of repairs required. The high stresses experienced by a monolith within the gate bay requires that immediate attention by given to repairing the damage.

Depth of deterioration

129. Five horizontal borings were drilled into the monolith. Frost damage was apparent in all except boring L-33. The average depth of deterioration is 0.8 ft, with the maximum depth being 2.1 ft in boring L-52. This boring was drilled into an exposed crack just above the emptying culvert. Alkali-silica gel was noted on the surface of the crack, which extended longitudinally to 2.19 ft, at which point the crack veered upstream. Borings L-31 and L-32 were drilled on the downstream vertical face of the monolith into an exposed vertical crack. The crack extended longitudinally from the free surface to 6.4 ft in boring L-31, and from the free surface to 9.3 ft in boring L-32. Alkali-silica gel was present on the crack surfaces in both cores. Borings L-33 and L-34 were drilled into the vertical face of the monolith on the river side of the wall.

130. One vertical boring (L-2) was drilled into monolith 57. Approximately 0.9 ft of new concrete, brown in color with 3/4-in. maximum size aggregate, was encountered in the boring. The underlying old concrete exhibited frost damage from 0.9 to 1.8 ft; the deterioration occurred prior to placing the overlay. A longitudinal crack was noted in the core from 1.8 to 7.3 ft. Alkali-silica gel was present on 10 percent of the crack surface and in void spaces within the concrete core. The reaction product was found on the core as deep as 47.6 ft, and the reaction itself may have caused the longitudinal crack. A diagonal heavy stained crack at about el 538 was correlated with the structural crack observed above the emptying culvert.

Average physical properties

131. The average physical properties of the concrete from the horizontal holes in monolith 57 are presented below:

Test	Near Surface Concrete	Bottom of Core Specimens	Percentage Difference
Effective Unit Wt, pcf	151.8	153.0	-2.0
Comp Wave Velocity, fps	--	15,972	--
Compressive Strength, psi	6,470	7,890	-18.0
Modulus of Elasticity, x 10^6 psi	--	5.56	--
Poisson's Ratio	--	0.28	--

132. The bottom of core physical properties are slightly higher than those of the near surface cores, apparently due to the adverse effects of freezing and thawing of concrete near the surface.

133. The physical properties of the near surface, middle, and bottom of core specimens obtained from boring L-2 are in close keeping with the average values. However, the near surface specimen from L-2 was taken below the areas of frost damage and longitudinal cracking. Therefore, the near surface compressive strength of 6240 psi is not necessarily representative of the strength of the concrete within the cracked and deteriorated regions. No samples could be obtained from the deteriorated zone just beneath the new concrete overlay due to the longitudinal crack.

Upper Approach Wall

Depth of deterioration

134. These horizontal borings were drilled into the upper approach wall. No new concrete was encountered in any of the borings. The average depth of frost damage within the concrete cores was 0.5 ft; the maximum depth was 1.1 ft in boring L-28. The concrete from this hole has undergone a high degree of weathering, resulting in fractured pieces throughout the first 0.9 ft. Alkali-silica gel deposits were present in air voids in each of the cores.

Average physical properties

135. The average physical properties of the upper approach wall concrete are presented below:

Test	Near Surface Concrete	Bottom of Core Specimens	Percentage Difference
Effective Unit Wt, pcf	150.8	156.7	-3.8
Comp Wave Velocity, fps	--	16,420	
Compressive Strength, psi	8,320	6,690	+24.4
Modulus of Elasticity, x 10^6 psi	--	5.56	
Poisson's Ratio	--	0.22	

The bottom of core concrete physical properties were determined from boring L-28. The values indicate that sound concrete exists beyond the deteriorated area. The average unit weight and compressive strength of the near surface specimens indicate that the concrete is probably sound beyond the damaged concrete of the vertical face of the upper approach wall.

Lower Approach Wall

Depth of deterioration

136. The average depth of frost-damaged concrete in the vertical face of the lower approach wall is 0.6 ft, with the maximum depth of 1.0 ft in boring L-30. A longitudinal crack starting at the free surface and extending through the entire length of core L-30 was noted. The frost-damaged area of the core was highly weathered and fractured. Alkali-silica gel was present on the longitudinal crack surface of the core, which suggests that the alkali-silica reaction was a possible crack mechanism. No apparent frost damage was detected in boring L-29 except a small degree of scaling at the surface.

137. A single vertical boring (L-26) drilled into the lower approach wall revealed no new concrete in the core. No perceptible frost damage has occurred in the concrete, although the presence of numerous voids, resulting from poor consolidation, may assist potential freezing and thawing.

Average physical properties

138. The deteriorated condition of boring L-30 prohibited obtaining specimens for physical properties tests. Borings L-29 and L-11 were

used in the detailed petrographic examination of the concrete within the lock, and consequently, no physical properties were determined for the concrete from the horizontal borings.

139. Physical properties were determined for one specimen obtained from the near surface concrete of the vertical boring. The compressive strength and modulus of elasticity are 85 and 93 percent, respectively, of those average properties determined from near surface specimens, while the Poisson's ratio of the specimen is 130 percent of the average value. Poor consolidation of the concrete may account for the lower compressive strength and higher deformation response of the specimen.

Instrumentation Monitoring Program

140. The following information is taken in part or directly from Reference 10:

141. The instrumentation monitoring program, limited to three lock monoliths for a period of 7 months, indicated that monolith 63 (downstream-most forebay monolith of the river wall) to be stable relative to monolith 57 to within 0.10 in. Monolith 63 underwent axial movement (upstream-downstream movement) of $\pm$0.10 in. with a residual displacement of +0.10 in.; this corresponds to a separation of joint opening of 0.10 in. Lateral movement was -0.10 in. toward the river side from the centerline of the lock chamber. A similar amount of shortening was recorded in the vertical direction. No significant movement was indicated by the four title meters.

142. Extensometers located across the cracks in the gallery in monolith 50, land lock wall, showed movement up to 0.04 in. in a horizontal plane. This movement shows the crack increasing in width. The extensometers were mounted perpendicular to the lock wall and monitored movement of the wedge of concrete (see Figure 12) toward the lock chamber.

PART VII: SUMMARY OF SIGNIFICANT CRACKS, FOUNDATION CONDITION, CONCRETE QUALITY, AND RECOMMENDED DESIGN VALUES

Significant Cracks

143. The crack above the emptying culvert in monolith 57 extends upward about 18 ft and exists over the full length of the culvert in the monolith. The crack in the downstream face of monolith exists from the top of the monolith to the top of the ledge; it is believed to extend below the ledge. It was traced 9 ft into the block. It is believed not to be connected to the crack on top of the emptying culvert. The crack on the back side of monolith 57 was not traced into the block; ultrasonic measurements could not be transmitted through the deteriorated concrete on the back of the block. This crack is connected to a borehole 23 ft away; it could be connected by horizontal construction joints and or cracks.

144. Cracks observed in monoliths 48, 50, and 52 (land wall) on the chamber face, in the cable gallery, and in boring L-1 are connected. In monoliths 48 and 50 a wedge exists with a low angle base that extends about 5 ft into the wall from the chamber side. In monolith 52 the wedge extends the same distance into the wall but with a base inclined at about 45°. Cracks similarly located are present in monoliths 51 and 53 but are not developed to the extent as those in monoliths 50 and 52.

145. Considering the available information, it was concluded that none of the structural cracks studied in monoliths 48, 50, and 52 and 51, 53, and 57 appear to pose any immediate problems. Consideration should be given to the use of adequately arranged post-tensioned tendons in monolith 57. It is suggested that the wedge-shaped concrete mass in monolith 52 be anchored down with tendons installed perpendicular to the base of the wedge; this should be carried out as soon as feasible. Continued freezing and thawing and alkali-silica reaction could worsen these cracks.

Bedrock Stratigraphy

146. Bedrock beneath Lockport Lock is Silurian in age and belongs to the Joliet Formation of the Niagaran Series. Each of the three members of the Joliet Formation is present: The Brandon Bridge, the Markgraf, and the Romeo. The top of the Brandon Bridge is identified by strong shaley partings. The three members consist of fine-grained, light gray to light tan dolomite. Clay- and shale-filled bedding planes and clay-filled fractures are found throughout the Joliet. The rock is highly to intensely fractured and contains many high-angle joints. The bedding is stylolitic in nature with a few well defined stylolites; asperity height is about 1/2 in.

Geologic Cross Section

147. Two cross sections were drawn; one along the lock land wall and one across the lock at the upper gate sill. Borings drilled in 1970 by CD were included in the cross sections. A tight contact (between concrete and bedrock) was noted in six of the eight vertical borings. These sections give an overview of the bedrock under the lock. The log of borings sheet (Plate 1) shows the 30-ft offset of the base of the Markgraf Member. The offset occurs about 200 ft downstream of the end of the land wall. The base of the Markgraf was identified in four of the eight borings drilled by WES (Plates 1 and 3). Clay- and shale-filled bedding planes are rarely more than 1/64-in. thick, with the thickest one about 1/8 in. in thickness. Many of the bedding planes are open and stained, indicating water flow. Chert bands are present in the bedrock, but they are not traceable across the foundation.

Bedrock Structural Characteristics

148. The bedding is essentially horizontal at the lock with only a minor regional dip, as indicated in Reference 2. The major structural feature in the bedrock is the stylolitic bedding. Although open bedding

planes were found, the stylolitic bedding is predominantly tight (cemented or healed) and has a relatively high resistance to shearing; bedding planes are essentially interlocked with relief averaging about 1/2 in. The stylolitic planes are not considered continuous under the lock because none could be so traced. The intermediate structural feature in the bedrock is the vertical jointing. Joints occur in two sets at nearly 90° to one another. The joints within the Joliet Formation trend N40-50°W and N50-60°E.[2] The joints are probably shear joints due to their smooth and straight nature. Small faults were detected with up to 1-in. displacement; displacement was nearly vertical. Slickensides were also found on a few vertical joint surfaces and on pieces of intensely fractured rock from beneath the upper gate sill. The minor structural features are treated collectively under "possible weak zones."

149. Evidence indicates the presence of a 30-ft upthrown block between the lower gate blocks and the midpoint of the lower approach wall. The strong shale partings at the base of the Markgraf member along an E-W line are at el 501.5, 509.7, and 517.0 ft. Borings on either side of this line show the strong shale partings at an elevation range of 483.0 to 490.0 ft. The relatively high incidence of cracking in the concrete of the gate monolith blocks and the possible movement of monolith 63 (end of ledge, river lock wall) could be associated with settlement or lateral movement of bedrock adjacent to an upthrown block. Additional drilling is recommended to verify the block's presence, and if present, its extent.

150. An intensely fractured zone (1- to 4-in. angular pieces of bedrock) exists under the upper gate sill. The zone is 18-ft deep at its center and about 50-ft long, as detected by drilling. The zone appears to be a shear zone associated with faulting. Borings in this area did not go deep enough to encounter the strong shale partings at the base of the Markgraf; therefore, it is not known if a fault exists in this area. The direction or extent of this zone was not defined by the borings at the lock. Extensive grouting in this zone may be required prior to installing an anchorage system. The fact that the bedrock contains many open bedding planes, fissures, joints, intensely fragmented

rock, and solution cavities indicates that grouting prior to the installation of anchors would be required at the lock site. Drilling for installation of anchors could assist in determining the extent of this scattered zone beneath the sill.

151. Ground water in the dolomite at the lock occurs in joints, fissures, fractures, solution cavities, and other openings. These openings are distributed both vertically and horizontally. The rate at which the upper porous dolomite is eroded by solution activity is not addressed in this report. Evidence of caving was indicated during the drilling operation. Just north of the lock on the west entrance road to the Chicago Sanitary District powerhouse, a cavity formed. A WES engineer observed the hole just after it was formed; it was about 18-ft deep with running water at the bottom. The water continued underground while washing away the material that had fallen in the hole. It is not known if the cavity developed in bedrock or fill for the canal embankment; the elevation of bedrock in the area where the cave-in occurred is not available. No solution cavities were encountered during the WES drilling; this is not to say cavities do not exist at the lock site. It is well documented in the literature that the Joliet Formation contains many clay-filled cavities.

152. Local possible weak zones in the bedrock beneath the lock include the intensely fractured zones found in the top of several borings, parallel vertical joints, clay- and shale-filled bedding planes (filled partings), the porous friable dolomite, stained solution channels, and the upthrown block (strongly indicated) at the downstream end of the lock. No one weak zone is continuous under the lock with the exception of the possible upthrown block.

153. After consideration of the available engineering and geological information and because there was not evidence of past horizontal movement along seams or bedding planes, it is believed that peak shearing resistances would control failure in the bedrock beneath the lock walls and land side lower approach wall. Peak shear values are recommended for use when making a stability analysis for these lock sections. This conclusion is in agreement with the conclusion presented in

Reference 2 concerning the bedrock feature likely to control failure in competent bedrock. Bedrock beneath the sill is intensely fractured. There were no direct shear tests run on concrete cast to fractured rock or precut concrete against fractured rock. It is suggested that a conservative design strength of c=0 and $\phi=26^{o}$ be used for the sill. The sill was found to be resting on intensely fractured rock. The $\phi=26^{o}$ was obtained from precut specimens of concrete and dolomite.

Concrete Quality

154. The back side of the river wall has numerous areas where chamber water is leaking out through the lock wall via construction joints. If waterstops were used during construction, it is now assumed that they are is in various stages of deterioration, thus allowing the leakage. No immediate problem is posed by this condition. Remedial measures to correct this condition could be taken during the upcoming major rehabilitation; i.e., a joint sealant could be injected in the construction joint or a waterstop could be installed to bridge the joints.

155. The new concrete along the top of the lock wall is in good condition. It is air entrained and has resisted the harsh winter environment on the river. However, the old underlying concrete is non-air entrained and exhibits frost damage, particularly in the lock chamber land wall. Because the new concrete appears to be providing an adequate cap over the old concrete, the frost damage probably occurred prior to the resurfacing operation. No major cracking was detected in the new concrete overlay atop the lock walls. This overlay covers about 1.2 ft of deteriorated concrete in the land wall. Should major cracking develop, then with the pentration of water, freezing and thawing would likely occur in the deteriorated zones causing additional cracking in the new overlay, especiaaly where the overlay is thin (0.02 ft, as observed in boring L-3).

156. If the lock walls are stabilized using prestressed tendons, then it is recommended that the frost-damaged concrete be removed before

installation of the bearing pads. Local removal of damaged concrete to 3-ft depths should be anticipated. Local honeycombing concrete would not be affected by the prestressing.

157. Some concern has been expressed about the effect of the concentrated loading from vertical tendons on vertical cracks in the concrete. If a significant structural crack is located where a tendon bearing pad is to be placed, an alternative location should be sought. The extent of the crack should be determined and appropriate measures taken for its repair. Any vertical cracks caused by alkali-silica reaction would generally be restricted to the outer 5 ft of concrete and are generally narrow (< 2 mm wide). If these cracks are detected where a pad is to be placed, they should be pressure grouted prior to placing the pad. The extent and orientation of the crack, the load exerted on the surrounding concrete, etc., would have to be known before a statement could be made concerning crack growth. It is believed that a short crack beneath moderate vertical loads applied by a tendon pad would not grow significantly. Constraining forces applied by the pad at and adjacent to the pad-concrete interface would somewhat restrain lateral movement of the concrete and hence, the crack. Of course if the tensile stress of the concrete at the tip of the crack exceeds the tensile strength of the concrete, then crack growth would occur. The average compressive strength of the concrete in the lock walls is 6000 psi plus; tensile strength should be about 10 percent of compressive strength, or a minimum of 600 psi. Narrow cracks outside the bearing pad area should be pressure grouted and watched for growth during application of the tendon load.

158. The exposed and near surface old concrete in the chamber side lock walls and gate recesses are lightly to moderately deteriorated. Freezing and thawing is the major cause of the damaged concrete. The near surface old concrete in the lock chamber river wall, river side, upper and lower approach walls, and monolith 57 is moderately to severely deteriorated. The damage in these structures is also primarily due to frost damage, although alkali-silica reaction is also a cause in some localized areas. The average depth of deterioration is as follows:

lock chamber land wall, 0.4 ft; lock chamber river wall, upstream of lower gate bay, 0.2 ft; lock chamber river wall, downstream of lower gate bay, 1.3 ft; lock chamber river wall, river side, 0.9 ft; lower gate bay recesses, 0.1 ft; monolith 57, 0.9 ft; upper approach wall, 0.5 ft; and the lower approach wall, 0.6 ft. Severe erosion of the concrete is evident at most monolith joints, particularly on the river side of the lock chamber river wall. The concrete portion of the ledge adjacent to the river wall is almost completely deteriorated, due to freezing and thawing, and should be replaced with quality air-entrained concrete.

159. The vertical faces of the lock chamber walls have a relatively shallow depth of deterioration when compared to other sections at the lock. The average depth of deteriorated concrete in the land wall is 0.4 ft and in the river wall it is 0.2 ft. Beyond the deteriorated zone the concrete is strong (6000 psi plus) and appears structurally adequate. It is believed that the chamber walls should not be resurfaced at this time. It does not appear that savings would be realized by resurfacing the chamber walls at this time rather than at some later date when the walls show a greater loss of concrete caused by increased deterioration.

160. It is suggested that 9 to 12 in. of concrete in the following sections be removed and replaced with air-entrained concrete:

a. Vertical and sloping walls, river side of river wall.

b. Upper and lower approach walls, the upper approach wall to the extent controlled by the US Government.

c. Downstream of the lower gate bays, including the ledge.

Local areas may require deeper removal.

161. The thickness of concrete required to bring the existing wall out to its original position is not addressed in this report.

162. Although alkali-silica gel is present throughout the lock structure, cracks resulting from the reaction are confined generally to the outer 5 ft except in monoliths 52 and 57. Since the serious alkali-silica reaction seems to be expressed most often in association with cracks normal to the free surfaces, it seems reasonable to assume that

the alkali-silica reation was encouraged when the exterior concrete began to crack up because of freezing and thawing, progressively letting water penetrate into the concrete. If the outer fragile concrete is repaired with air-entrained concrete, the potential for alkali-silica damage should be reduced, and the structure should be stable in terms of the anticipated behavior of the concrete. The rate at which the alkali-silica reaction is now taking place is not known. In addition, it is not known if the rate of reaction is increasing or decreasing. Work at the 43-year-old William Bacon Oliver Lock and Spillway near Tuscaloosa, Alabama, indicates that over a 20-year period concrete cracking due to alkali-silica reaction has stabilized. The cracking has stabilized even though the concrete still has the potential for expansion due to alkali-silica reaction.

Recommended Design Values for Rock

163. Design should consider rock type and the various bedrock structural characteristics described herein. Guidance is presented in the following tabulation as to proper choice of design parameters. Design values for lock backfill are presented in Plate 4 of Reference 2.

	Dolomite
Characterization Properties	
Effective Unit Weight, lb/ft^3	168.0
Dry Unit Weight, lb/ft^3 (from Reference 2)	164.3
Compressive Strength, psi	13,820
Direct Tensile Strength, psi	95.0
Shear Strength	
Concrete-on-rock	$c=18$ tsf, $\phi=67^o$
Cross bed, 45^o (from Reference 2)	$c=29$ tsf, $\phi=68^o$
Clay-filled parting (along stylolitic bedding)	$c=9.2$ tsf, $\phi=48^o$
Bedding plane (along stylolitic bedding)	$c=49$ tsf, $\phi=61.5^o$
Precut, rock-on-rock (from Reference 6)	$c=0$, $\phi_r=22^o$

Precut, ·rete-on-rock (from R ·ence 6)	c=0, ϕ_r=26°
Natural jo... smooth (from Reference 6)	c=12.4 tsf, ϕ=23.2°
Bond Strength, tsf	117.4
Modulus of Elasticity x 10^6 psi (from Reference 2)	8.94
Poisson's Ratio (from Reference 2)	0.28
Shear Modulus x 10^6 psi	3.49

Instrumentation Monitoring

164. The following conclusions can be drawn from the 7-month monitoring program at Lockport Lock; these conclusions are taken from Reference 10.

a. "At Lockport Lock extensometers 1, 2, and 3 show monolith 63 to be stable relative to monolith 57 to within 0.10 in. The long extensometers and temperature corrections required indicate that the precision of the measurement is not better than ±0.010 in.

b. The relative stability of monoliths 57 and 63 is also confirmed by the results from the tilt meters in which little tilting was indicated.

c. The east or land side lock wall measurements in the gallery showed the existing cracks to be widening by a maximum of 0.040 in. during this monitoring period."

165. The cause of movements of monolith 63 relative to monolith 57 is not postulated in Reference 10. However, boring information from L-25, which was drilled through monolith 63 and 50 ft in bedrock, indidates that the movement could be caused by poor foundation rock beneath at least a portion of monolith 63. Boring L-25 shows concrete founded in friable, vuggy (vugs to 1.5 in.), fossiliferous dolomite; portions of the core near the concrete-bedrock contact crumbled in the hand. Drill water circulation was lost for the full depth of L-25. The poor foundation rock observed could be associated with the formation of solution cavities or sinks. Numerous solution channels have been

observed in foundation cores and the formation of a sink in the canal embankment was observed by a WES engineer in 1978.

Recommendations

166. Additional drilling is recommended to verify if an upthrown fault block exists between the lower gate blocks and the midpoint of the lower approach wall. If a fault exists in this area, its extent should be traced, as it could possibly influence a structural stability analysis.

167. The following work is recommended for investigating the bedrock in the area of the upper gate sill. The planning and field work should be coordinated with NCD.

a. Ascertain the condition of bedrock beneath the sill including orientation and extent of the shear zone. This effort should include drilling and a reexaminatin of available core from borings near the sill for intensely fractured rock and the strong shale partings of the Brandon Bridge Member.

b. Drill at least two 6-in. core borings inclined 30° from the vertical on a bearing perpendicular to the strike of the joints ($N50^{\circ}$-$60^{\circ}E$). Conduct pressure tests on each 5-ft increment of bedrock as measured on the vertical segment of the inclined boring, then grout or case when necessary to maintain an open hole. If the hole remains open without grouting, use borehole photography. Drill borings to at least the Brandon Bridge Member and carry borings to competent rock.

c. Where rock anchors are considered, drill at least 10 ft below the maximum (proposed) depth of anchors. The condition of rock adjacent to the anchorage point could influence an anchorage design system.

d. Conduct dye tests between borings and between borings, lock, and river. In the event that dye tests are unsuccessful, then low level radioactive trace techniques could be considered.

e. Conduct crosshole seismic tests in an attempt to delineate the shear zone.

168. A study of air photographs of the lock and vicinity shows, and a review of Illinois geological literature of the Lockport Lock area

describes the presence of sinkholes and cavities. The literature describes some cavities as being clay-filled. The formation of sinks has occurred in the vicinity and adjacent to the Lockport Lock. The authors have been informed that at least two sinks formed near the lock in the past 10 or so years. One additional sink formed within the access road to the Sanitary District of Chicago Facility across the canal from the lock in 1978. The access road is atop the Chicago Sanitary and Ship Canal embankment. It's possible that sinkholes are developing in the bedrock beneath monolith 63 (river wall) and contributing to the measured movement of monolith 63. In view of this information, it is recommended that future studies be conducted at Lockport Lock in an attempt to detect the presences of solution cavities and underground caves.

169. A number of geophysical methods are available for conducting such a study. The following methods have been shown to be useful, and ongoing research at the WES in FY 80-81 will allow for the sensitivity of some of these methods to be better documented. The methods that could be used include crosshole and ground radar, gravity and microgravity, magnetic-induction survey, refraction seismic, crosshole seismic, and surface electric resistivity survey.

170. It is recommended that future studies address shear strength design values for concrete-bedrock interface when the bedrock is intensely fractured, as beneath the upper gate sill at Lockport. A review of available literature indicates that very little work has been done in this area. It is expected that shear strength values would be quite different for the concrete-bedrock interface, depending on the nature of the contact, i.e., bonded to or loose contact on intensely fractured rock.

REFERENCES

1. U. S. Army Engineer District, Chicago, subject, "Field Inspection of Existing Locks and Dam, Illinois Waterway," Memorandum for Record, NCCOD-PO, dated 3 Jun 1972.
2. U. S. Army Engineer District, Chicago, "Appendix A, Soils and Geology for Structural Stability Analysis, Lockport Lock, Illinois Waterway," Sep 1972, Revised Dec 1972.
3. U. S. Army Engineer District, Chicago, "Reconnaisance Report, Major Rehabilitation, Illinois Waterway, Lockport Lock and Appurtenant Structures, Preliminary," Jul 1977.
4. Willman, H., E. Atherton, et al, "Handbook of Illinois Stratigraphy," Bulletin 95, Illinois State Geological Survey, Urbana.
5. M. L. Sargent, Illinois Geological Survey, private communication.
6. Stowe, R. L., "Concrete and Rock Tests, Rehabilitation Work, Brandon Road Dam, Illinois Waterway, Chicago District," Miscellaneous Paper C-78-4, May 1978, U. S. Army Engineer Waterways Experiment Station, CE, Vicksburg, Miss.
7. U. S. Army Engineer District, Chicago, "Appendix F, Geology and Soils Report, Duplicate Locks, Illinois Waterway, Illinois and Indiana, General Design Memorandum, Phase I, Plan Formulation and Site Selection," Apr 1975.
8. ACI Committee 201, "Guide for Making a Condition Survey of Concrete in Service," Journal, American Concrete Institute, Proceedings, Vol 65, pp 905-918, Nov 1968; also in "ACI Manual of Concrete Practice," Vol I.
9. U. S. Army Engineer Waterways Experiment Station, CE, "Handbook for Concrete and Cement," with quarterly supplements, Vicksburg, Miss., Aug 1949.
10. Glass, D., and B. R. Sullivan, "Monitoring Deflection at Lockport and at Brandon Road Locks, Chicago District," WES Miscellaneous Paper, in press.
11. Stowe, R. L., B. A. Pavlov, and G. S. Wong, "Concrete and Rock Core Tests, Major Rehabilitation of Starved Rock Lock and Dam, Illinois Waterway, Chicago District, Phase I, Rehabilitation," Miscellaneous Paper C-78-12, Sep 1978, U. S. Army Engineer Waterways Experiment Station, CE, Vicksburg, Miss.
12. Woodruff, Seth D., Methods of Working Coal and Metal Mines, Vol 3, Pergamon Press, NY, 1966, p 504.

Table 1

Types, Location, Elevation, and Starting Dates of Borings

Boring No.	Type of Boring	Location	El Top Boring, ft	El Top Rock, ft	El Bottom Boring, ft	Start Date
SACLP-1	4-in. core	Backfill, lock	584.9	546.3	493.0	20 Aug 1970
SACLP-2	4-in. core	Backfill, lock	584.3	542.9	495.2	29 Aug 1970
SACLP-3	4-in. core	W of river wall	521.5	518.5	493.6	14 Aug 1970
SACLP-4	4-in. core	N of river wall	560.0	543.2	518.0	15 Aug 1970
CLP 500	4-in. core	Backfill	584.3	544.9	501 (?)	13 Dec 1966
CLP 502	4-in. core	5 ft rt of baseline	540.8	540.8	460.1	8 Sep 1967
CLP 503	4-in. core	77 ft rt of baseline	548.2	543.6	483.8	16 Dec 1966
CLP 504	4-in. core	40 ft rt of baseline	539.4	539.4	479.5	27 Jul 1967
CLP 505	4-in. core	114 ft L of baseline	552.8	542.0	481.3	2 Aug 1967
CLP 506	4-in. core	72 ft L of baseline	541.7	541.7	479.9	17 Jul 1967
CLP 507	4-in. core	60 ft L of baseline	540.4	540.4	480.1	24 Jul 1967
COP 508	4-in. core	65 ft L of baseline	541.5	541.5	480.6	8 Mar 1967
CLP 509	4-in. core	62 ft L of baseline	542.1	542.1	480.6	23 Jan 1967
CLP 510	NX core	NE of lock	553.3	547.5	472.0	8 Nov 1969
CLP 511	NX core	NE of lock	553.3	547.4	478.4	14 Nov 1969
CLP 512	NX core	NE of lock	553.2	547.5	474.0	28 Oct 1969
CLP 514	--	NE of lock	556.2	550.7	480.2	7 Jan 1970
CLP 515	--	NE of lock	556.2	550.7	505.2	7 Jan 1970
CLP 516	--	NE of lock	556.5	551.5	512.5	15 Jan 1970
CLP 517	--	NE of lock	557.0	551.0	507.0	22 Jan 1970
CLP 518	--	NE of lock	555.7	552.2	505.7	23 Jan 1970
CLP 519	--	NE of lock	555.7	554.2	512.7	2 Feb 1970
CLP 520	NX core	NE of lock	555.8	555.3	480.8	28 Jan 1970
CLP 530	--	S of lock	--	--	--	--
CLP 531	NX core	270 ft rt of baseline	546.4	515.4	504.2	10 Feb 1970
CLP 532	4-in. core	280 ft rt of baseline	549.0	544.4	524.0	9 Feb 1970
CLP 533	280 ft rt of baseline		550.2	546.4	524.3	6 Feb 1970

(Continued)

Table 1 (Concluded)

Boring No.	Type of Boring	Location	El Top Boring, ft	El Top Rock, ft	El Bottom Boring, ft	Start Date
CLP 600	4-in. core	55 ft rt of baseline	552.1	547.1	513.4	3 Feb 1971
CLP 602-N	NX core	10 ft rt of baseline	552.0	524.3	476.2	22 Jan 1971
CLP 602-W	NX core	210 ft rt of baseline	552.0	536.8	522.3	28 Jan 1971
CLP 603	4-in. core	5 ft rt of baseline	551.1	539.7	493.9	21 Nov 1970
CLP 604	4-in. core	180 ft L of baseline	553.3	542.9	434.6	16 Nov 1970
CLP 605	4-in. core	60 ft rt of baseline	554.5	548.7	495.4	29 Jan 1971
CLP 700	--	N of 9th st locksite	560.0	552.3	420.2	17 Mar 1973
CLP 701	--	N of 9th st locksite	573.1	563.0	447.0	10 Mar 1973
CLP 702	--	N of 9th st locksite	566.9	562.0	442.0	28 Feb 1973
CLP 704	--	N of 9th st locksite	568.0	563.3	436.9	1973
L WES L1-78	6-in. core	Land lock wall	585	517.3	485.8	6 Feb 1978
L WES L2-78	6-in. core	River lock wall	585	--	537.4	10 Feb 1978
L WES L 25-78	6-in. core	River wall, D/S end	547	520.9	471.3	22 Mar 1978
L WES L3-78	6-in. core	Land lock wall	585	518.5	486.5	20 Feb 1978
L WES L 13-78	6-in. core	River lock wall	585	518.2	488.4	10 Feb 1978
L WES L 23-78	6-in. core	Upper gate sill	558	530.0	521.9	7 Mar 1978
L WES L 24-78	6-in. core	Upper gate sill	558	529.8	491.9	23 Mar 1978
L WES L 26-78	6-in. core	Lower approach wall	547	540.3	511.7	30 Mar 1978
L WES L 38-78	6-in. core	River lock wall	585	520.0	511.3	22 Apr 1978

Table 2

River Wall Velocities

Monoliths No. 17-49

Monolith No.	Data Point	Velocity, fps	Signal Strength	Monolith No.	Data Point	Velocity, fps	Signal Strength
17	1	NR*	--	33	1	Blocked by drill rig	
	2	13,750	Good		2	NR	--
19	1	12,515	Weak	35	1	Manhole	
	2	12,165	"		2	NR	--
21	1	11,905	"			13,965	Weak
	2	10,930	"			13,795	"
23	1	12,065	"	37	1	14,430	Good
	2	10,050	"		2	15,040	"
		13,105	"	39	1	NR	--
		11,615	"		2	NR	--
25	1	NR	--	41	1	NR	--
	2	10,255	Weak		2	9,345	Weak
27	1	10,005	"	43	1	11,835	"
	2	11,300	"		2	11,670	"
29	1	14,620	Good	45	1	13,210	Good
	2	13,570	"		2	10,005	Weak
31	1	14,685	"			13,245	"
	2	11,535	Weak			15,040	Good
				47	1	11,260	Weak
					2	13,175	"
				49	1	11,790	"
					2	NR	--

* NR denotes that no reading could be obtained through the wall at this data point.

Table 3

River Wall Velocities

Monolith No. 57

Depth, ft	Velocities, fps							
	Data Point No. 1	Signal Strength	Data Point No. 2	Signal Strength	Data Point No. 3	Signal Strength	Data Point No. 4	Signal Strength
3	11,675	Weak	8,100	Weak	10,260	Weak	Inaccessible	
8	12,710	Good	11,450	"	10,500	"	7,160	Weak
13	13,825	"	11,140	"	11,125	"	6,965	"
18	13,955	"	12,525	"	13,505	Good	8,230	"
23	14,085	"	13,020	Good	13,740	"	7,570	"
28	13,955	"	13,385	"	13,620	"	9,860	"
33	10,715	Weak	13,950	"	14,045	"	13,460	"
38	11,630	"	13,890	"	13,505	Weak	13,205	Good

Table 4

Land Wall Velocities

Monolith No. 52

Borehole to Chamber Wall			
Borehole Depth, ft	Wall Depth, ft	Path Length, ft	Velocity, fps
10.5	10.5	15.0	10,380
12.0	10.5	15.1	9,025
14.0	10.5	15.4	NR*
14.3	14.3	15.0	13,635
12.0	14.3	15.2	13,615
10.0	14.3	15.6	13,805
8.0	14.3	16.3	12,910
16.0	14.3	15.1	13,605

Borehole to Gate Recess			
Borehole Depth, ft	Wall Depth, ft	Path Length, ft	Velocity, fps
12.0	7.5	17.6	10,530
15.0	7.5	18.6	9,885
12.0	12.0	17.0	14,845
11.0	12.0	17.0	14,875
10.0	12.0	17.1	14,885
9.0	12.0	17.3	14,755
15.0	12.0	17.3	14,385

Gallery to Gate Recess			
From Point in	Distance from Top of Wall, ft	Path Length, ft	Velocity, fps
Gallery to:	4.0	12.4	7,090
	7.0	12.6	6,025
	10.0	13.6	7,235
	13.0	15.0	12,845
	15.0	16.2	13,890

* NR denotes that no reading could be obtained through the concrete at this location.

Table 5

WES Core from Lockport Lock, Illinois Waterway, Chicago District

WES Reference	Drill Hole #	Date Rec'd	Core Diam, in.	Bag/Box No.	Depth, ft	Elevation, ft Depth Intervals	Elevation, ft Top of Hole	Remarks
CHI-14 CON-1(A)	L-WES-L1-78	3-8-78	6	1 of 24	0.0-4.6	585.0-580.4	585.0	Concrete
CHI-14 CON-1(B)	L-WES-L1-78	3-8-78	6	2 of 24	4.6-9.5	580.4-575.5	585.0	Concrete
CHI-14 CON-1(C)	L-WES-L1-78	3-8-78	6	3 of 24	9.5-13.6	575.5-571.4	585.0	Concrete
CHI-14 CON-1(D)	L-WES-L1-78	3-8-78	6	4 of 24	13.6-17.9	571.4-567.1	585.0	Concrete
CHI-14 CON-1(E)	L-WES-L1-78	3-8-78	6	5 of 24	17.9-19.5	567.1-565.5	585.0	Concrete
CHI-14 CON-1(F)	L-WES-L1-78	3-8-78	6	6 of 24	19.5-24.3	565.5-560.7	585.0	Concrete
CHI-14 CON-1(G)	L-WES-L1-78	3-8-78	6	7 of 24	24.3-29.3	560.7-555.7	585.0	Concrete
CHI-14 CON-1(H)	L-WES-L1-78	3-8-78	6	8 of 24	29.3-33.1	555.7-551.9	585.0	Concrete
CHI-14 CON-1(I)	L-WES-L1-78	3-8-78	6	9 of 24	3.1-37.4	551.9-547.6	585.0	Concrete
CHI-14 CON-1(J)	L-WES-L1-78	3-8-78	6	10 of 24	37.4-41.8	547.6-543.2	585.0	Concrete
CHI-14 CON-L(K)	L-WES-L1-78	3-8-78	6	11 of 24	41.8-41.6	543.2-538.9	585.0	Concrete
CHI-14 CON-L(L)	L-WES-L1-78	3-8-78	6	12 of 24	46.1-50.6	538.9-534.4	585.0	Concrete
CHI-14 CON-L(M)	L-WES-L1-78	3-8-78	6	13 of 24	50.6-55.6	534.4-529.4	585.0	Concrete
CHI-14 CON-1(N)	L-WES-L1-78	3-8-78	6	14 of 24	55.6-60.2	529.4-524.8	585.0	Concrete
CHI-14 CON-1(O)	L-WES-L1-78	3-8-78	6	15 of 24	60.2-64.2	529.4-524.8	585.0	Concrete
CHI-14 CON-1(P)	L-WES-L1-78	3-8-78	6	16 of 24	64.2-68.4	524.8-520.8	585.0	Concrete, Dolomite
CHI-14 DC-1(A)	L-WES-L1-78	3-8-78	6	17 of 24	68.4-72.7	520.8-516.6	585.0	Concrete
CHI-14 DC-1(B)	L-WES-L1-78	3-8-78	6	18 of 24	72.7-77.1	512.3-507.9	585.0	Dolomite
CHI-14 DC-1(C)	L-WES-L1-78	3-8-78	6	19 of 24	77.1-81.15	507.9-503.85	585.0	Dolomite
CHI-14 DC-1(D)	L-WES-L1-78	3-8-78	6	20 of 24	81.15-85.7	503.85-499.3	585.0	Dolomite
CHI-14 DC-1(E)	L-WES-L1-78	3-8-78	6	21 of 24	85.7-87.7	499.3-497.3	585.0	Dolomite
CHI-14 DC-1(F)	L-WES-L1-78	3-8-78	6	22 of 24	87.7-91.8	497.3-493.2	585.0	Dolomite
CHI-14 DC-1(G)	L-WES-L1-78	3-8-78	6	23 of 24	91.8-95.4	493.2-489.6	585.0	Dolomite
CHI-14 DC-1(H)	L-WES-L1-78	3-8-78	6	24 of 24	95.4-99.2	489.6-485.8	585.0	Dolomite
CHI-14 CON-2(A)	L-WES-L2-78	3-8-78	6	1 of 12	0.0-4.1	585.0-580.9	585.0	Concrete
CHI-14 CON-2(B)	L-WES-L2-78	3-8-78	6	2 of 12	4.1-8.3	580.9-576.7	585.0	Concrete

(Continued)

Table 5 (Continued)

WES Reference	Drill Hole #	Date Rec'd	Core Diam, in.	Bag/Box No.	Depth, ft	Elevation, ft Depth Intervals	Top of Hole	Remarks
CHI-14 CON-2(C)	L-WES-L2-78	3-8-78	6	3 of 12	8.3-11.2	576.7-573.8	585.0	Concrete
CHI-14 CON-2(D)	L-WES-L2-78	3-8-78	6	4 of 12	11.2-15.7	573.8-569.3	585.0	Concrete
CHI-14 CON-2(E)	L-WES-L2-78	3-8-78	6	5 of 12	15.7-20.3	569.3-564.7	585.0	Concrete
CHI-14 CON-2(F)	L-WES-L2-78	3-8-78	6	6 of 12	20.3-23.55	564.7-561.45	585.0	Concrete
CHI-14 CON-2(G)	L-WES-L2-78	3-8-78	6	7 of 12	23.55-28.0	561.45-557.0	585.0	Concrete
CHI-14 CON-2(H)	L-WES-L2-78	3-8-78	6	8 of 12	28.0-32.0	557.0-553.0	585.0	Concrete
CHI-14 CON-2(I)	L-WES-L2-78	3-8-78	6	9 of 12	32.0-35.8	553.0-549.2	585.0	Concrete
CHI-14 CON-2(J)	L-WES-L2-78	3-8-78	6	10 0f 12	35.8-40.15	549.2-544.85	585.0	Concrete
CHI-14 CON-2(K)	L-WES-L2-78	3-8-78	6	11 of 12	40.15-44.65	544.85-540.35	585.0	Concrete
CHI-14 CON-2(L)	L-WES-L2-78	3-8-78	6	12 of 12	44.65-47.76	540.35-537.35	585.0	Concrete
CHI-14 CON-3(A)	L-WES-L3-78	3-8-78	6	1 of 23	0.0-5.15	585.0-579.85	585.0	Concrete
CHI-14 CON-3(B)	L-WES-L3-78	3-8-78	6	2 of 23	5.15-10.1	579.85-574.9	585.0	Concrete
CHI-14 CON-3(C)	L-WES-L3-78	3-8-78	6	3 of 23	10.1-14.55	574.9-570.45	585.0	Concrete
CHI-14 CON-3(D)	L-WES-L3-78	3-8-78	6	4 of 23	14.55-19.3	570.45-565.7	585.0	Concrete
CHI-14 CON-3(E)	L-WES-L3-78	3-8-78	6	5 of 23	19.3-24.0	565.7-561.0	585.0	Concrete
CHI-14 CON-3(F)	L-WES-L3-78	3-8-78	6	6 of 23	24.0-29.0	561.0-556.0	585.0	Concrete
CHI-14 CON-3(G)	L-WES-L3-78	3-8-78	6	7 of 23	29.0-32.65	556.0-552.35	585.0	Concrete
CHI-14 CON-3(H)	L-WES-L3-78	3-8-78	6	8 of 23	32.65-36.35	552.35-548.65	585.0	Concrete
CHI-14 CON-3(I)	L-WES-L3-78	3-8-78	6	9 of 23	36.35-40.25	548.65-544.75	585.0	Concrete
CHI-14 CON-3(J)	L-WES-L3-78	3-8-78	6	10 of 23	40.25-44.6	544.75-540.4	585.0	Concrete
CHI-14 CON-3(K)	L-WES-L3-78	3-8-78	6	11 of 23	44.6-49.5	540.4-535.5	585.0	Concrete
CHI-14 CON-3(L)	L-WES-L3-78	3-8-78	6	12 of 23	49.5-53.8	535.5-531.2	585.0	Concrete
CHI-14 CON-3(M)	L-WES-L3-78	3-8-78	6	13 of 23	53.8-58.1	531.2-526.9	585.0	Concrete
CHI-14 CON-3(N)	L-WES-L3-78	3-8-78	6	14 of 23	58.1-62.2	526.9-522.8	585.0	Concrete
CHI-14 CON-3(O)	L-WES-L3-78	3-8-78	6	15 of 23	62.2-66.55	522.8-518.45	585.0	Concrete
CHI-14 DC-3(A)	L-WES-L3-78	3-8-78	6	16 of 23	66.55-69.3	518.45-515.7	585.0	Dolomite
CHI-14 DC-3(B)	L-WES-L3-78	3-8-78	6	17 of 23	69.3-73.45	515.7-511.55	585.0	Dolomite
CHI-14 DC-3(C)	L-WES-L3-78	3-8-78	6	18 of 23	73.45-77.8	511.55-507.2	585.0	Dolomite

(Continued)

Table 5 (Continued)

WES Reference	Drill Hole	Date Rec'd	Core Diam, in.	Bag/Box No.	Depth, ft	Elevation, ft Depth Intervals	Top of Hole		Remarks
CHI-14 DC-3(D)	L-WES-L3-78	3-8-78	6	19 of 23	77.8-82.3	507.2-502.7	585.0	Dolomite	
CHI-14 DC-3(E)	L-WES-L3-78	3-8-78	6	20 of 23	82.3-86.75	502.7-498.25	585.0	Dolomite	
CHI-14 DC-3(F)	L-WES-L3-78	3-8-78	6	21 of 23	86.75-90.2	498.25-494.8	585.0	Dolomite	
CHI-14 DC-3(G)	L-WES-L3-78	3-8-78	6	22 of 23	90.2-94.4	494.8-490.6	585.0	Dolomite	
CHI-14 DC-3(H)	L-WES-L3-78	3-8-78	6	23 of 23	94.4-98.45	490.6-486.55	585.0	Dolomite	
CHI-14 CON-4	L-WES-L4-78	3-8-78	6	1 of 1	0.0-3.1	574.2	574.2	Concrete	
CHI-14 CON-5	L-WES-L5-78	3-8-78	6	1 of 1	0.0-3.1	574.2	574.2	Concrete	
CHI-14 CON-6	L-WES-L6-78	3-8-78	6	1 of 1	0.0-3.0	573.2	573.2	Concrete	
CHI-14 CON-7	L-WES-L7-78	3-8-78	6	1 of 1	0.0-3.0	541.0	541.0	Concrete	
CHI-14 CON-8	L-WES-L8-78	3-8-78	6	1 of 1	0.0-3.45	561.2	561.2	Concrete	
CHI-14 CON-9	L-WES-L9-78	3-8-78	6	1 of 1	0.0-3.2	537.0	537.0	Concrete	
CHI-14 CON-10	L-WES-L10-78	3-8-78	6	1 of 1	0.0-3.2	537.0	537.0	Concrete	
CHI-14 CON-11	L-WES-L11-78	3-8-78	6	1 of 1	0.0-3.1	544.0	544.0	Concrete	
CHI-14 CON-12	L-WES-L12-78	3-8-78	6	1 of 1	0.0-3.45	576.2	576.2	Concrete	
CHI-14 CON-13(A)	L-WES-L13-78	4-24-78	6	1 of 24	0.0-4.1	585.0-580.9	585.0	Concrete	
CHI-14 CON-13(B)	L-WES-L13-78	4-24-78	6	2 of 24	4.1-8.4	580.9-576.6	585.0	Concrete	
CHI-14 CON-13(C)	L-WES-L13-78	4-24-78	6	3 of 24	8.4-12.4	576.6-572.6	585.0	Concrete	
CHI-14 CON-13(D)	L-WES-L13-78	4-24-78	6	4 of 24	12.4-16.7	572.6-568.3	585.0	Concrete	
CHI-14 CON-13(E)	L-WES-L13-78	4-24-78	6	5 of 24	16.7-21.55	568.3-563.45	585.0	Concrete	
CHI-14 CON-13(F)	L-WES-L13-78	4-24-78	6	6 of 24	21.55-26.2	563.45-558.8	585.0	Concrete	
CHI-14 CON-13(G)	L-WES-L13-78	4-24-78	6	7 of 24	26.2-29.85	558.8-555.15	585.0	Concrete	
CHI-14 CON-13(H)	L-WES-L13-78	4-24-78	6	8 of 24	29.85-31.1	555.15-553.9	585.0	Concrete	
CHI-14 CON-13(I)	L-WES-L13-78	4-24-78	6	9 of 24	31.1-35.45	553.9-549.55	585.0	Concrete	
CHI-14 CON-13(J)	L-WES-L13-78	4-24-78	6	10 of 24	35.45-40.15	549.55-544.85	585.0	Concrete	
CHI-14 CON-13(K)	L-WES-L13-78	4-24-78	6	11 of 24	40.15-44.7	544.85-540.3	585.0	Concrete	
CHI-14 CON-13(L)	L-WES-L13-78	4-24-78	6	12 of 24	44.7-49.35	540.3-535.65	585.0	Concrete	
CHI-14 CON-13(M)	L-WES-L13-78	4-24-78	6	13 of 24	49.35-54.25	535.65-530.75	585.0	Concrete	
CHI-14 CON-13(N)	L-WES-L13-78	4-24-78	6	14 of 24	54.25-58.32	530.75-526.68	585.0	Concrete	

(Continued)

Table 5 (Continued)

WES Reference	Drill Hole	Date Rec'd	Core Diam, in.	Bag/Box No.	Depth, ft	Elevation, ft Depth Intervals	Top of Hole		Remarks
CHI-14 CON-13(O)	L-WES-L13-78	4-24-78	6	15 of 24	58.32-62.75	526.68-522.25	585.0	Concrete	
CHI-14 CON-13(P)	L-WES-L13-78	4-24-78	6	16 of 24	62.75-66.8	522.25-518.2	585.0	Concrete	
CHI-14 CON-13(A)	L-WES-L13-78	4-24-78	6	17 of 24	66.8-70.6	518.2-514.4	585.0	Concrete	
CHI-14 CON-13(B)	L-WES-L13-78	4-24-78	6	18 of 24	70.6-73.75	514.4-511.25	585.0	Concrete	
CHI-14 CON-13(C)	L-WES-L13-78	4-24-78	6	19 of 24	73.75-77.95	511.25-507.05	585.0	Concrete	
CHI-14 CON-13(D)	L-WES-L13-78	4-24-78	6	20 of 24	77.95-82.15	507.05-502.85	585.0	Concrete	
CHI-14 CON-13(E)	L-WES-L13-78	4-24-78	6	21 of 24	82.15-86.2	502.85-489.8	585.0	Concrete	
CHI-14 CON-13(F)	L-WES-L13-78	4-24-78	6	22 of 24	86.2-89.8	498.8-495.2	585.0	Concrete	
CHI-14 CON-13(G)	L-WES-L13-78	4-24-78	6	23 of 24	89.8-93.85	495.2-491.15	585.0	Concrete	
CHI-14 DC-13(H)	L-WES-L13-78	4-24-78	6	24 of 24	93.85-96.6	491.15-488.4	585.0	Dolomite	
CHI-14 CON-14	L-WES-L14-78	3-8-78	6	1 of 1	0.0-3.0	573.2	573.2	Concrete	
CHI-14 CON-15	L-WES-L15-78	3-8-78	6	1 of 1	0.0-3.2	565.0	565.0	Concrete	
CHI-14 CON-16	L-WES-L16-78	3-8-78	6	1 of 1	0.0-3.5	571.2	571.2	Concrete	
CHI-14 CON-17	L-WES-L17-78	4-24-78	6	1 of 1	0.0-2.95	555.0	555.0	Concrete	
CHI-14 CON-18	L-WES-L18-78	4-24-78	6	1 of 1	0.0-3.05	573.2	573.2	Concrete	
CHI-14 CON-19	L-WES-L19-78	4-24-78	6	1 of 1	0.0-3.4	573.2	573.2	Concrete	
CHI-14 CON-20	L-WES-L20-78	4-24-78	6	1 of 1	0.0-3.25	571.2	571.2	Concrete	
CHI-14 CON-21(A)	L-WES-L21-78	4-24-78	6	1 of 2	0.0-2.6	573.2	573.2	Concrete	
CHI-14 CON-21(B)	L-WES-L21-78	4-24-78	6	1 of 2	2.6-4.6	573.2	573.2	Concrete	
CHI-14 CON-22	L-WES-L22-78	4-24-78	6	1 of 1	0.0-3.45	539.0	539.0	Concrete	
CHI-14 CON-23(A)	L-WES-L23-78	4-24-78	6	1 of 11	0.0-3.0	558.0-555.0	558.0	Concrete	
CHI-14 CON-23(B)	L-WES-L23-78	4-24-78	6	2 of 11	3.0-5.5	555.0-552.5	558.0	Concrete	
CHI-14 CON-23(C)	L-WES-L23-78	4-24-78	6	3 of 11	5.5-8.6	552.5-549.4	558.0	Concrete	
CHI-14 CON-23(D)	L-WES-L23-78	4-24-78	6	4 of 11	8.6-13.0	549.4-545.0	558.0	Concrete	
CHI-14 CON-23(E)	L-WES-L23-78	4-24-78	6	5 of 11	13.0-17.37	545.0-540.63	558.0	Concrete	
CHI-14 CON-23(F)	L-WES-L23-78	4-24-78	6	6 of 11	17.37-22.35	540.63-535.65	558.0	Concrete	
CHI-14 CON-23(G)	L-WES-L23-78	4-24-78	6	7 of 11	22.35-25.3	535.65-532.7	558.0	Concrete	
CHI-14 CON-23(H)	L-WES-L23-78	4-24-78	6	8 of 11	25.3-28.12	532.7-529.88	558.0	Concrete	

(Continued)

Table 5 (Continued)

WES Reference	Drill Hole	Date Rec'd	Core Diam, in.	Bag/Box No.	Depth, ft	Elevation, ft Depth Intervals	Top of Hole		Remarks
CHI-14 DC-23(A)	L-WES-L23-78	4-24-78	6	9 of 11	28.12-32.0	529.88-526.0	558.0	Dolomite	
CHI-14 DC-23(B)	L-WES-L23-78	4-24-78	6	10 of 11	32.0-35.0	526.0-523.0	558.0	Dolomite	
CHI-14 DC-23(C)	L-WES-L23-78	4-24-78	6	11 of 11	35.0-36.15	523.0-521.85	558.0	Dolomite	
CHI-14 CON-24(A)	L-WES-L24-78	4-24-78	6	1 of 18	0.0-4.1	558.0-553.9	558.0	Concrete	
CHI-14 CON-24(B)	L-WES-L24-78	4-24-78	6	2 of 18	4.1-6.7	553.9-551.3	558.0	Concrete	
CHI-14 CON-24(C)	L-WES-L24-78	4-24-78	6	3 of 18	6.7-10.1	551.3-547.9	558.0	Concrete	
CHI-14 CON-24(D)	L-WES-L24-78	4-24-78	6	4 of 18	10.1-14.35	547.9-543.65	558.0	Concrete	
CHI-14 CON-24(E)	L-WES-L24-78	4-24-78	6	5 of 18	14.35-17.8	543.65-540.2	558.0	Concrete	
CHI-14 CON-24(F)	L-WES-L24-78	4-24-78	6	6 of 18	17.8-21.85	540.2-536.15	558.0	Concrete	
CHI-14 CON-24(G)	L-WES-L24-78	4-24-78	6	7 of 18	21.85-25.6	536.15-532.4	558.0	Concrete	
CHI-14 CON-24(H)	L-WES-L24-78	4-24-78	6	8 of 18	25.6-28.2	532.4-529.8	558.0	Concrete	
CHI-14 CON-24(A)	L-WES-L24-78	4-24-78	6	9 of 18	28.2-34.15	529.8-523.85	558.0	Concrete	
CHI-14 CON-24(B)	L-WES-L24-78	4-24-78	6	10 of 18	34.15-38.5	523.85-519.5	558.0	Concrete	
CHI-14 CON-24(C)	L-WES-L24-78	4-24-78	6	11 of 18	38.5-41.2	519.5-516.8	558.0	Concrete	
CHI-14 CON-24(D)	L-WES-L24-78	4-24-78	6	12 of 18	41.2-46.1	516.8-511.9	558.0	Concrete	
CHI-14 CON-24(E)	L-WES-L24-78	4-24-78	6	13 of 18	46.1-49.25	511.9-508.75	558.0	Concrete	
CHI-14 CON-24(F)	L-WES-L24-78	4-24-78	6	14 of 18	49.25-53.35	508.75-504.65	558.0	Concrete	
CHI-14 CON-24(G)	L-WES-L24-78	4-24-78	6	15 of 18	53.35-56.0	504.65-502.0	558.0	Concrete	
CHI-14 CON-24(H)	L-WES-L24-78	4-24-78	6	16 of 18	56.0-60.0	502.0-498.0	558.0	Concrete	
CHI-14 CON 24(I)	L-WES-L24-78	4-24-78	6	17 of 18	60.0-63.65	489.0-494.35	558.0	Concrete	
CHI-14 CON-24(J)	L-WES-L24-78	4-24-78	6	18 of 18	63.65-66.15	494.35-491.85	558.0	Concrete	
CHI-14 CON-25(A)	L-WES-L25-78	4-24-78	6	1 of 19	0.0-4.1	547.0-542.9	547.0	Concrete	
CHI-14 CON-25(B)	L-WES-L25-78	4-24-78	6	2 of 19	4.1-8.8	542.9-538.2	547.0	Concrete	
CHI-14 CON-25(C)	L-WES-L25-78	4-24-78	6	3 of 19	8.8-13.65	538.2-533.35	547.0	Concrete	
CHI-14 CON-25(D)	L-WES-L25-78	4-24-78	6	4 of 19	13.65-18.5	533.35-528.5	547.0	Concrete	
CHI-14 CON-25(E)	L-WES-L25-78	4-24-78	6	5 of 19	18.5-23.3	528.5-523.7	547.0	Concrete	
CHI-14 CON-25(F)	L-WES-L25-78	4-24-78	6	6 of 19	23.3-28.3	523.7-518.7	547.0	Concrete	

(Continued)

Table 5 (Continued)

WES Reference	Drill Hole	Date Rec'd	Core Diam, in.	Bag/Box No.	Depth, ft	Elevation, ft Depth Intervals	Elevation, ft Top of Hole	Remarks
CHI-14 DC-25(A)	L-WES-L25-78	4-24-78	6	7 of 19	28.3-31.1	518.7-515.9	547.0	Dolomite
CHI-14 DC-25(B)	L-WES-L25-78	4-24-78	6	8 of 19	31.1-34.8	515.9-512.2	547.0	Dolomite
CHI-14 DC-25(C)	L-WES-L25-78	4-24-78	6	9 of 19	34.8-38.7	512.2-508.3	547.0	Dolomite
CHI-14 DC-25(D)	L-WES-L25-78	4-24-78	6	10 of 19	38.7-42.7	508.3-504.3	547.0	Dolomite
CHI-14 DC-25(E)	L-WES-L25-78	4-24-78	6	11 of 19	42.7-46.95	504.3-500.05	547.0	Dolomite
CHI-14 DC-25(F)	L-WES-L25-78	4-24-78	6	12 of 19	46.95-50.45	500.05-496.55	547.0	Dolomite
CHI-14 DC-25(G)	L-WES-L25-78	4-24-78	6	13 of 19	50.45-54.2	496.55-492.8	547.0	Dolomite
CHI-14 DC-25(H)	L-WES-L25-78	4-24-78	6	14 of 19	54.2-57.6	492.8-489.4	547.0	Dolomite
CHI-14 DC-25(I)	L-WES-L25-78	4-24-78	6	15 of 19	57.6-62.1	489.4-484.9	547.0	Dolomite
CHI-14 DC-25(J)	L-WES-L25-78	4-24-78	6	16 of 19	62.1-65.8	484.9-481.2	547.0	Dolomite
CHI-14 DC-25(K)	L-WES-L25-78	4-24-78	6	17 of 19	65.8-69.85	481.2-477.15	547.0	Dolomite
CHI-14 DC-25(L)	L-WES-L25-78	4-24-78	6	18 of 19	69.85-74.1	477.15-472.9	547.0	Dolomite
CHI-14 DC-25(M)	L-WES-L25-78	4-24-78	6	19 of 19	74.1-75.75	472.9-471.25	547.0	Dolomite
CHI-14 CON-26(A)	L-WES-L26-78	4-24-78	6	1 of 9	0.0-3.5	547.0-543.5	547.0	Concrete
CHI-14 CON-26(B)	L-WES-L26-78	4-24-78	6	2 of 9	3.5-8.05	543.5-538.95	547.0	Concrete and Dolomite
CHI-14 CON-26(A)	L-WES-L26-78	4-24-78	6	3 of 9	8.05-11.75	538.95-535.25	547.0	Dolomite
CHI-14 CON-26(B)	L-WES-L26-78	4-24-78	6	4 of 9	11.75-15.85	535.25-531.15	547.0	Dolomite
CHI-14 CON-26(C)	L-WES-L26-78	4-24-78	6	5 of 9	15.85-19.65	531.15-527.35	547.0	Dolomite
CHI-14 CON-26(D)	L-WES-L26-78	4-24-78	6	6 of 9	19.65-24.1	527.35-522.9	547.0	Dolomite
CHI-14 CON-26(E)	L-WES-L26-78	4-24-78	6	7 of 9	24.1-27.65	522.9-519.35	547.0	Dolomite
CHI-14 CON-26(F)	L-WES-L26-78	4-24-78	6	8 of 9	27.65-31.2	519.35-515.8	547.0	Dolomite
CHI-14 DC-26(G)	L-WES-L26-78	4-24-78	6	9 of 9	31.2-35.3	515.8-511.7	547.0	Dolomite
CHI-14 CON-27	L-WES-L27-78	4-24-78	6	1 of 1	0.0-3.15	576.2	576.2	Concrete
CHI-14 CON-28	L-WES-L28-78	4-24-78	6	1 of 1	0.0-3.0	576.2	576.2	Concrete
CHI-14 CON-29	L-WES-L29-78	4-24-78	6	1 of 1	0.0-2.75	539.0	539.0	Concrete
CHI-14 CON-30	L-WES-L30-78	4-24-78	6	1 of 1	0.0-2.7	539.0	539.0	Concrete
CHI-14 CON-31(A)	L-WES-L31-78	4-24-78	6	1 of 3	0.0-3.6	569.2	569.2	Concrete

(Continued)

Table 5 (Concluded)

WES Reference	Drill Hole	Date Rec'd	Core Diam, in.	Bag/Box No.	Depth, ft	Elevation, ft Depth Intervals	Elevation, ft Top of Hole	Remarks
CHI-14 CON-31(B)	L-WES-L31-78	4-24-78	6	2 of 2	3.6-8.3	569.2	569.2	Concrete
CHI-14 CON-32(A)	L-WES-L32-78	4-24-78	6	1 of 3	0.0-3.1	565.0	565.0	Concrete
CHI-14 CON-32(B)	L-WES-L32-78	4-24-78	6	2 of 3	3.1-6.8	565.0	565.0	Concrete
CHI-14 CON-32(C)	L-WES-L32-78	4-24-78	6	3 of 3	6.8-10.3	565.0	565.0	Concrete
CHI-14 CON-33	L-WES-L33-78	4-24-78	6	1 of 1	0.0-3.4	573.0	573.0	Concrete
CHI-14 CON-34	L-WES-L34-78	4-24-78	6	1 of 1	0.0-3.75	557.0	557.0	Concrete
CHI-14 CON-35	L-WES-L35-78	4-24-78	6	1 of 1	0.5-3.85	556.5	557.0	Concrete
CHI-14 CON-36	L-WES-L36-78	4-24-78	6	1 of 1	0.0-3.7	573.0	573.0	Concrete
CHI-14 CON-37	L-WES-L37-78	4-24-78	6	1 of 1	0.0-3.5	560.0	560.0	Concrete
CHI-14 CON-39	L-WES-L39-78	6-22-78	6	1 of 1	0.0-3.2			Concrete
CHI-14 CON-40	L-WES-L40-78	6-22-78	6	1 of 1	0.0-2.65			Concrete
CHI-14 CON-41	L-WES-L41-78	6-22-78	6	1 of 1	0.0-3.55			Concrete
CHI-14 CON-42	L-WES-L42-78	6-22-78	6	1 of 1	0.0-3.45			Concrete
CHI-14 CON-43	L-WES-L43-78	6-22-78	6	1 of 1	0.0-3.8			Concrete
CHI-14 CON-44	L-WES-L44-78	6-22-78	6	1 of 1	0.0-2.0			Concrete
CHI-14 CON-45	L-WES-L45-78	6-22-78	6	1 of 1	0.0-3.4			Concrete
CHI-14 CON-46	L-WES-L46-78	6-22-78	6	1 of 1	0.0-3.2			Concrete
CHI-14 CON-47	L-WES-L47-78	6-22-78	6	1 of 1	0.0-1.8			Concrete
CHI-14 CON-48	L-WES-L48-78	6-22-78	6	1 of 1	0.0-3.15			Concrete
CHI-14 CON-49	L-WES-L49-78	6-22-78	6	1 of 1	0.0-3.5			Concrete
CHI-14 CON-50	L-WES-L50-78	6-22-78	6	1 of 1	0.0-3.2			Concrete
CHI-14 CON-51	L-WES-L51-78	6-22-78	6	1 of 1	0.0-3.3			Concrete
CHI-14 CON-52	L-WES-L52-78	6-22-78	6	1 of 1	0.0-3.15			Concrete
CHI-14 CON-53	L-WES-L53-78	6-22-78	6	1 of 1	0.0-2.9			Concrete
CHI-14 CON-54	L-WES-L54-78	6-22-78	6	1 of 1	0.0-3.4			Concrete
CHI-14 CON-55	L-WES-L55-78	6-22-78	6	1 of 1	0.0-3.0			Concrete
CHI-14 CON-56	L-WES-L56-78	6-22-78	6	1 of 1	0.0-2.8			Concrete
CHI-14 CON-57	L-WES-L38-78	4-24-78	6	None	None	585.0	511.4*	Cores not received at WES

* Elevation computed for vertical segment of inclined boring at 25°.

Table 6

Test Results of Dolomite Cores, Lockport Lock

Drill Hole No. L-WES- -78	Depth, ft	Elev, ft	Characterization Tests: Effective Unit Wt, γ_m, lb/ft^3	Dry Unit Wt, γ_d, lb/ft^3	Water Content, w %	Comp Wave Velocity Vp, fps	Comp Strength, psi	Tensile Strength, psi	Eng Design Tests: Elastic Modulus, E, 10^6 psi	Poisson's Ratio
L1	70.9	514.1	167.9	164.8	1.9	20,066	13,480*		9.62	0.25
L1	84.5	500.5	171.7			19,629	16,090*		9.47	0.26
L3	92.8	492.2	167.9			16,611	16,090*		6.44	0.20
L13	72.7	512.3	167.3	163.9	2.1	19,526	13,480		8.99	0.30
L13	76.5	508.5	168.6					65		
L25	33.8	513.2	166.1	162.8	2.0	19,280	11,270		10.74	0.42
L26	22.1	524.9	167.3	165.6	1.0	18,931	12,520		8.35	0.23
L26	31.7	515.3	167.3					95		
L26	32.7	514.3	166.7					130		
	Average		168.0	164.3	1.75	19,007	13,820	95	8.94	0.28
	Range		5.6	2.8	1.1	3,455	2,210	65	4.3	0.22
	No. of Tests		6	4	4	6	4	3	6	6

* Core did not fail, tested to capacity of 440,000 lb.

Rebar pullout strength, average of 2 tests is 117.4 tsf.

Table 7

Laboratory Test Results, Lockport Lock

Direct Shear Tests

Lithology	Drill Hole No. L WES	Elevation, ft	Test	Normal Stress, tsf	Peak Shear Stress, tsf	Ultimate Shear Stress, tsf	Peak Shear Strength	Ultimate Shear Strength
Dolomite	L 3-78	515.7	Concrete	2	38.1	2.1		
	L25-78	520.9	to rock	4	27.5	7.7	ϕ=67.4°	ϕ_u=61.9
	L26-78	540.3		8	37.1	13.7	c=18 tsf	c_u=0
<1/8-in. green shale parting in dolomite	L13-78	505.8	Filled parting *	2	27.2	20.9		
				4	13.5	10.4		
				8	14.6	12.3		
<1/8-in. green shale parting in dolomite	L26-78	537.5	Filled parting	2	10.1	7.6		
				4	11.4	10.3	ϕ=48°	ϕ_u=52°
				8	17.6	19.4	c=9.2tsf	c_u=6.4 tsf
<1/8-in. green shale parting in dolomite	L26-78	532.3	Filled parting	2	12.6	12.0		
				4	16.3	11.6		
				8	22.0	19.4		
Dolomite	L26-78	519.7	Bedding plane	2	61.1	$14.2\frac{1}{2}$		
				4	18.1	15.5_2		
				8	23.3	21.8	ϕ=61.5 c=49 tsf]1	
Dolomite	L25-78	511.8	Bedding plane	2	46.6	$26.3\frac{1}{2}$		
				4	26.8	14.2_2		
				8	28.4	24.7	ϕ=40.3° c=19.5 tsf] 2	
Dolomite	L25-78	506.5	Bedding plane	2	43.5	$42.8\frac{1}{1}$		
				4	53.1	11.7		

(Continued)

Table 7 (Concluded)

Lithology	Drill Hole No. L WES	Elevation, ft	Test	Normal Stress, tsf	Peak Shear Stress, tsf	Ultimate Shear Stress, tsf	Peak Shear Strength	Ultimate Shear Strength
Dolomite	L26-78	517.7	Bedding plane	2	62.3	59.5_1^1		
				4	58.8	54.6_1^1		
				8	64.7	83.1^1		
Dolomite	L-1	501.6	Natural joint	2	41.1	35.8	$\phi=68.4^o$	
				4	46.5	44.9	c=36 tsf	
				8	56.3	22.4		
Dolomite	L-1	510.8	Natural joint	2	12.0	11.4		
				4	16.0	13.1	$\phi=23.2^o$	
				8	15.2	11.3	c=12.4 tsf	

* Filled parting specimens have about 35% surface coated with thin green clay coating, coating thickness about <1/64 in.

1 and 2 denote groupings for calculating shear strength parameters.

Table 8

Laboratory Test Results, Lockport Lock

Surface Descriptions of Direct Shear Specimens

Drill Hole/Elev, ft	Surface Description and Remarks
L 3/515.7	Shear in concrete, very rough relief about 1/2 in., 100% concrete contact
L25/520.9	Shear at contact, rough relief about 1/4 in., 25% concrete contact
L26/540.3	Shear at contact, rough relief about 1/4 in., 20% concrete contact, rock surface was old solution surface.
L13/505.8	Shear surface, very rough relief about 1/2 in., 6-8 peaks sheared at base, 30% surface contact, thin green (< 1/64 in.) clay coating on 70% surface, minor solution activity, rock flour at base of 5 sheared peaks, 1/2-in. deep by 2-in. edge broken.
L26/537.5	Shear surface, rough relief about 1/4 in., 4 peaks sheared at base, 15% surface contact, thin green clay coating on 15% surface, no solution activity, rock flour at base of peaks.
L26/532.3	Shear surface, rough relief about 1/4 in., 10% surface contact, thin green clay coating on about 20% surface, heavy solution activity, rock flour at base of sheared peaks.
L26/519.7	Shear surface, very rough relief about 1/2 in., 6-8 peaks sheared at base, 50% surface contact, thin green clay coating on 15% of surface, no solution activity.
L25/511.8	Shear surface, very rough relief about 1/2 in., 3 peaks sheared at base, 60% surface contact, thin green clay coating about 40% of surface, no solution activity.
L25/506.5	Shear surface, very rough relief about 1/2 in., 6 peaks sheared at base, 75% surface contact, thin green clay coating on 25% of surface, dark stain on solution channel surfaces.
L26/517.7	Shear surface on bedding plane, very smooth w/no relief, 100% surface contact, chip 1-in. wide and 4-in. long off edge, 2-4% thin green clay coating.
L 1/501.6	Rough relief about 1/4 in., 60% of specimen edge sheared off.
L 1/510.8	Relief about 1/32 in., rock flour present.

Table 9

Test Results of Concrete Cores, Lockport Lock

Drill Hole No. L-WES- -78	Depth Ft	Elev Ft	Characterization Tests: Effective Unit wt γ_m, lb/ft^3	Dry Unit Wt γ_d, lb/ft^3	Water Content W %	Comp Wave Velocity Vp, fps	Comp Strength UC, psi	Eng Design Tests: Elastic Modulus E x 10^6	Poisson's Ratio
L1	1.9	583.1	153.6	145.0	5.9	16,815	7860	5.90	0.18
L1	34.5	550.5	154.1	145.2	6.1	16,461	8080	6.90	0.24
L1	64.7	520.3	153.0	143.0	7.0	15,111	4180	5.40	0.20
L2	7.8	577.2	149.2	141.2	5.7		6240		
L2	24.0	561.0	154.2	143.8	7.2		6460		
L2	45.0	540.0	151.8	140.9	7.7		6470		
L3	2.1	582.9	153.6	143.2	7.3		5800		
L3	32.1	552.9	155.2	146.3	6.1		8870		
L3	65.3	519.7	152.0	141.3	7.6		6400		
L4	1.3	574.2	155.5	145.7	6.7	15,508	6840	4.55	0.23
L5	0.5	574.2	152.3	144.8	5.2	15.586	7420	5.56	0.22
L5	2.5	574.2	150.5	141.8	6.1	14,404	6650	5.88	0.26
L6	0.5	573.2	152.3	142.1	7.2		5930		
L6	2.5	573.2	151.7	142.3	6.6		7270		
L7	0.5	541.0	153.0	143.5	6.6	16,209	7390	5.00	0.25
L7	2.5	541.0	153.6	143.3	7.2	16,129	7290	5.56	0.28
L8	0.7	561.2	151.7	141.0	7.6	15,651	6690	5.56	0.28
L9	0.5	537.0	148.6	137.8	7.8		5710		
L12	0.5	576.2	151.1	143.0	5.7		8970		
L13	0.8	584.2	151.1	143.0	5.7	14,705	6180	5.45	0.15
L13	33.5	551.5	150.5	141.6	6.3	15,625	6730	5.45	0.24
L13	64.7	520.3	151.1	143.0	5.7	16,129	6080	5.47	0.22
L15	0.6	565.0	149.8	140.4	6.7		5410		
L16	0.8	571.2	155.5	144.8	7.4		6630		
L16	3.0	571.2	154.2	143.3	7.6		5840		
L17	0.7	555.0	153.0	144.5	5.9	15,385	7640	5.10	0.20
L17	2.4	555.0	151.1	140.7	7.4	15,151	6920	5.56	0.28
L18	0.5	573.2	153.0	144.7	5.7	14,539	6790	5.00	0.25
L18	2.5	573.2	152.3	142.6	6.8	14,404	5310	5.33	0.20
L19	0.5	573.2	149.2	139.4	7.0		6470		

(Continued)

Table 9 (Continued)

Drill Hole No. L-WES- 78	Depth Ft	Elev Ft	Characterization Tests: Effective Unit wt γ_m, lb/ft^3	Dry Unit wt γ_d, lb/ft^3	Water Content W %	Comp Wave Velocity Vp, fps	Comp Strength UC, psi	Eng Design Tests: Elastic Modulus E x 10^6	Poisson's Ratio
L20	0.5	571.2	153.0	142.9	7.1		6860		
L20	2.3	571.2	153.6	144.0	6.7		6470		
L21	0.7	573.2	150.5	142.2	5.8	14,392	6700	3.85	0.19
L21	4.0	573.2	149.2	140.6	6.1	14,800	7130	5.26	0.26
L24	1.5	556.5	151.7	143.9	5.4		6440		
L24	13.2	544.8	151.7	142.8	6.2		7030		
L24	27.7	530.3	154.8	146.7	5.5		6800		
L25	7.9	539.1	152.3	142.3	7.0		6450		
L25	13.1	533.9	153.6	142.9	7.5		7420		
L25	22.8	524.2	149.8	138.6	8.1		7280		
L26	1.3	545.7	152.3	143.5	6.1	15,625	5580	5.10	0.26
L27	0.7	576.2	150.5	142.2	5.8		7670		
L28	1.6	576.2	156.7	149.4	4.9	16,420	6690	5.56	0.22
L32	9.8	565.0	153.0	143.7	6.5	15,972	7890	5.56	0.28
L33	0.5	573.0	150.5	139.6	7.8		6320		
L34	1.3	557.0	153.0	142.6	7.3		6620		
L35	1.0	557.0	151.7	142.6	6.4		6660		
L36	1.1	573.0	152.3	142.2	7.1		6290		
L36	3.2	573.0	151.7	141.2	7.4		6610		
L39	0.7	551.0	154.2	145.7	5.8	14,345	6040	3.92	0.16
L39	2.7	551.0	153.6	144.6	6.2	16,193	7610	5.10	0.20
L40	0.5	566.0	151.7	141.0	7.6		7160		
L40	2.1	566.0	150.5	139.2	8.1		5920		
L41	0.5	574.0	152.3	143.1	6.4		7440		
L41	3.0	574.0	153.0	143.4	6.7		5870		
L42	1.5	554.0	153.0	142.1	7.7		5440		
L45	0.9	566.0	151.1	139.5	8.3		4850		
L45	2.9	566.0	150.5	138.7	8.5		5080		
L46	0.7	551.0	149.2	137.1	8.8		4280		

(Continued)

Table 9 (Concluded)

Drill Hole No. L-WES- -78	Depth Ft	Elev Ft	Characterization Tests: Effective Unit Wt γ_m, lb/ft^3	Characterization Tests: Dry Unit Wt γ_d, lb/ft^3	Characterization Tests: Water Content W %	Characterization Tests: Comp Wave Velocity Vp, fps	Characterization Tests: Comp Strength UC, psi	Eng Design Tests: Elastic Modulus E x 10^6	Eng Design Tests: Poisson's Ratio
L47	0.5	579.0	150.5	142.2	5.8		6490		
L48	1.3	573.0	151.7	140.7	7.8		5670		
L48	2.6	573.0	151.7	141.1	7.5		7070		
L49	0.9	566.0	152.3	143.0	6.5	15,151	6040	4.76	0.21
L49	3.0	566.0	151.7	142.8	6.2	15,446	6880	5.00	0.25
L50	1.1	551.0	150.5	138.2	8.9		4200		
L51	2.8	541.0	152.3	141.7	7.5		6510		
L54	1.1	544.9	151.7	141.5	7.2		6210		

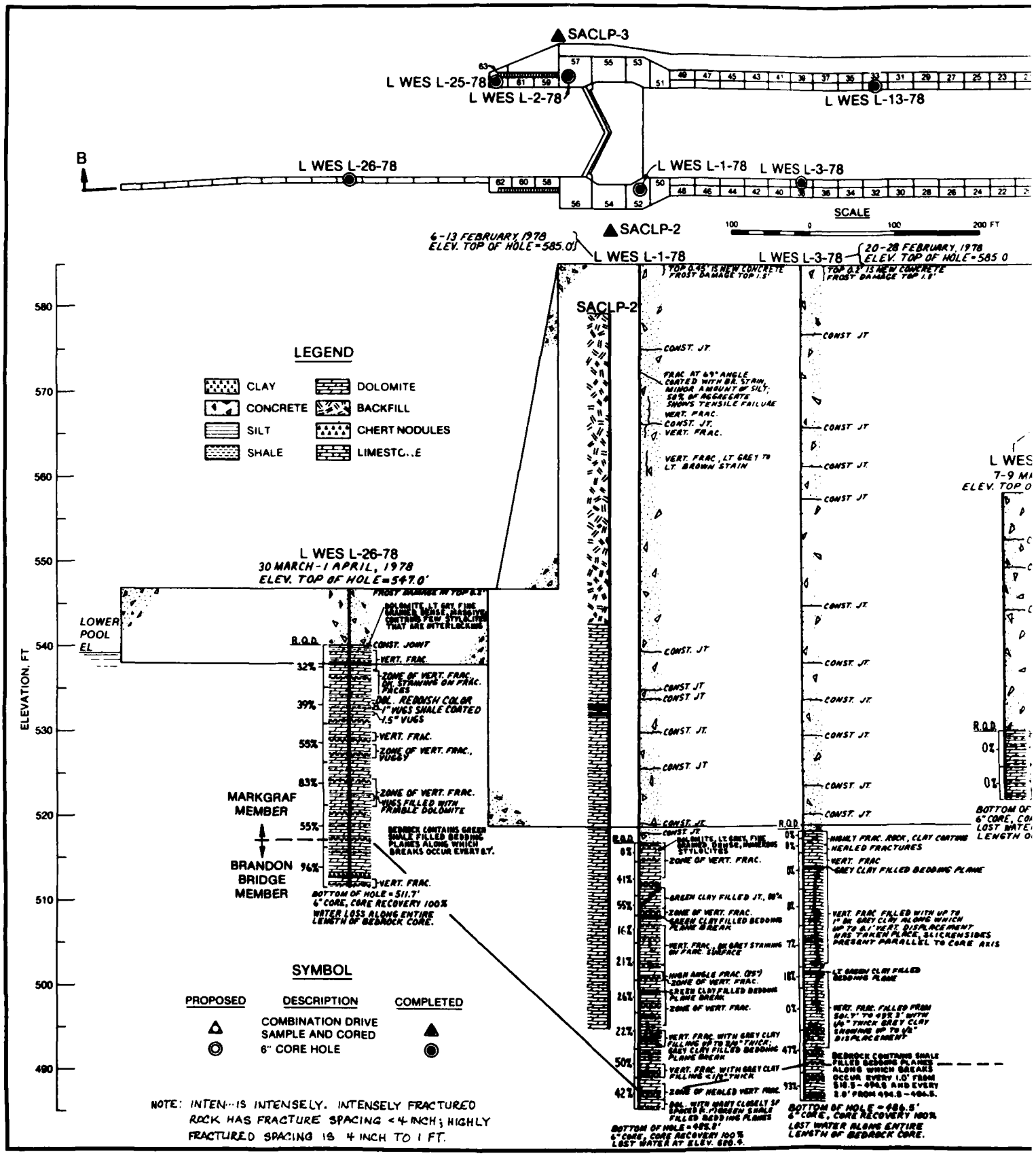
SACLP-3
L WES L-25-78
L WES L-2-78
L WES L-13-78
B
L WES L-26-78
L WES L-1-78
L WES L-3-78
SCALE
100 0 100 200 FT
SACLP-2
6-13 FEBRUARY, 1978
ELEV. TOP OF HOLE = 585.0'
20-28 FEBRUARY, 1978
ELEV. TOP OF HOLE = 585.0
ELEVATION, FT
580
570
560
550
540
530
520
510
500
490
LEGEND
CLAY
CONCRETE
SILT
SHALE
DOLOMITE
BACKFILL
CHERT NODULES
LIMESTONE
L WES L-26-78
30 MARCH - 1 APRIL, 1978
ELEV. TOP OF HOLE = 547.0'
LOWER POOL EL
MARKGRAF MEMBER
BRANDON BRIDGE MEMBER
BOTTOM OF HOLE = 511.7'
6" CORE, CORE RECOVERY 100%
WATER LOSS ALONG ENTIRE LENGTH OF BEDROCK CORE.
SYMBOL
PROPOSED
DESCRIPTION
COMPLETED
COMBINATION DRIVE SAMPLE AND CORED
6" CORE HOLE
NOTE: INTEN-- IS INTENSELY. INTENSELY FRACTURED ROCK HAS FRACTURE SPACING < 4 INCH; HIGHLY FRACTURED SPACING IS 4 INCH TO 1 FT.
BOTTOM OF HOLE = 495.9'
6" CORE, CORE RECOVERY 100%
LOST WATER AT ELEV. 680.9.
BOTTOM OF HOLE = 486.5'
6" CORE, CORE RECOVERY 100%
LOST WATER ALONG ENTIRE LENGTH OF BEDROCK CORE.

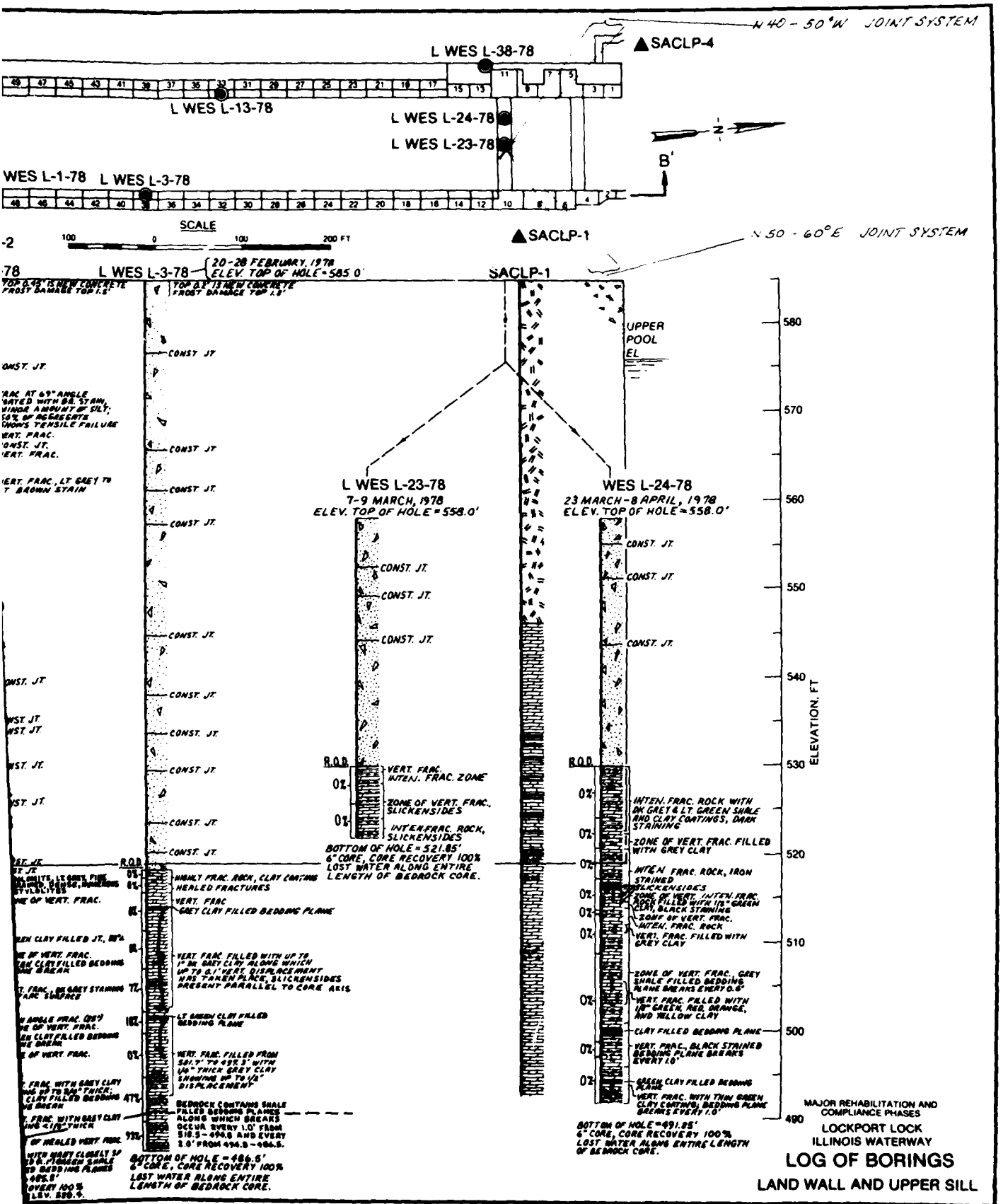

MAJOR REHABILITATION AND COMPLIANCE PHASES

LOCKPORT LOCK
ILLINOIS WATERWAY

LOG OF BORINGS

LAND WALL AND UPPER SILL

PLATE 1

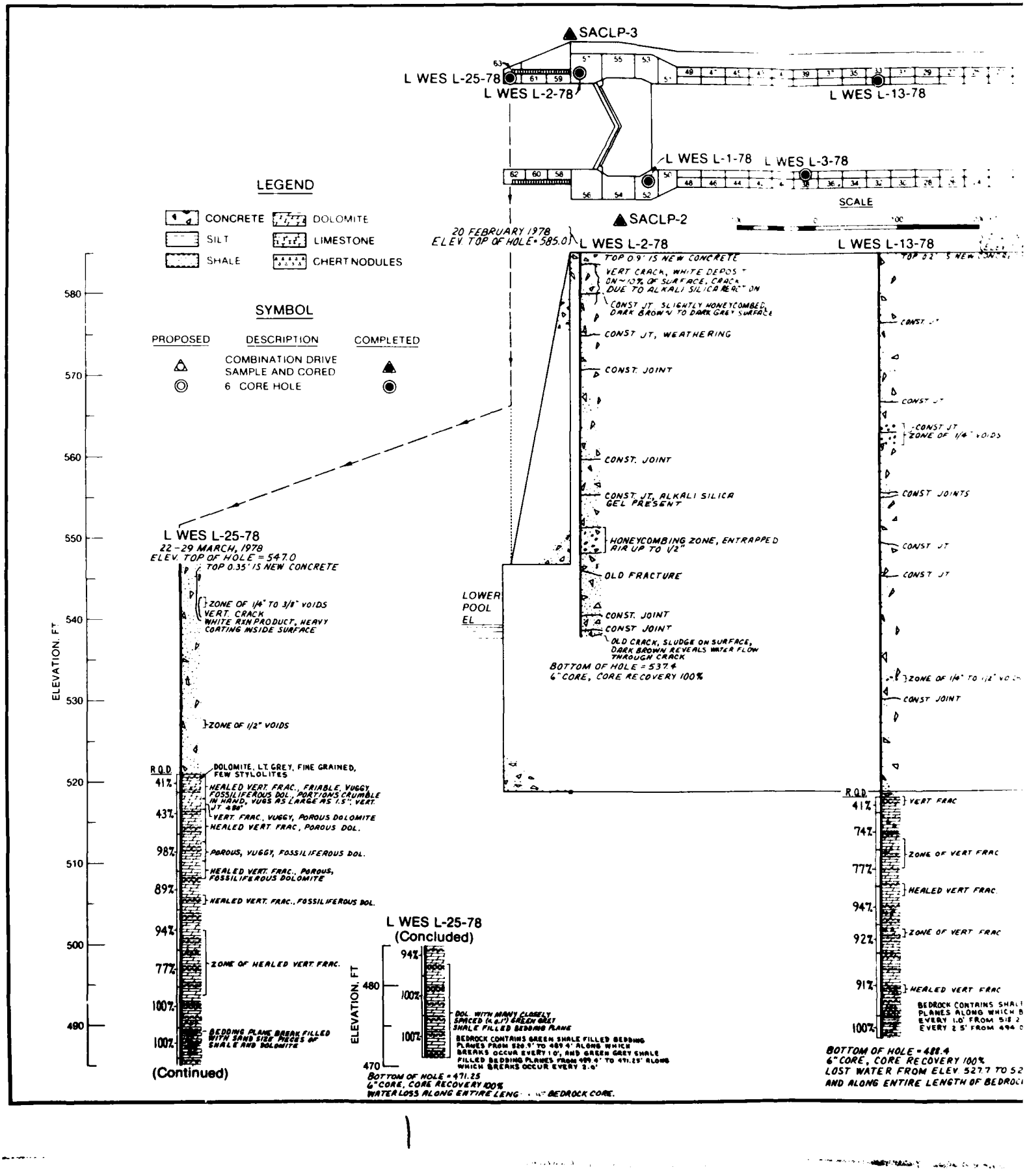
SACLP-3
L WES L-25-78
L WES L-2-78
L WES L-13-78
L WES L-1-78
L WES L-3-78
SACLP-2
SCALE
LEGEND
CONCRETE
DOLOMITE
SILT
LIMESTONE
SHALE
CHERT NODULES
SYMBOL
PROPOSED
DESCRIPTION
COMPLETED
COMBINATION DRIVE SAMPLE AND CORED
6 CORE HOLE
20 FEBRUARY 1978
ELEV. TOP OF HOLE = 585.0
ELEVATION, FT
580
570
560
550
540
530
520
510
500
490
L WES L-2-78
TOP 0.9' IS NEW CONCRETE
VERT CRACK, WHITE DEPOS ON ~10% OF SURFACE, CRACK DUE TO ALKALI SILICA REAC ON
CONST JT SLIGHTLY HONEYCOMBED, DARK BROWN TO DARK GRAY SURFACE
CONST JT, WEATHERING
CONST. JOINT
CONST. JOINT
CONST JT, ALKALI SILICA GEL PRESENT
HONEYCOMBING ZONE, ENTRAPPED AIR UP TO 1/2"
OLD FRACTURE
CONST. JOINT
CONST JOINT
OLD CRACK, SLUDGE ON SURFACE, DARK BROWN REVEALS WATER FLOW THROUGH CRACK
BOTTOM OF HOLE = 537.4
6" CORE, CORE RECOVERY 100%
LOWER POOL EL
L WES L-13-78
CONST JT
CONST JOINTS
CONST JT
CONST JT
CONST JOINT
L WES L-25-78
22-29 MARCH, 1978
ELEV. TOP OF HOLE = 547.0
TOP 0.35' IS NEW CONCRETE
ZONE OF 1/4" TO 3/8" VOIDS
VERT. CRACK WHITE RXN PRODUCT, HEAVY COATING INSIDE SURFACE
ZONE OF 1/2" VOIDS
RQD
41%
43%
98%
89%
94%
77%
100%
DOLOMITE, LT GREY, FINE GRAINED, FEW STYLOLITES
HEALED VERT. FRAC., FRIABLE, VUGGY FOSSILIFEROUS DOL., PORTIONS CRUMBLE IN HAND, VUGS AS LARGE AS 1.5", VERT. JT 48°
VERT. FRAC., VUGGY, POROUS DOLOMITE
HEALED VERT. FRAC., POROUS DOL.
POROUS, VUGGY, FOSSILIFEROUS DOL.
HEALED VERT. FRAC., POROUS, FOSSILIFEROUS DOLOMITE
HEALED VERT. FRAC., FOSSILIFEROUS DOL.
ZONE OF HEALED VERT. FRAC.
BEDDING PLANE BREAK FILLED WITH SAND SIZE PIECES OF SHALE AND DOLOMITE
(Continued)
L WES L-25-78
(Concluded)
ELEVATION, FT
480
470
94%
100%
100%
DOL. WITH MANY CLOSELY SPACED (4.0") GREEN GREY SHALE FILLED BEDDING PLANE
BEDROCK CONTAINS GREEN SHALE FILLED BEDDING PLANES FROM 520.9' TO 489.4' ALONG WHICH BREAKS OCCUR EVERY 1.0', AND GREEN GREY SHALE FILLED BEDDING PLANES FROM 489.4' TO 471.25' ALONG WHICH BREAKS OCCUR EVERY 2.0'
BOTTOM OF HOLE = 471.25
4" CORE, CORE RECOVERY 100%
WATER LOSS ALONG ENTIRE LENG
BEDROCK CORE.
RQD
41%
74%
77%
94%
92%
91%
100%
VERT FRAC
ZONE OF VERT FRAC
HEALED VERT FRAC
ZONE OF VERT FRAC
HEALED VERT FRAC
BEDROCK CONTAINS SHALE PLANES ALONG WHICH B
EVERY 1.0' FROM 518.2
EVERY 2.5' FROM 494.0
BOTTOM OF HOLE = 488.4
6" CORE, CORE RECOVERY 100%
LOST WATER FROM ELEV. 527.7 TO 52
AND ALONG ENTIRE LENGTH OF BEDROC

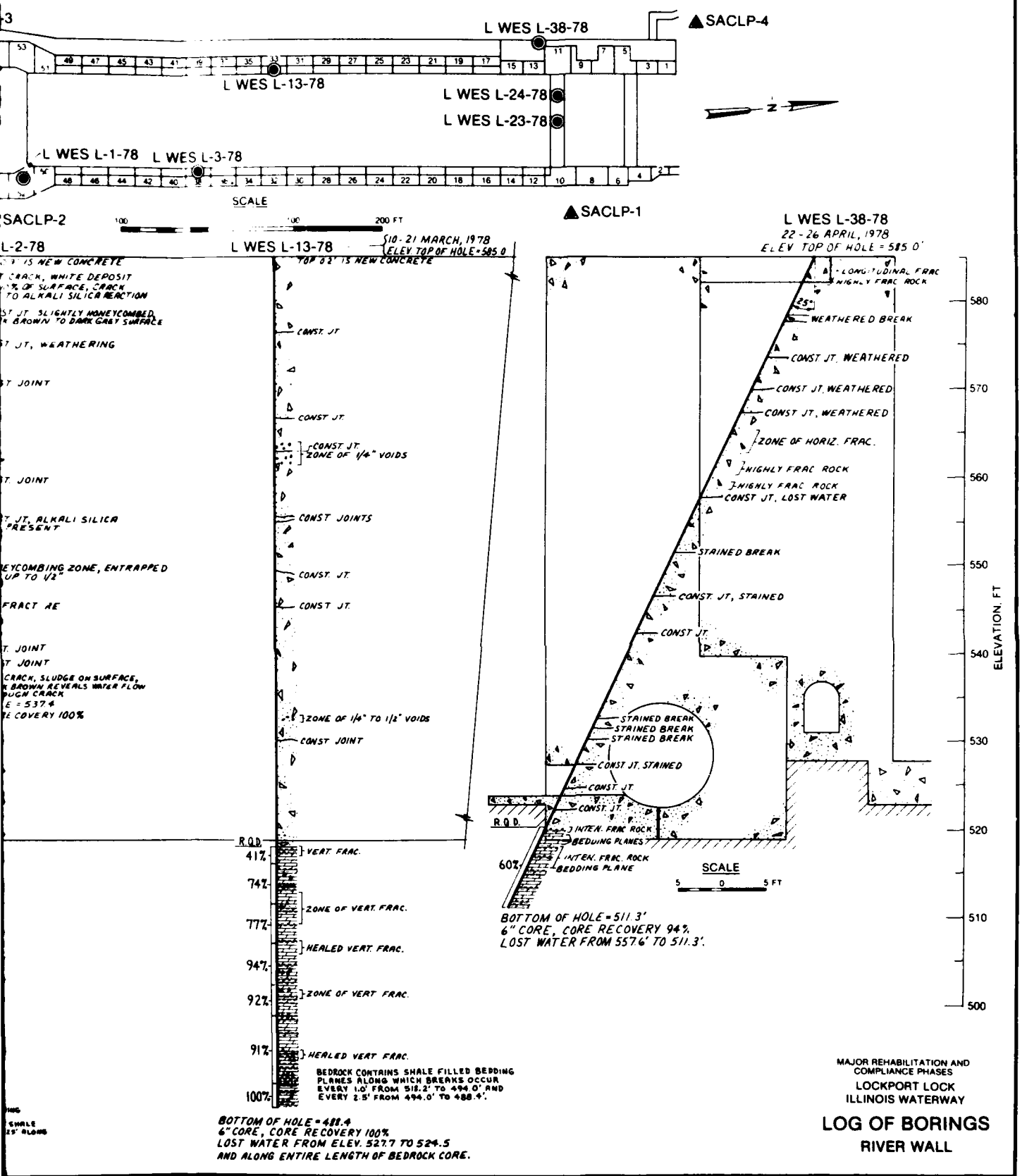

MAJOR REHABILITATION AND COMPLIANCE PHASES

LOCKPORT LOCK
ILLINOIS WATERWAY

LOG OF BORINGS
RIVER WALL

2

PLATE 2

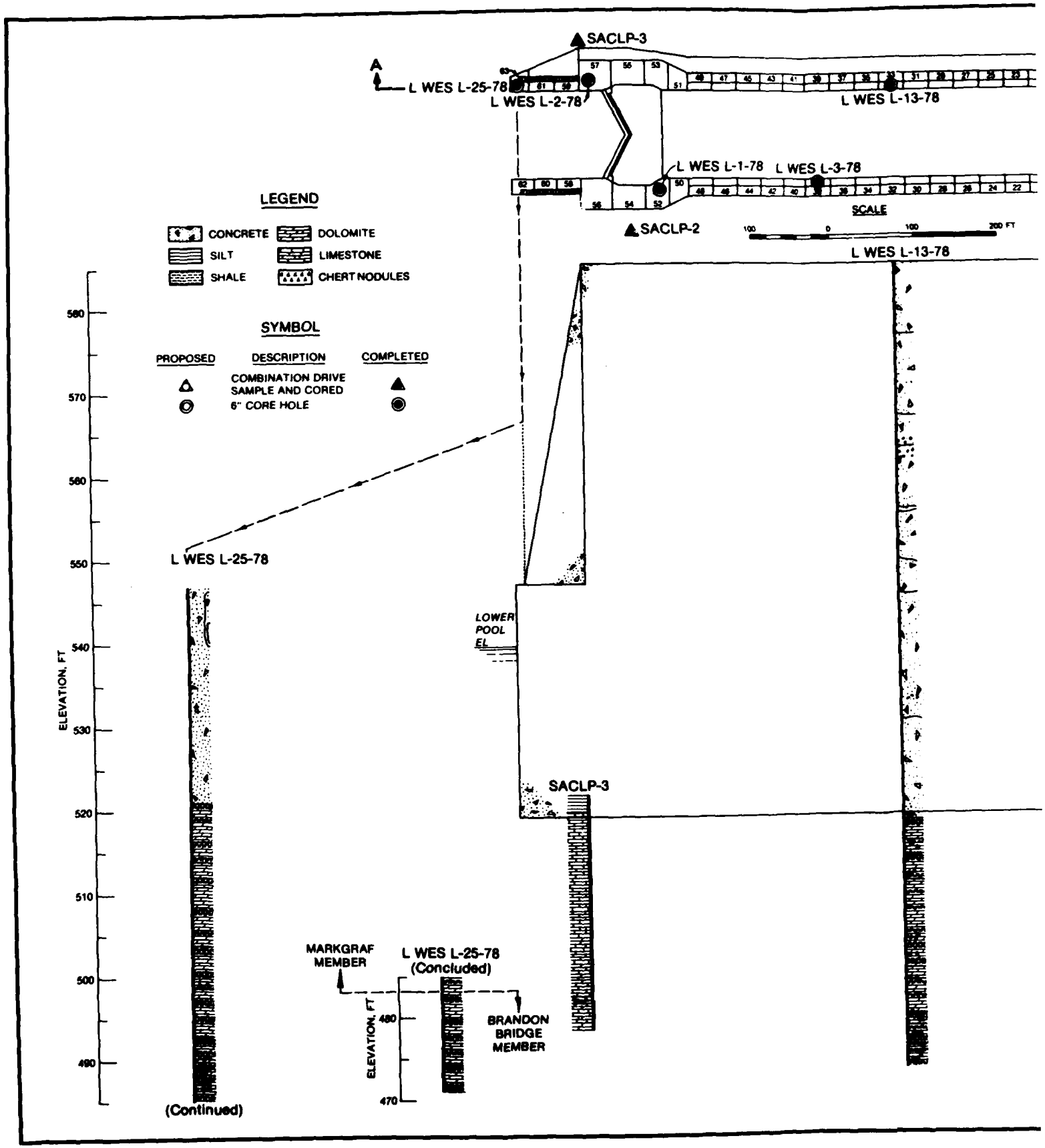
SACLP-3
A
L WES L-25-78
L WES L-2-78
L WES L-13-78
L WES L-1-78
L WES L-3-78
SACLP-2
SCALE
100 0 100 200 FT
LEGEND
CONCRETE
DOLOMITE
SILT
LIMESTONE
SHALE
CHERT NODULES
SYMBOL
PROPOSED
DESCRIPTION
COMPLETED
COMBINATION DRIVE SAMPLE AND CORED
6" CORE HOLE
L WES L-13-78
L WES L-25-78
LOWER POOL EL
SACLP-3
ELEVATION, FT
580
570
560
550
540
530
520
510
500
490
(Continued)
MARKGRAF MEMBER
L WES L-25-78 (Concluded)
BRANDON BRIDGE MEMBER
480
470

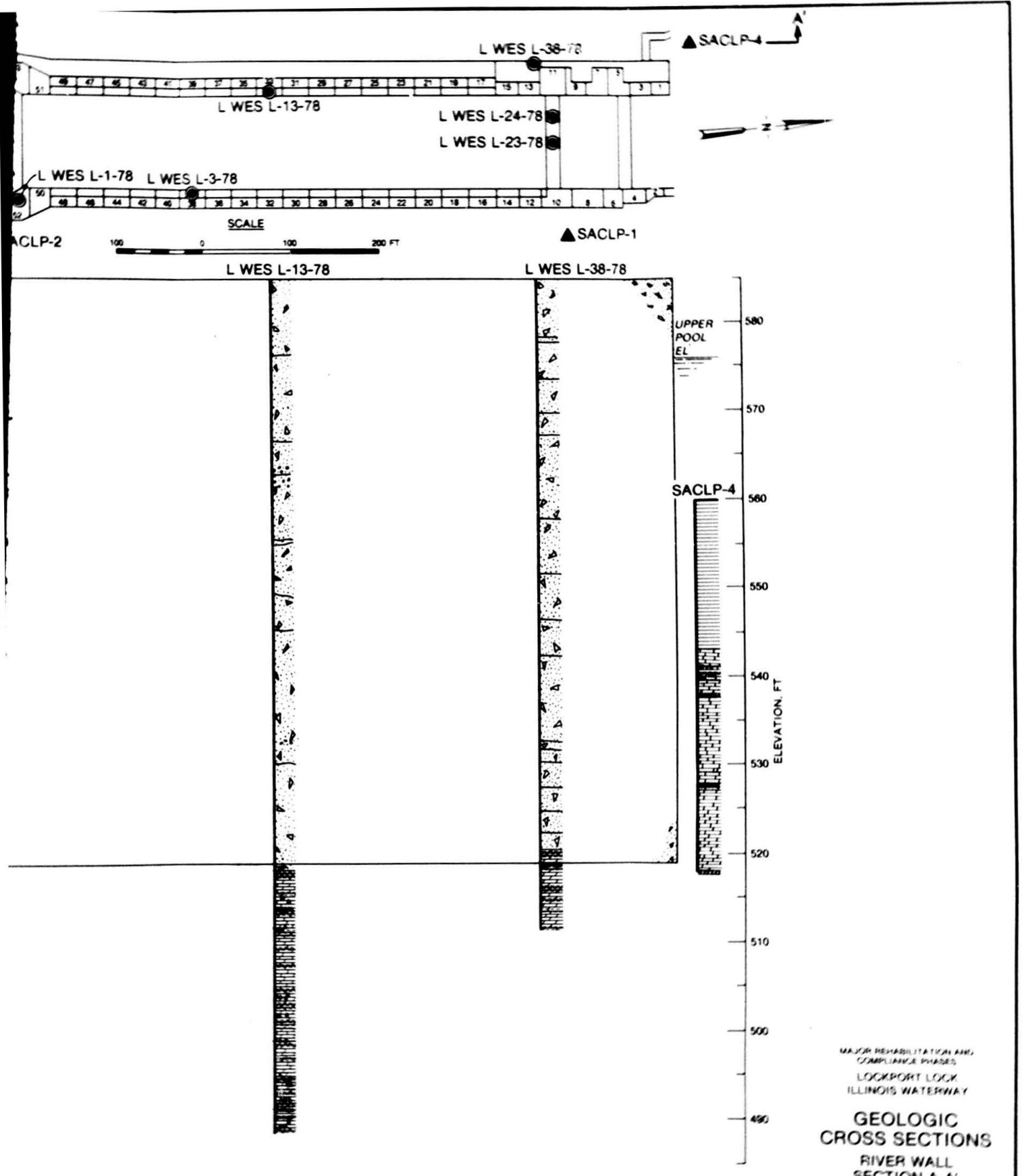

MAJOR REHABILITATION AND COMPLIANCE PHASES

LOCKPORT LOCK
ILLINOIS WATERWAY

GEOLOGIC CROSS SECTIONS

RIVER WALL
SECTION A-A'

2

PLATE 3

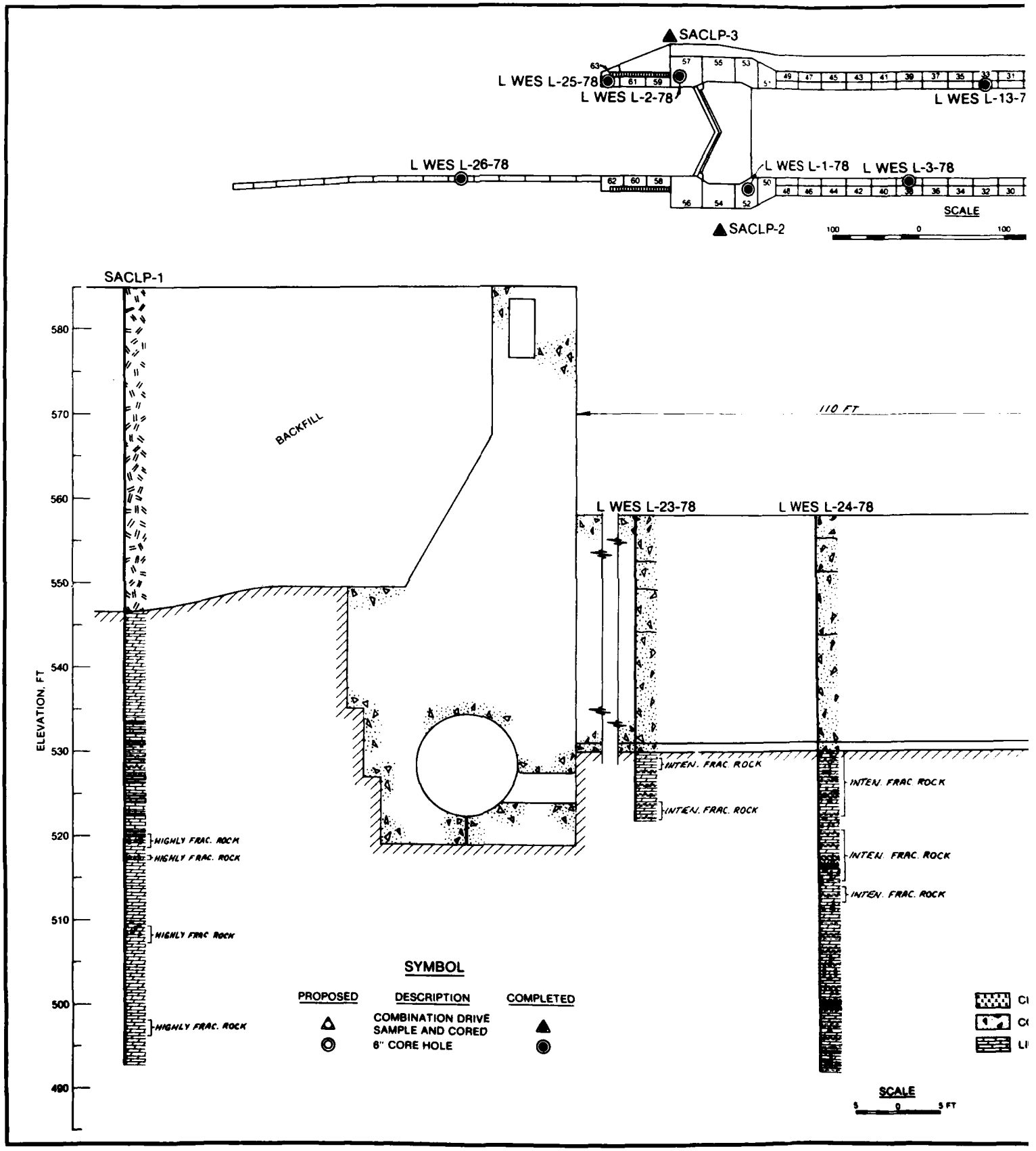
SACLP-3
L WES L-25-78
L WES L-2-78
L WES L-13-7
L WES L-26-78
L WES L-1-78
L WES L-3-78
SACLP-2
SCALE
100 0 100
SACLP-1
ELEVATION, FT
580
570
560
550
540
530
520
510
500
490
BACKFILL
110 FT
L WES L-23-78
L WES L-24-78
HIGHLY FRAC. ROCK
HIGHLY FRAC. ROCK
HIGHLY FRAC ROCK
HIGHLY FRAC. ROCK
INTEN. FRAC. ROCK
INTEN. FRAC. ROCK
INTEN. FRAC. ROCK
INTEN. FRAC. ROCK
INTEN. FRAC. ROCK
SYMBOL
PROPOSED
DESCRIPTION
COMPLETED
COMBINATION DRIVE SAMPLE AND CORED
6" CORE HOLE
SCALE
5 0 5 FT

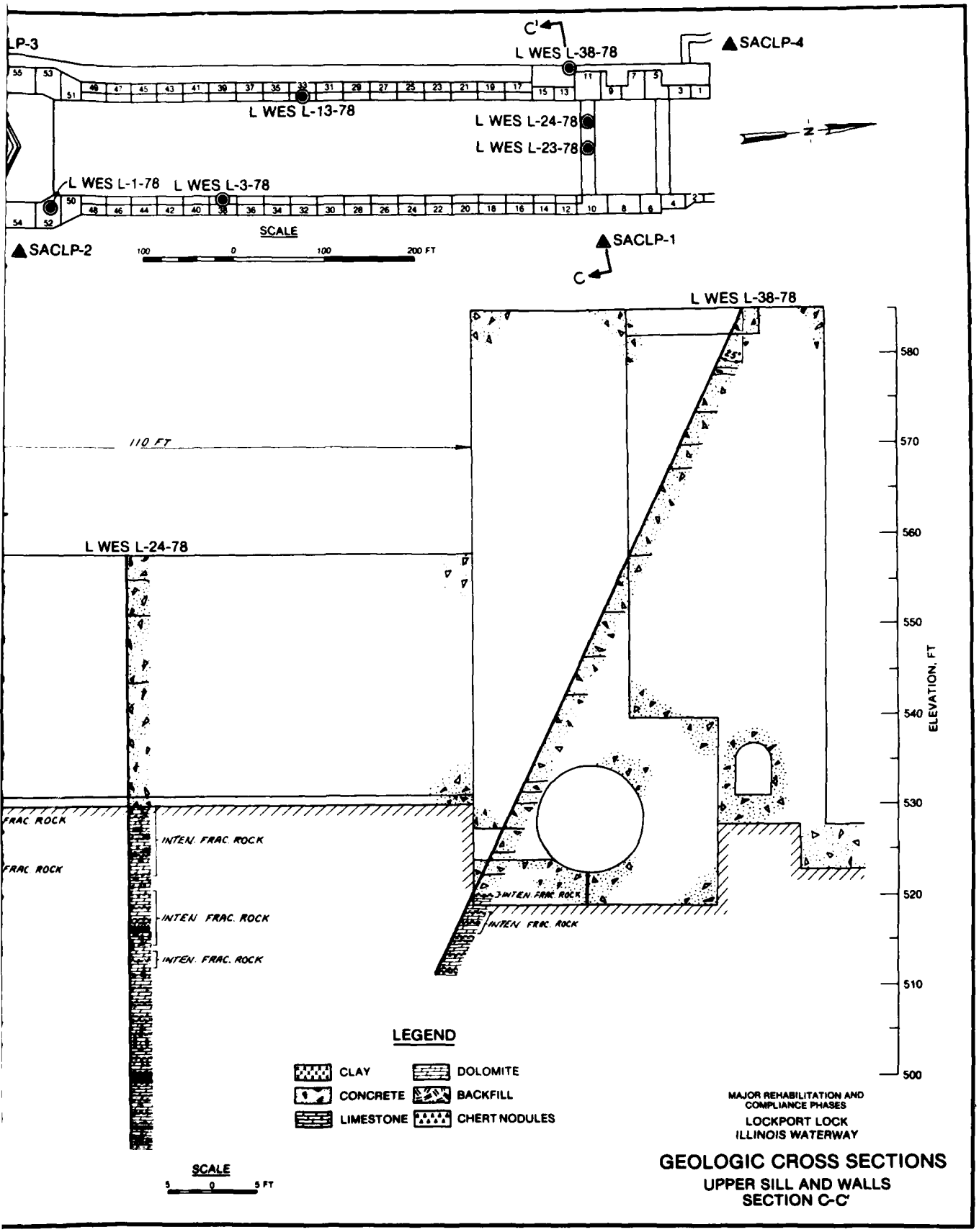

MAJOR REHABILITATION AND COMPLIANCE PHASES

LOCKPORT LOCK
ILLINOIS WATERWAY

GEOLOGIC CROSS SECTIONS

UPPER SILL AND WALLS
SECTION C-C'

2

PLATE 4

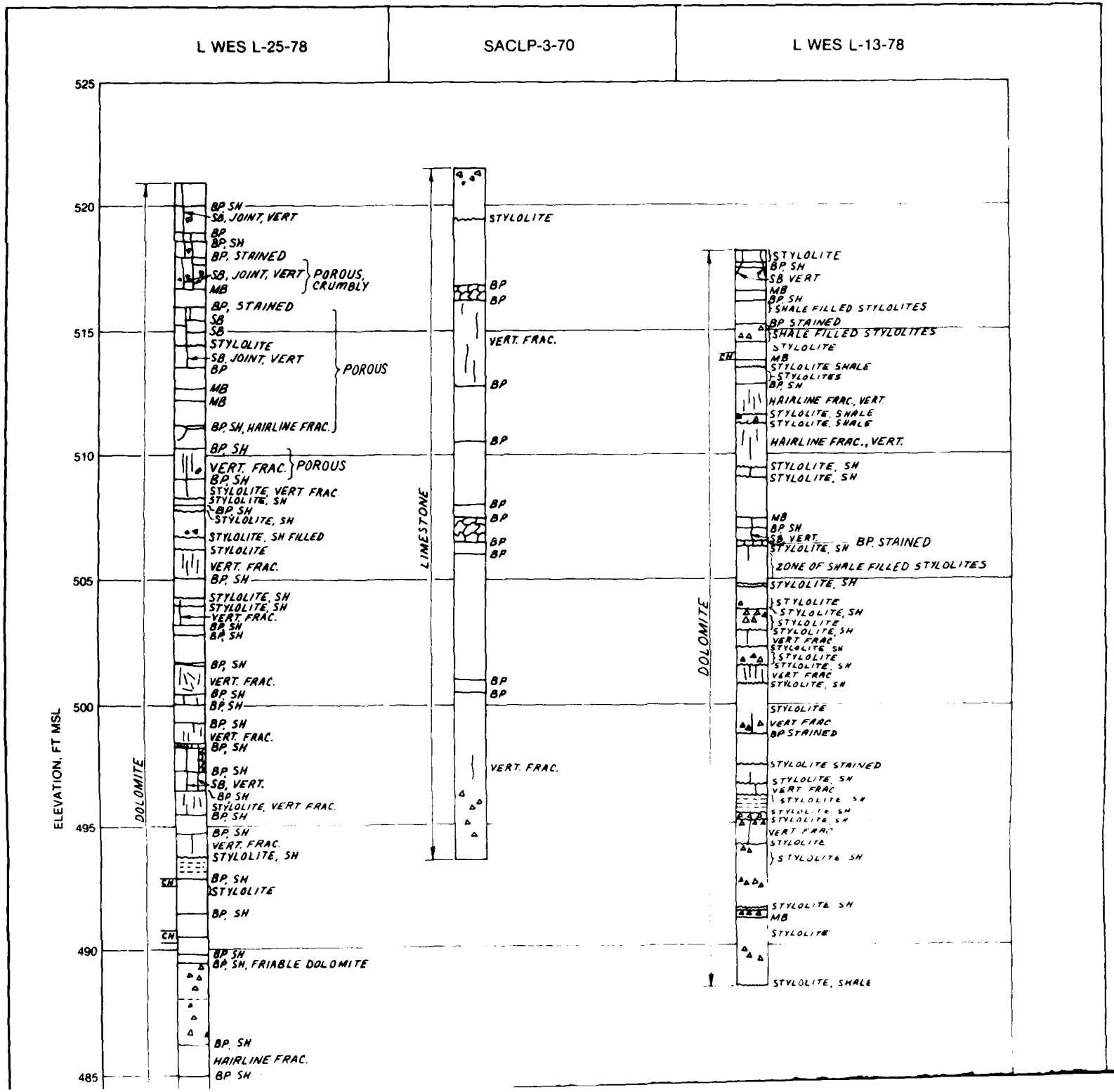
L WES L-25-78
SACLP-3-70
L WES L-13-78
ELEVATION, FT MSL
525
520
515
510
505
500
495
490
485
DOLOMITE
LIMESTONE
DOLOMITE
BP, SH
SB, JOINT, VERT
BP
BP, SH
BP, STAINED
SB, JOINT, VERT
POROUS, CRUMBLY
MB
BP, STAINED
SB
SB
STYLOLITE
SB, JOINT, VERT
POROUS
BP
MB
MB
BP, SH, HAIRLINE FRAC.
BP, SH
VERT. FRAC.
POROUS
BP, SH
STYLOLITE, VERT. FRAC.
STYLOLITE, SH
BP, SH
STYLOLITE, SH
STYLOLITE, SH FILLED
STYLOLITE
VERT. FRAC.
BP, SH
STYLOLITE, SH
STYLOLITE, SH
VERT. FRAC.
BP, SH
BP, SH
BP, SH
VERT. FRAC.
BP, SH
BP, SH
BP, SH
BP, SH
SB, VERT.
BP, SH
STYLOLITE, VERT. FRAC.
BP, SH
BP, SH
VERT. FRAC.
STYLOLITE, SH
CH
BP, SH
STYLOLITE
BP, SH
CM
BP, SH
BP, SH, FRIABLE DOLOMITE
BP, SH
HAIRLINE FRAC.
BP, SH
STYLOLITE
BP
BP
VERT. FRAC.
BP
BP
BP
BP
BP
BP
BP
BP
VERT. FRAC.
STYLOLITE
BP, SH
SB VERT
MB
BP, SH
SHALE FILLED STYLOLITES
BP STAINED
SHALE FILLED STYLOLITES
STYLOLITE
CH
MB
STYLOLITE SHALE
STYLOLITES
BP, SH
HAIRLINE FRAC., VERT.
STYLOLITE, SHALE
STYLOLITE, SHALE
HAIRLINE FRAC., VERT.
STYLOLITE, SH
STYLOLITE, SH
MB
BP, SH
SB VERT.
BP STAINED
STYLOLITE, SH
ZONE OF SHALE FILLED STYLOLITES
STYLOLITE, SH
STYLOLITE
STYLOLITE, SH
STYLOLITE
STYLOLITE, SH
VERT FRAC
STYLOLITE SH
STYLOLITE
STYLOLITE, SH
VERT FRAC
STYLOLITE, SH
STYLOLITE
VERT FRAC
BP STAINED
STYLOLITE STAINED
STYLOLITE, SH
VERT FRAC
STYLOLITE SH
STYLOLITE SH
STYLOLITE SH
STYLOLITE SH
VERT FRAC
STYLOLITE
STYLOLITE SH
STYLOLITE SH
MB
STYLOLITE
STYLOLITE, SHALE

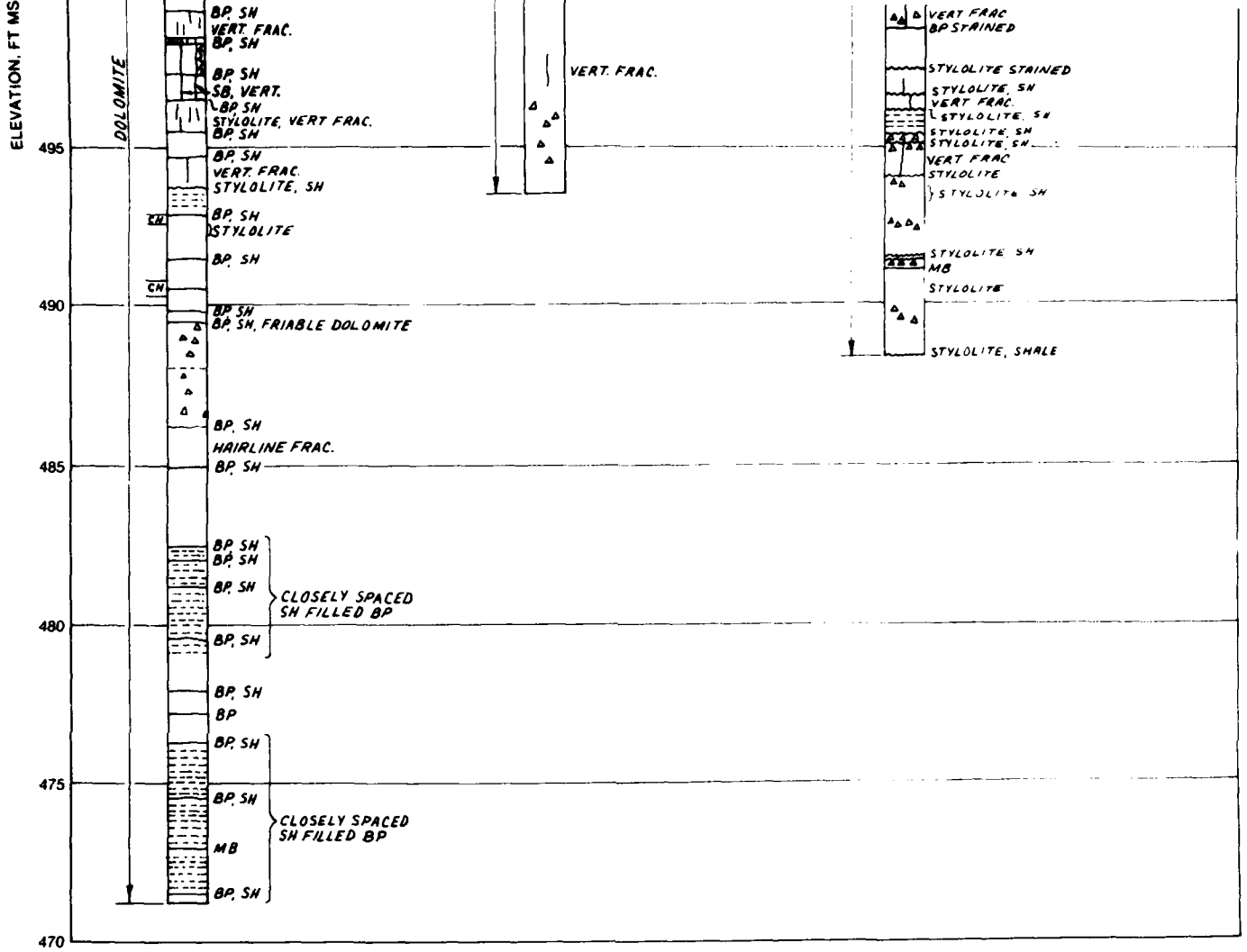

SYMBOLS

BP = BEDDING PLANE
SB = STRUCTURAL BREAK
MB = MECHANICAL BREAK

VUGS
BREAK AT STYLOLITE
SHALE SEAM
FRACTURED ROCK
CHERT NODULES

PREPARED FOR
U S ARMY ENGINEER DISTRICT
CORPS OF ENGINEERS
CHICAGO, ILLINOIS

LOCKPORT LOCK
ILLINOIS WATERWAY ILL

BEDROCK STRUCTURAL CHARACTERISTICS
RELEVANT TO FOUNDATIONS

PREPARED BY _____
DRAWN BY _____
DATE _____
SHEET ___ OF ___

PREPARED BY
U S ARMY ENGINEER
WATERWAYS EXPERIMENT STATION
CORPS OF ENGINEERS
VICKSBURG, MISSISSIPPI

PLATE 5

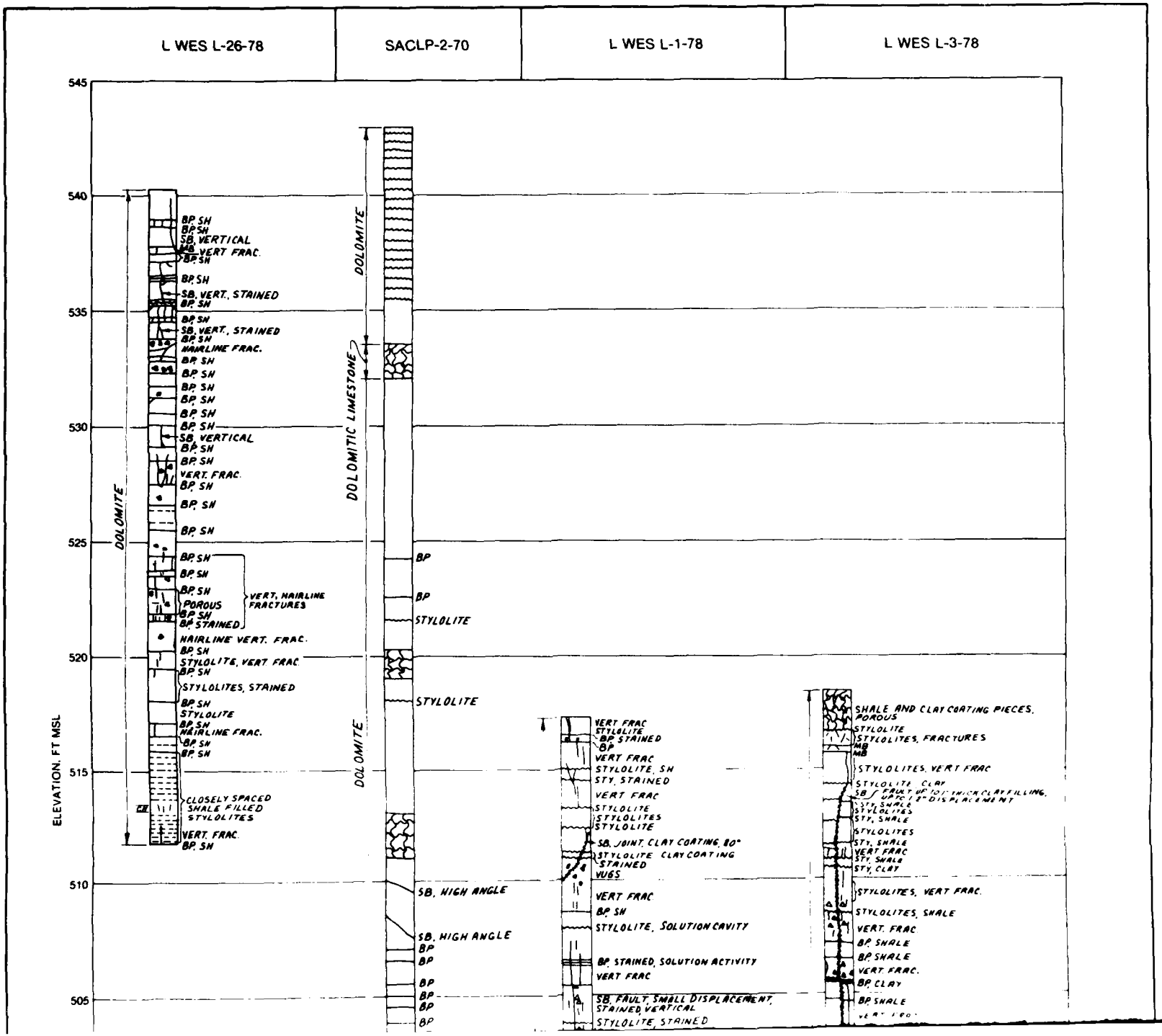
L WES L-26-78
SACLP-2-70
L WES L-1-78
L WES L-3-78
ELEVATION, FT MSL
545
540
535
530
525
520
515
510
505
DOLOMITE
DOLOMITIC LIMESTONE
DOLOMITE
BP, SH
SB, VERTICAL
VERT. FRAC.
SB, VERT., STAINED
HAIRLINE FRAC.
VERT, HAIRLINE FRACTURES
POROUS
STAINED
HAIRLINE VERT. FRAC.
STYLOLITE, VERT. FRAC.
STYLOLITES, STAINED
STYLOLITE
CLOSELY SPACED SHALE FILLED STYLOLITES
BP
STYLOLITE
SB, HIGH ANGLE
VERT FRAC
STYLOLITE, SH
STY, STAINED
STYLOLITES
SB, JOINT, CLAY COATING, 80°
STYLOLITE CLAY COATING
VUGS
STYLOLITE, SOLUTION CAVITY
BP, STAINED, SOLUTION ACTIVITY
SB, FAULT, SMALL DISPLACEMENT, STAINED, VERTICAL
STYLOLITE, STAINED
SHALE AND CLAY COATING PIECES, POROUS
STYLOLITES, FRACTURES
STYLOLITES, VERT FRAC
STYLOLITE CLAY
STY, SHALE
STY, CLAY
STYLOLITES, VERT FRAC.
STYLOLITES, SHALE
VERT. FRAC.
BP, SHALE
BP, CLAY

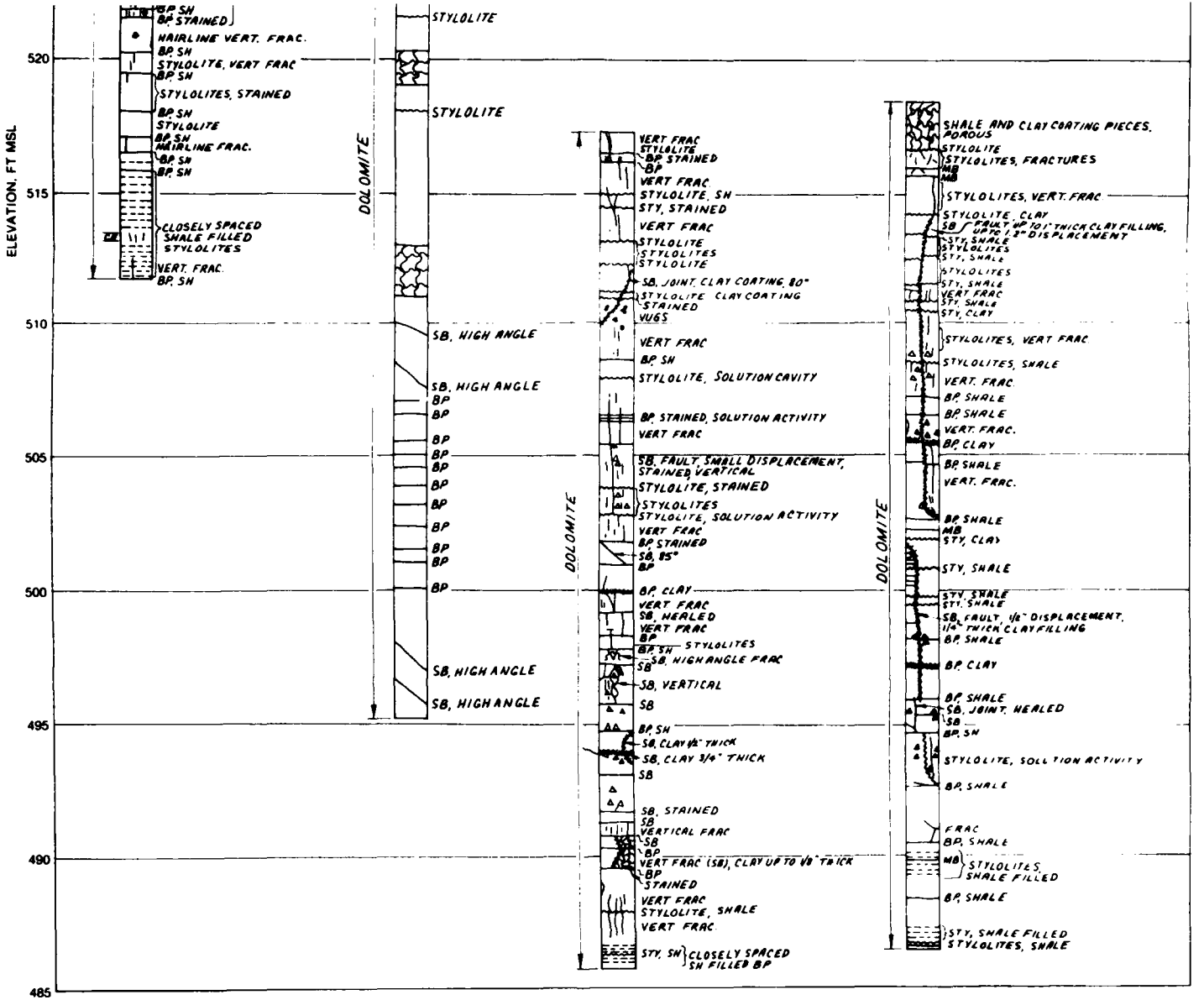

SYMBOLS

BP = BEDDING PLANE
SB = STRUCTURAL BREAK
MB = MECHANICAL BREAK

VUGS
BREAK AT STYLOLITE
SHALE SEAM
FRACTURED ROCK
CHERT NODULES
CLAY SEAM

U.S. ARMY ENGINEER DISTRICT
CORPS OF ENGINEERS

LOCKPORT LOCK
ILLINOIS WATERWAY

BEDROCK STRUCTURAL CHARACTERISTICS
RELEVANT TO FOUNDATIONS

U.S. ARMY ENGINEER
WATERWAYS EXPERIMENT STATION
CORPS OF ENGINEERS

PLATE 6

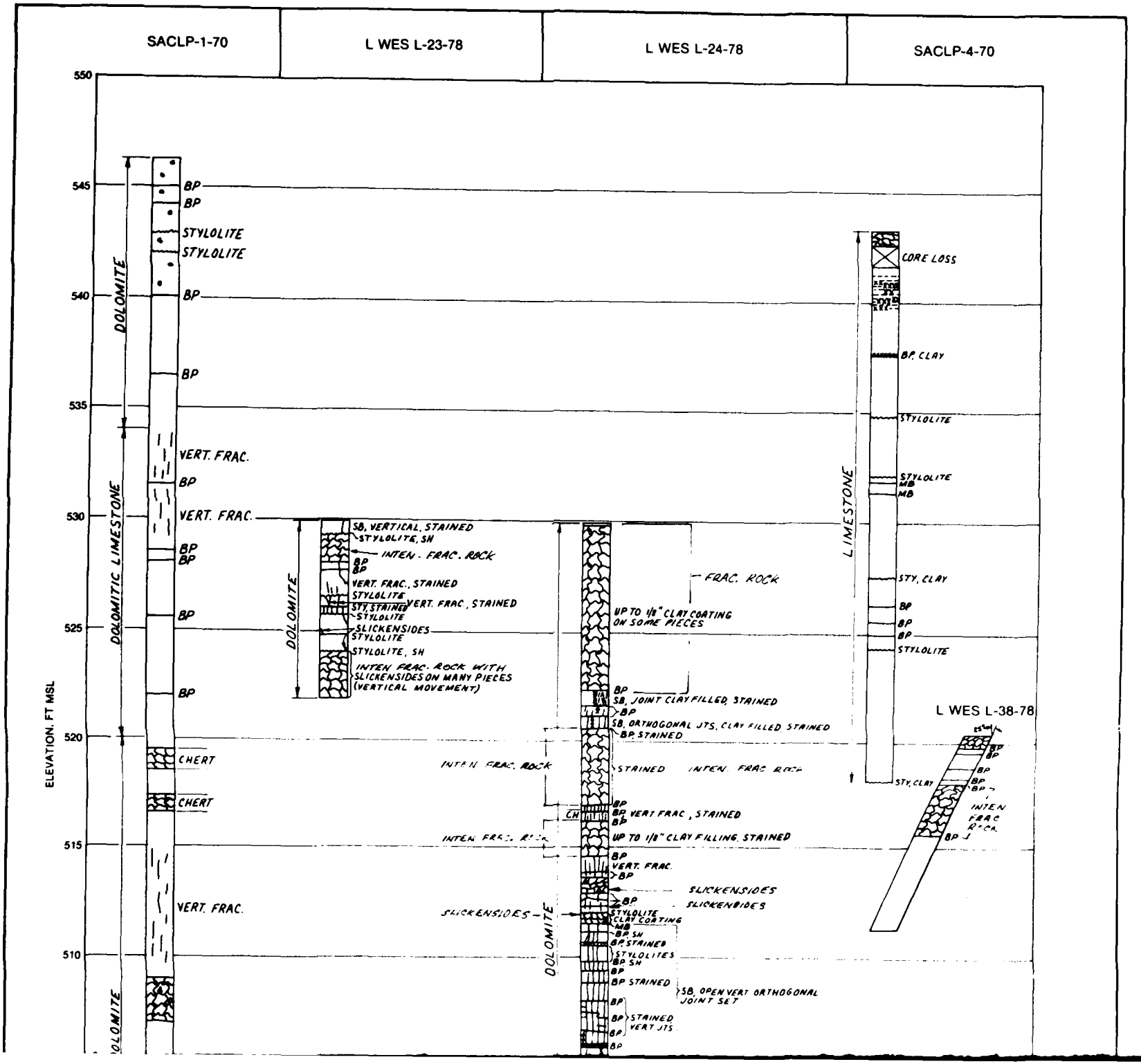
SACLP-1-70
L WES L-23-78
L WES L-24-78
SACLP-4-70
ELEVATION, FT MSL
550
545
540
535
530
525
520
515
510
DOLOMITE
DOLOMITIC LIMESTONE
DOLOMITE
LIMESTONE
DOLOMITE
BP
STYLOLITE
VERT. FRAC.
CHERT
SB, VERTICAL, STAINED
STYLOLITE, SH
INTEN. FRAC. ROCK
VERT. FRAC., STAINED
STYLOLITE
STY, STAINED
SLICKENSIDES
STYLOLITE, SH
INTEN. FRAC. ROCK WITH SLICKENSIDES ON MANY PIECES (VERTICAL MOVEMENT)
FRAC. ROCK
UP TO 1/8" CLAY COATING ON SOME PIECES
SB, JOINT CLAY FILLED, STAINED
SB, ORTHOGONAL JTS, CLAY FILLED STAINED
BP, STAINED
INTEN. FRAC. ROCK
STAINED
CH
UP TO 1/8" CLAY FILLING, STAINED
SLICKENSIDES
STYLOLITE
CLAY COATING
MB
BP, SH
BP, STAINED
STYLOLITES
SB, OPEN VERT ORTHOGONAL JOINT SET
STAINED VERT JTS
CORE LOSS
BP, CLAY
STY, CLAY
L WES L-38-78

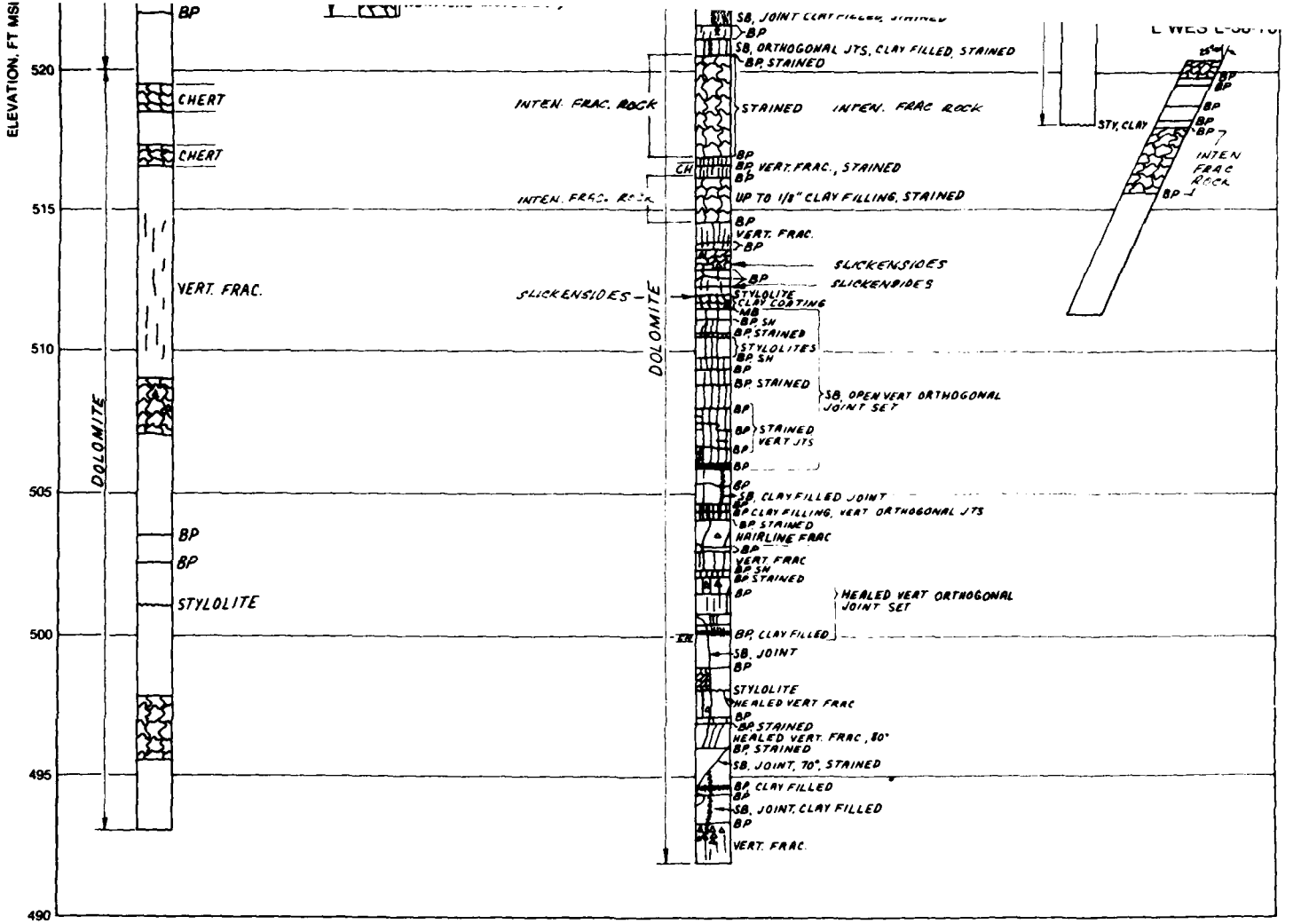

BP = BEDDING PLANE
SB = STRUCTURAL BREAK
MB = MECHANICAL BREAK

SYMBOLS

- FRACTURED ROCK
- VUGS
- SHALE SEAM
- BREAK AT STYLOLITE
- CLAY SEAM
- CHERT NODULES

PREPARED FOR
U. S. ARMY ENGINEER DISTRICT
CORPS OF ENGINEERS
[illegible]
ILLINOIS WATERWAY ILL

BEDROCK STRUCTURAL CHARACTERISTICS
RELEVANT TO FOUNDATIONS

PREPARED BY
DRAWN BY
DATE
SHEET

PREPARED BY
U. S. ARMY ENGINEER
WATERWAYS EXPERIMENT STATION
CORPS OF ENGINEERS

PLATE 7

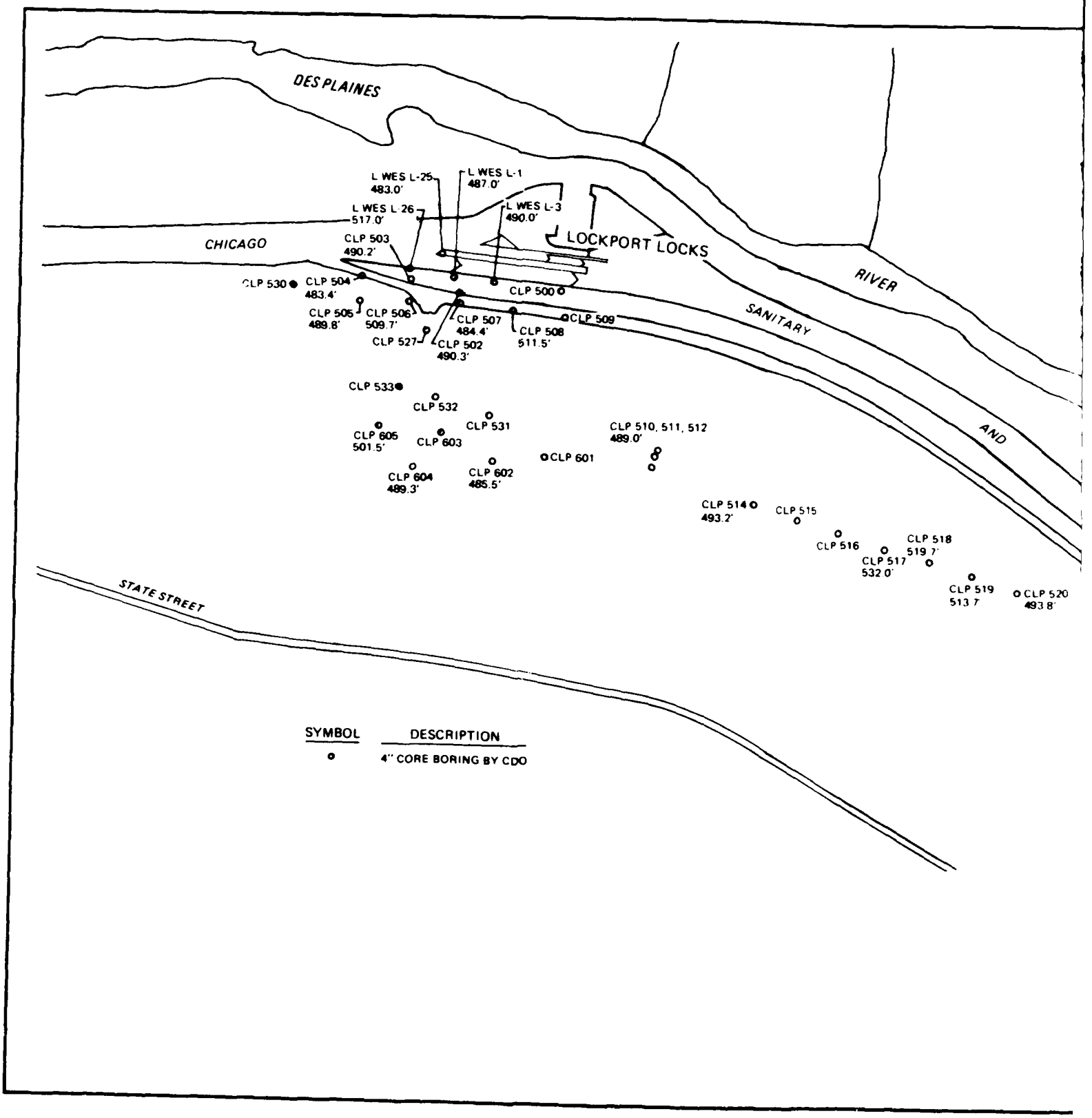
DES PLAINES
L WES L-25
483.0'
L WES L-1
487.0'
L WES L-26
517.0'
L WES L-3
490.0'
CHICAGO
CLP 503
490.2'
LOCKPORT LOCKS
RIVER
CLP 530
CLP 504
483.4'
CLP 500
SANITARY
CLP 505
489.8'
CLP 506
509.7'
CLP 507
484.4'
CLP 509
AND
CLP 527
CLP 502
490.3'
CLP 508
511.5'
CLP 533
CLP 532
CLP 531
CLP 605
501.5'
CLP 603
CLP 510, 511, 512
489.0'
CLP 601
CLP 604
489.3'
CLP 602
485.5'
CLP 514
493.2'
CLP 515
CLP 516
CLP 518
519.7'
CLP 517
532.0'
CLP 519
513.7
CLP 520
493.8'
STATE STREET
SYMBOL
DESCRIPTION
4" CORE BORING BY CDO

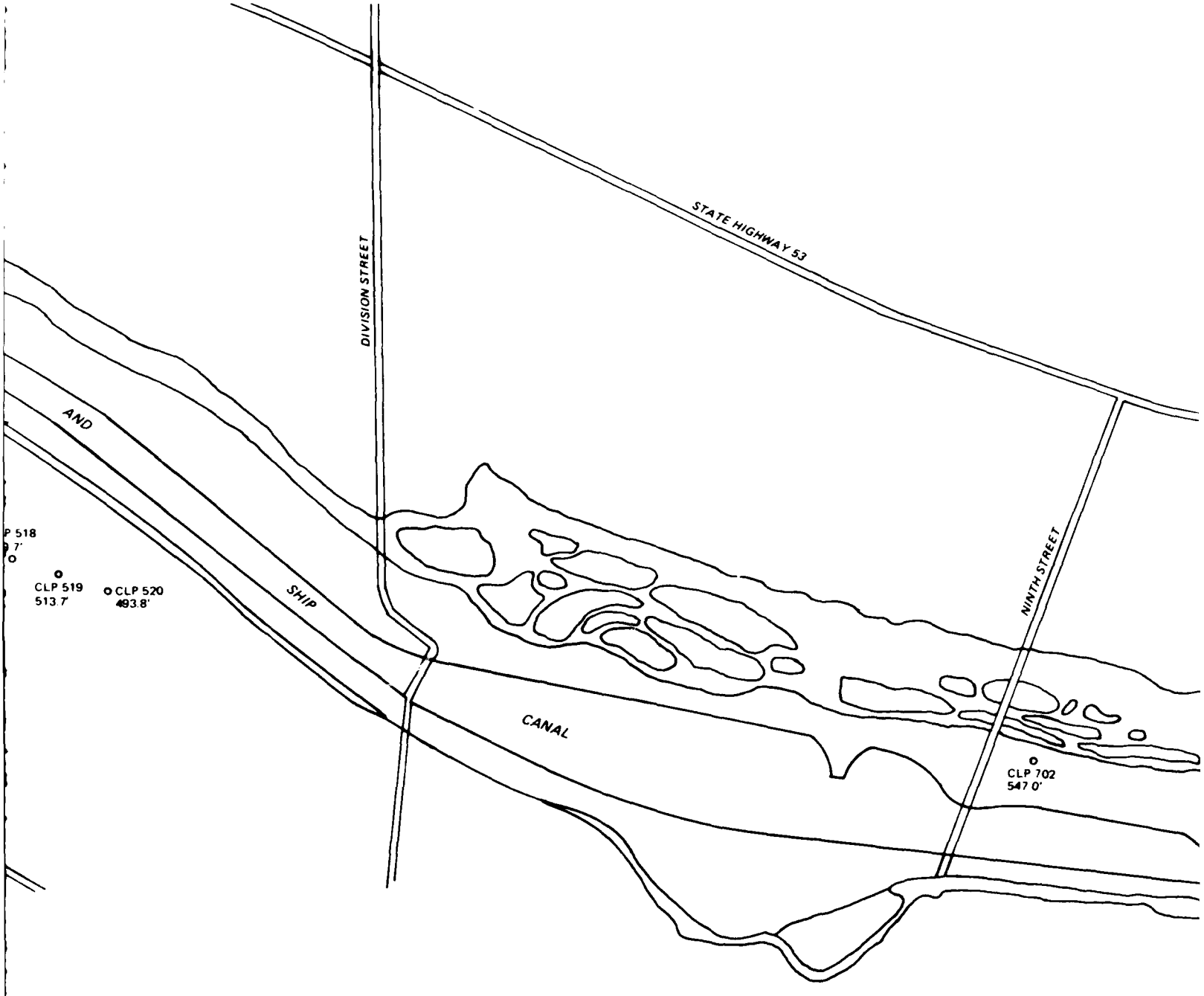

LOCKPOI
ILLINOIS W

SURFACE ELEV
BRANDON BRI

2

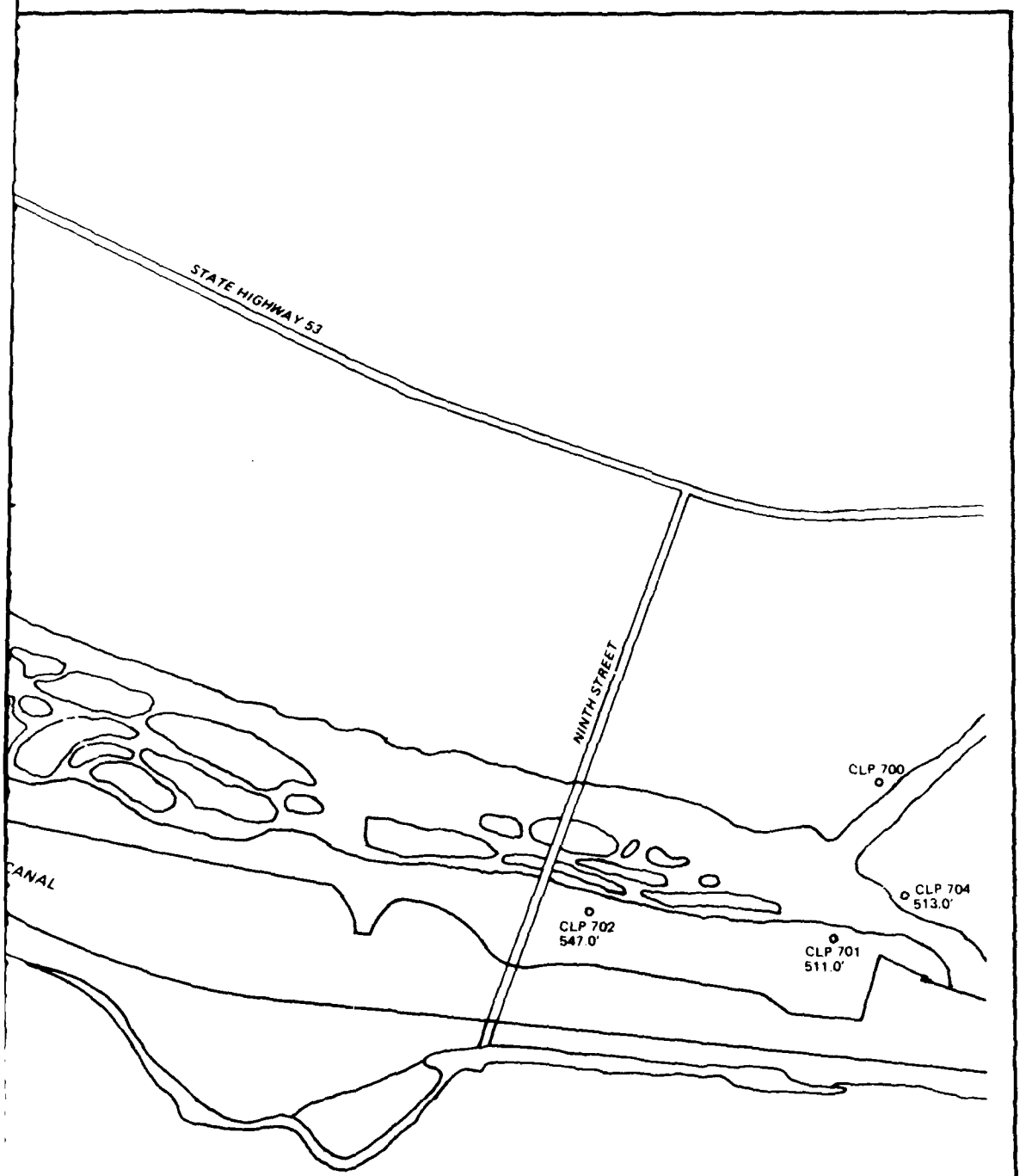

LOCKPORT LOCK
ILLINOIS WATERWAY

SURFACE ELEVATION TOP OF BRANDON BRIDGE MEMBER

PLATE 8

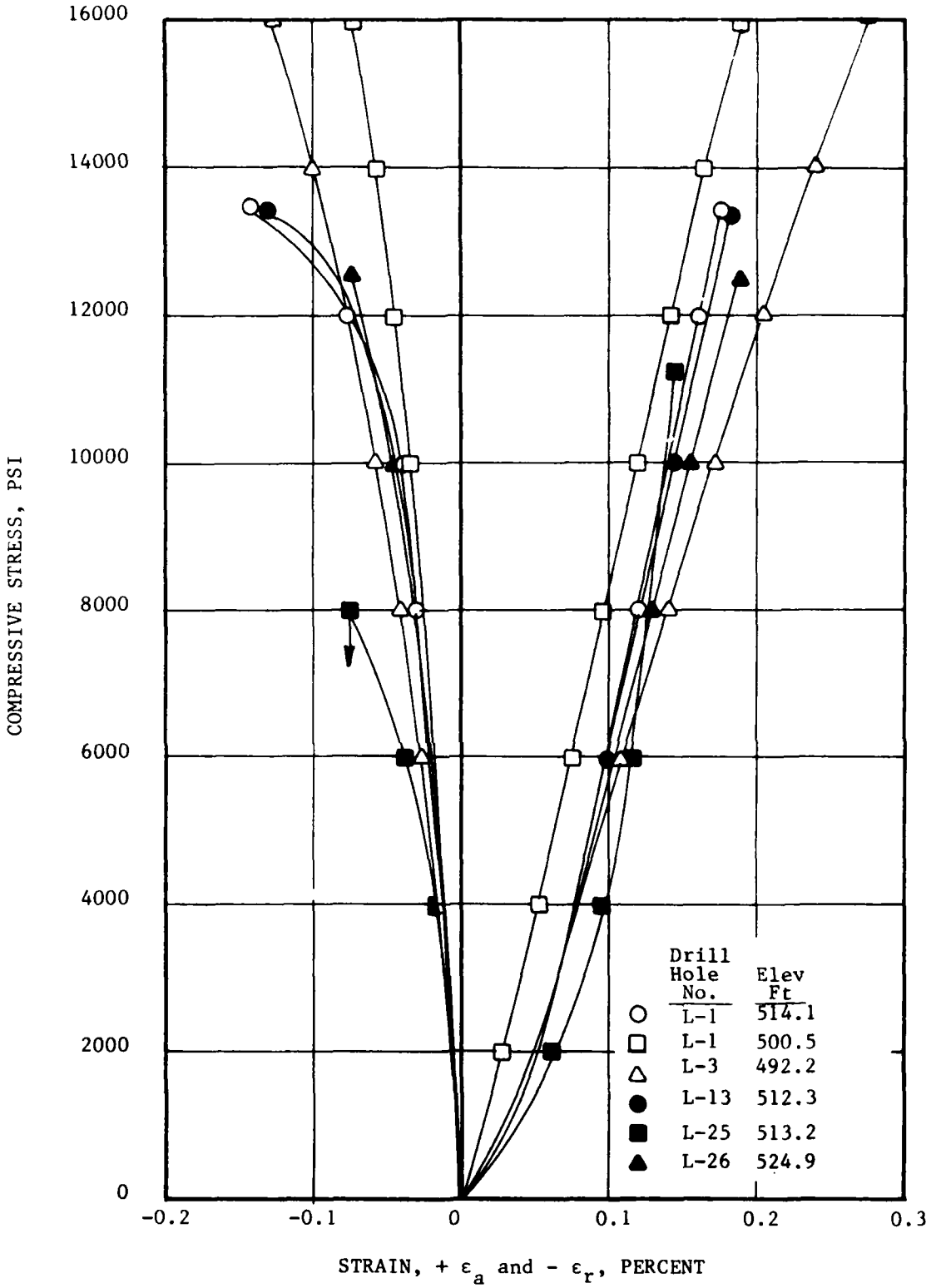

Stree-strain relation for dolomite, Lockport Lock.

PLATE 9

LOCKPORT LOCK

COMPLIANCE & MAJOR REHAB

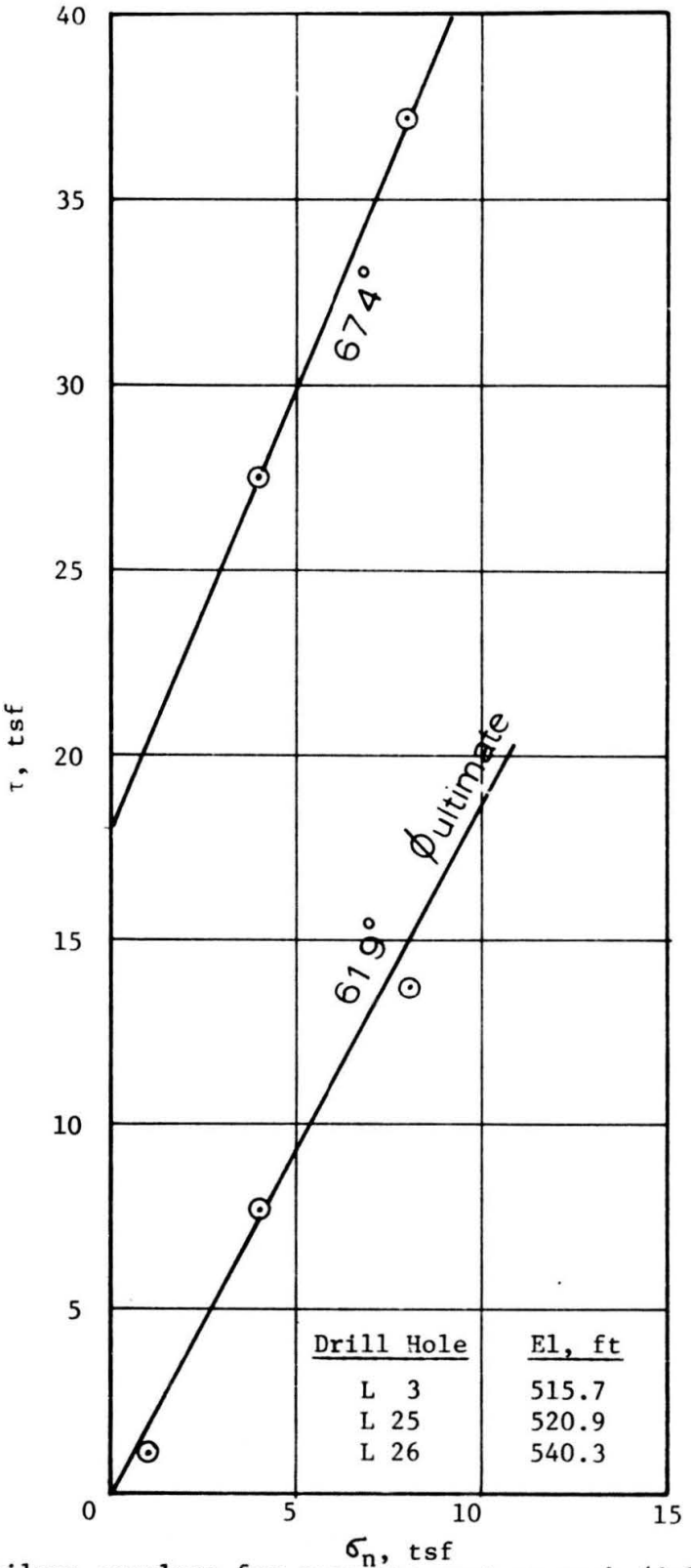

PLATE 10 Failure envelope for concrete cast on rock (dolomite).

LOCKPORT LOCK

COMPLIANCE & MAJOR REHAB

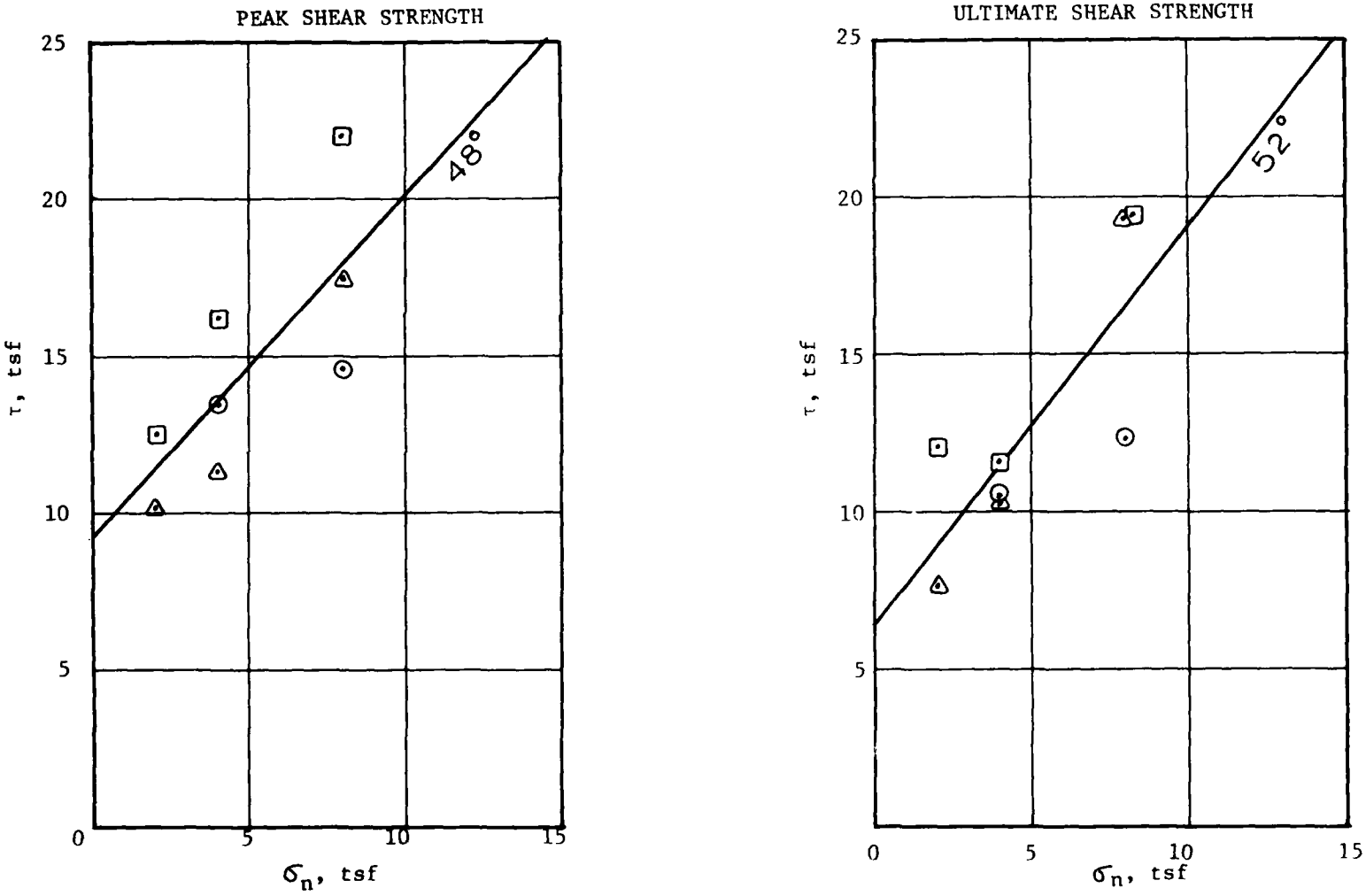

PLATE 11

Failure envelope for filled partings in dolomite.

LOCKPORT LOCK
COMPLIANCE & MAJOR REHAB

PEAK SHEAR STRENGTH

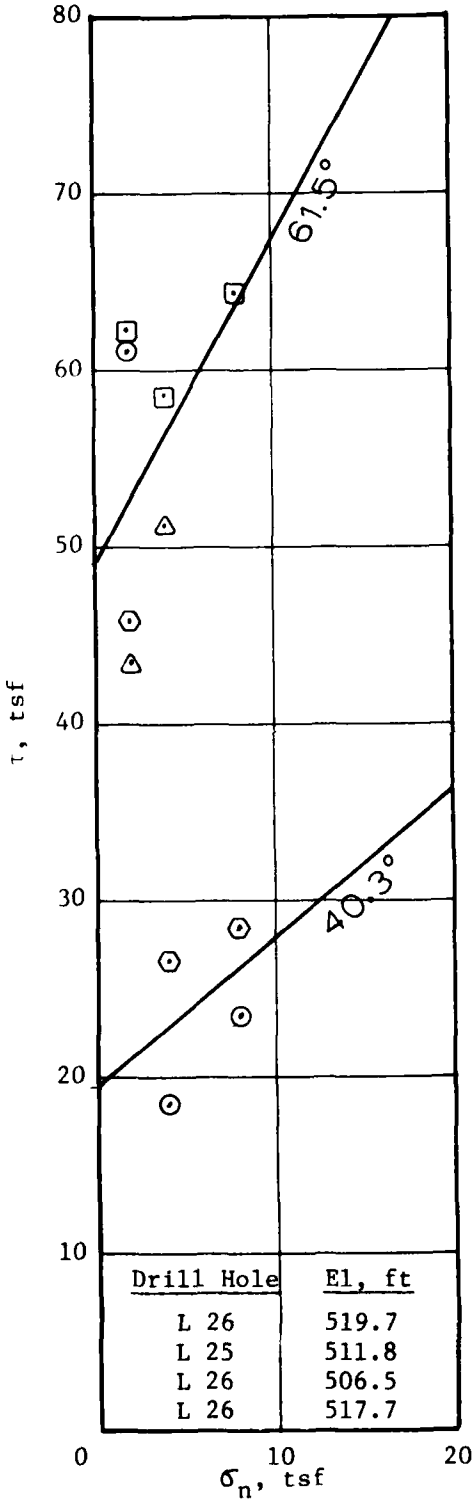

Drill Hole	El, ft
L 26	519.7
L 25	511.8
L 26	506.5
L 26	517.7

ULTIMATE SHEAR STRENGTH

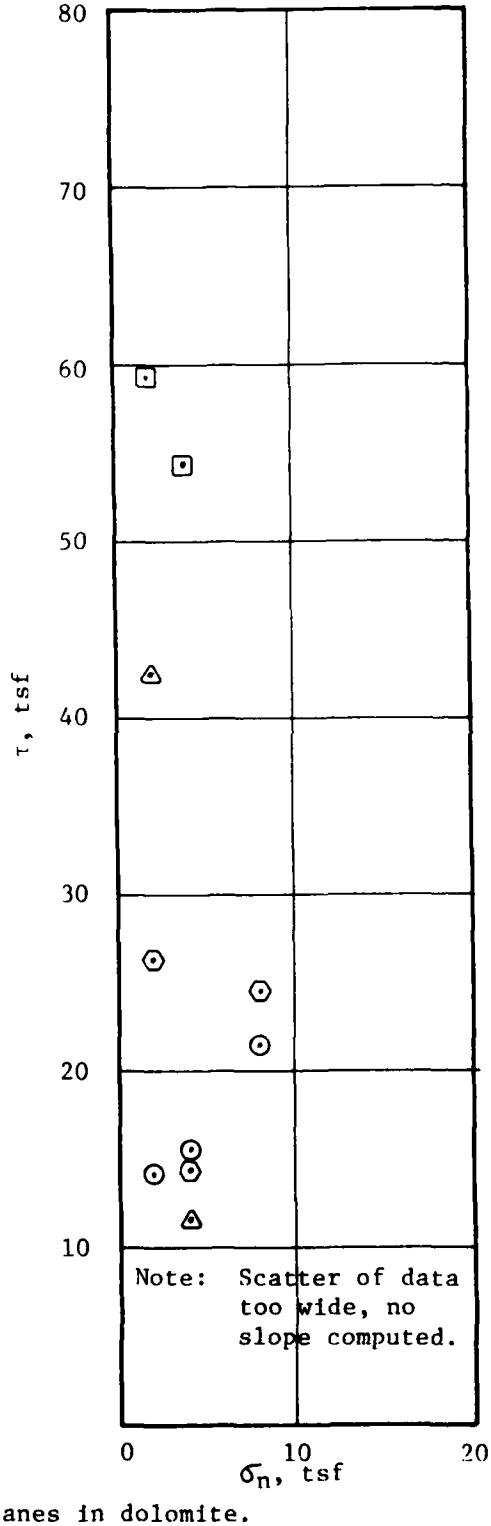

Note: Scatter of data too wide, no slope computed.

Failure envelope for bedding planes in dolomite.

PLATE 12

LOCKPORT LOCK

COMPLIANCE & MAJOR REHAB

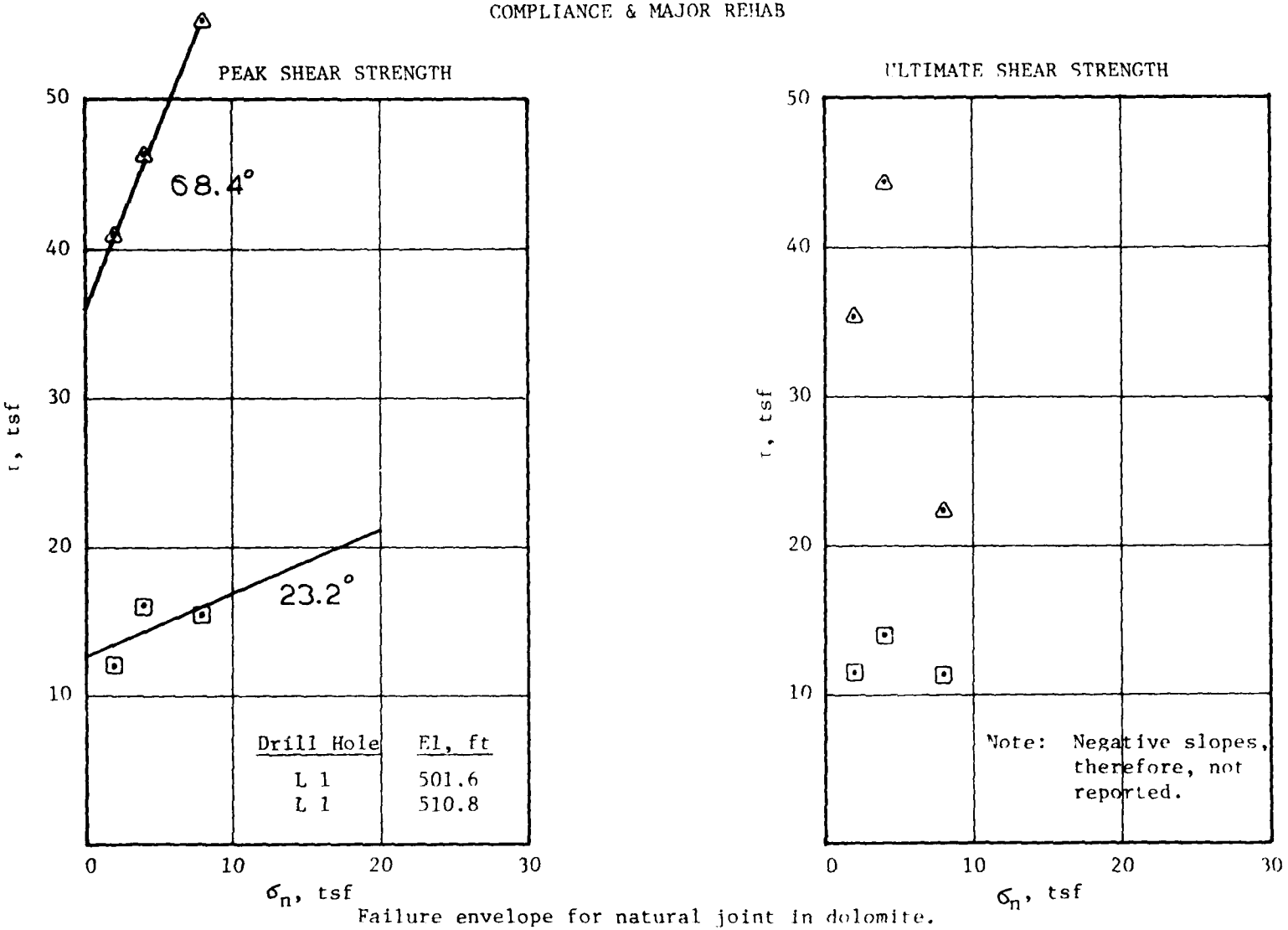

PLATE 13

Failure envelope for natural joint in dolomite.

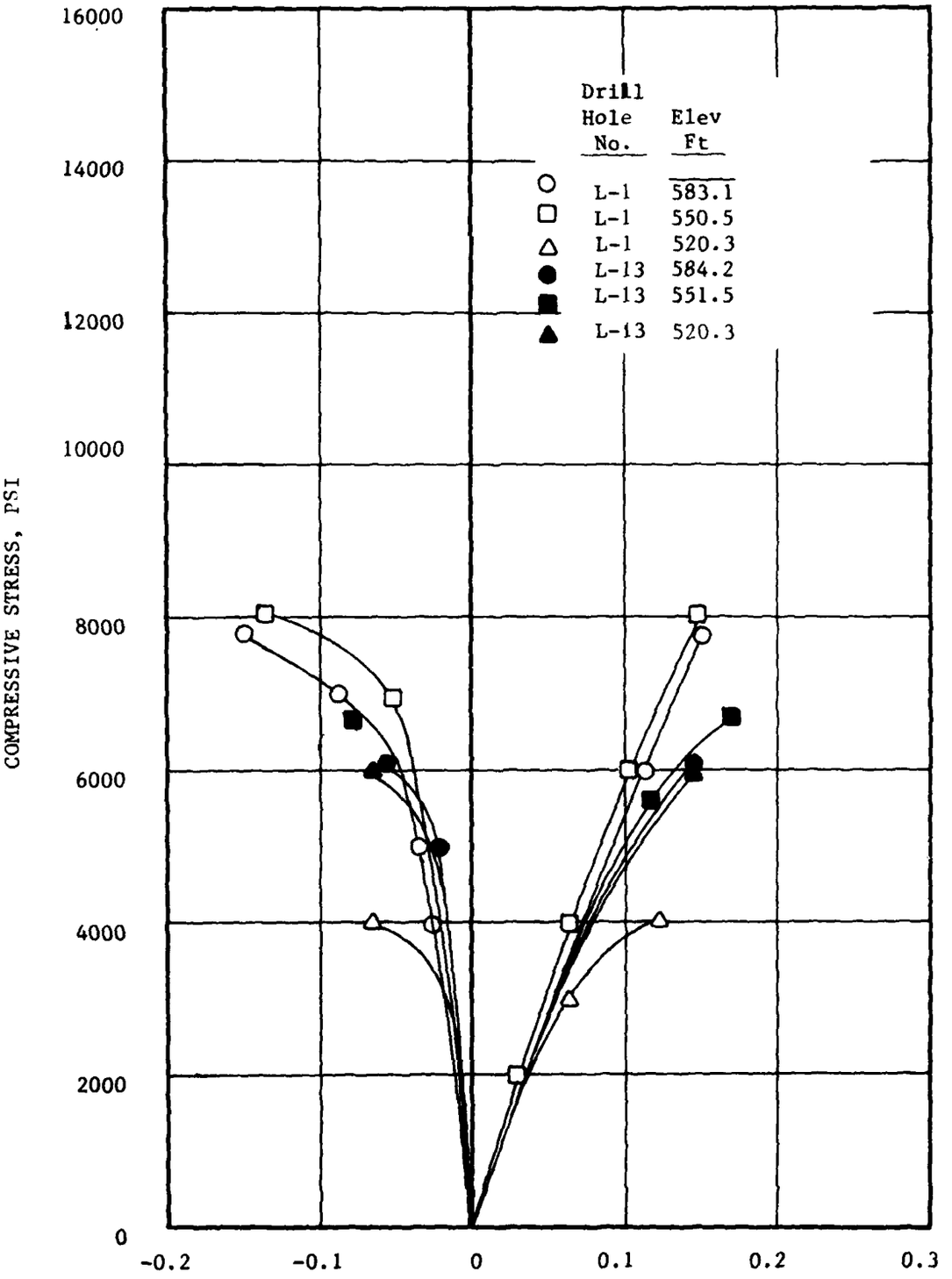

Stress-strain relation for concrete (vertical holes), Lockport Lock.

PLATE 14

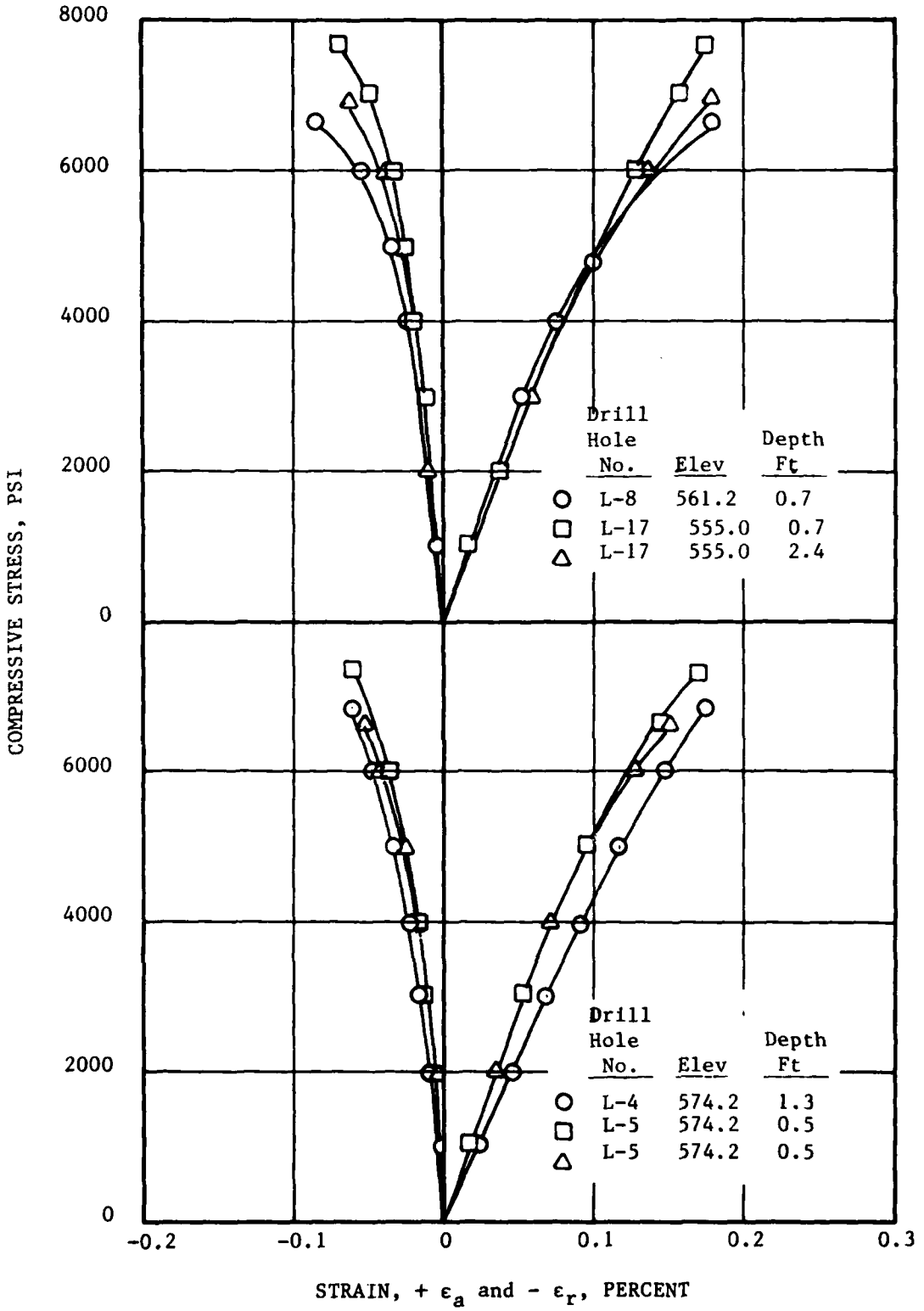

Stress-strain relation for concrete (horizontal holes) land wall chamber side, near surface and deeper core; Lockport Lock

PLATE 15

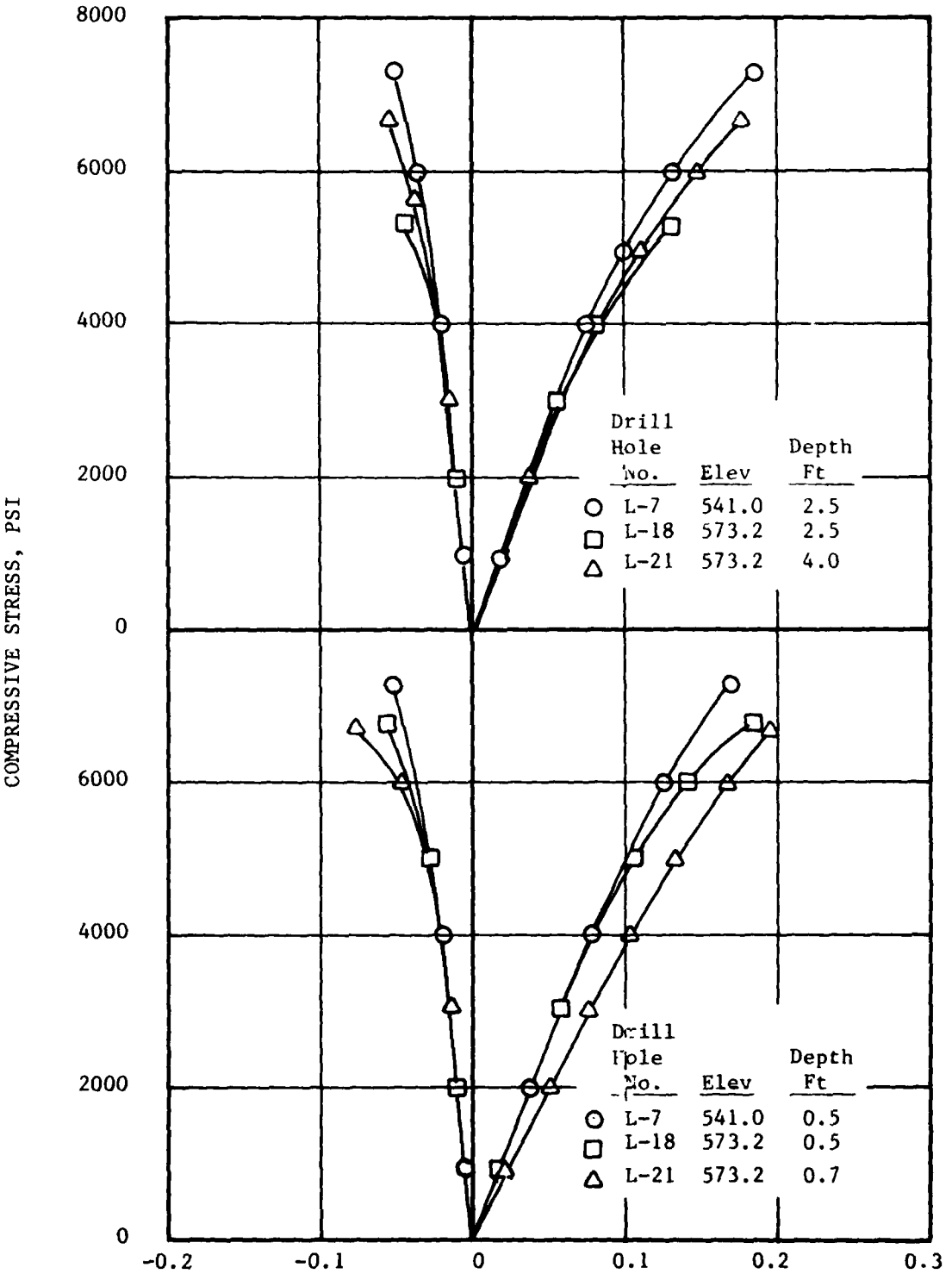

Stress-strain relation for concrete (horizontal holes) river wall chamber side, near surface and deeper core; Lockport Lock.

PLATE 16

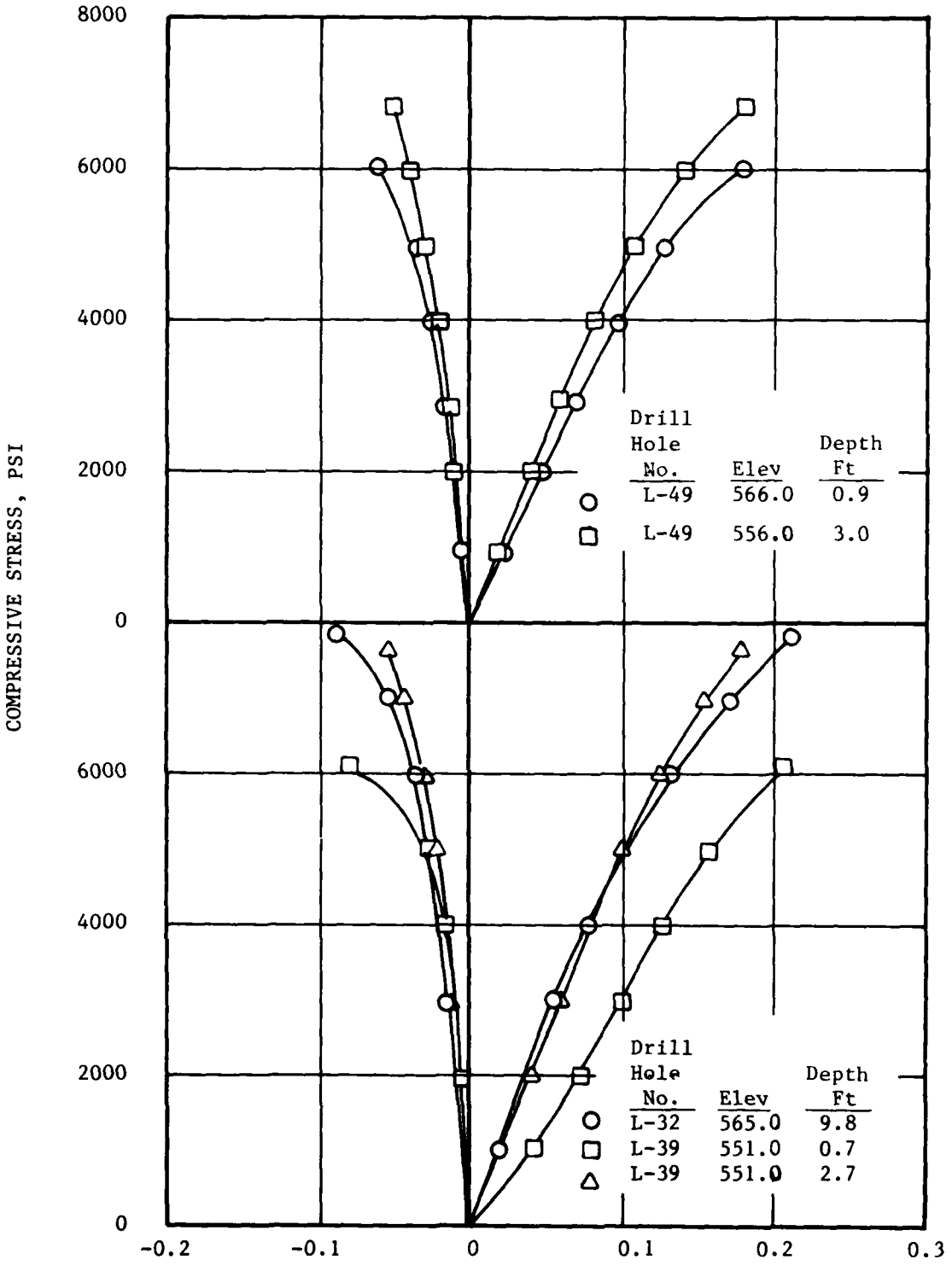

Stress-strain relation for concrete (horizontal holes) river side of river wall, near surface and deeper core; Lockport Lock.

PLATE 17

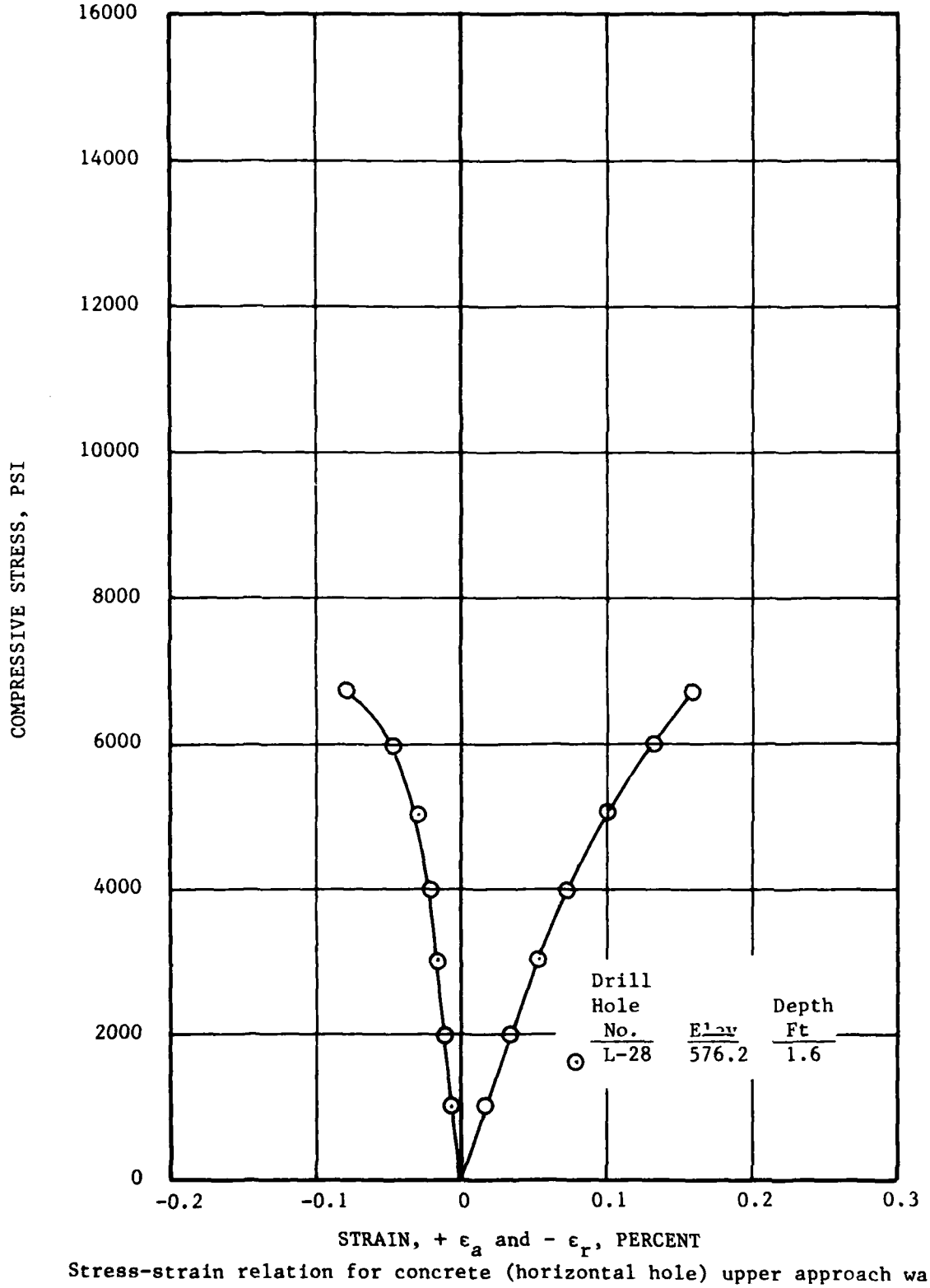

Stress-strain relation for concrete (horizontal hole) upper approach wall, Lockport Lock.

PLATE 18

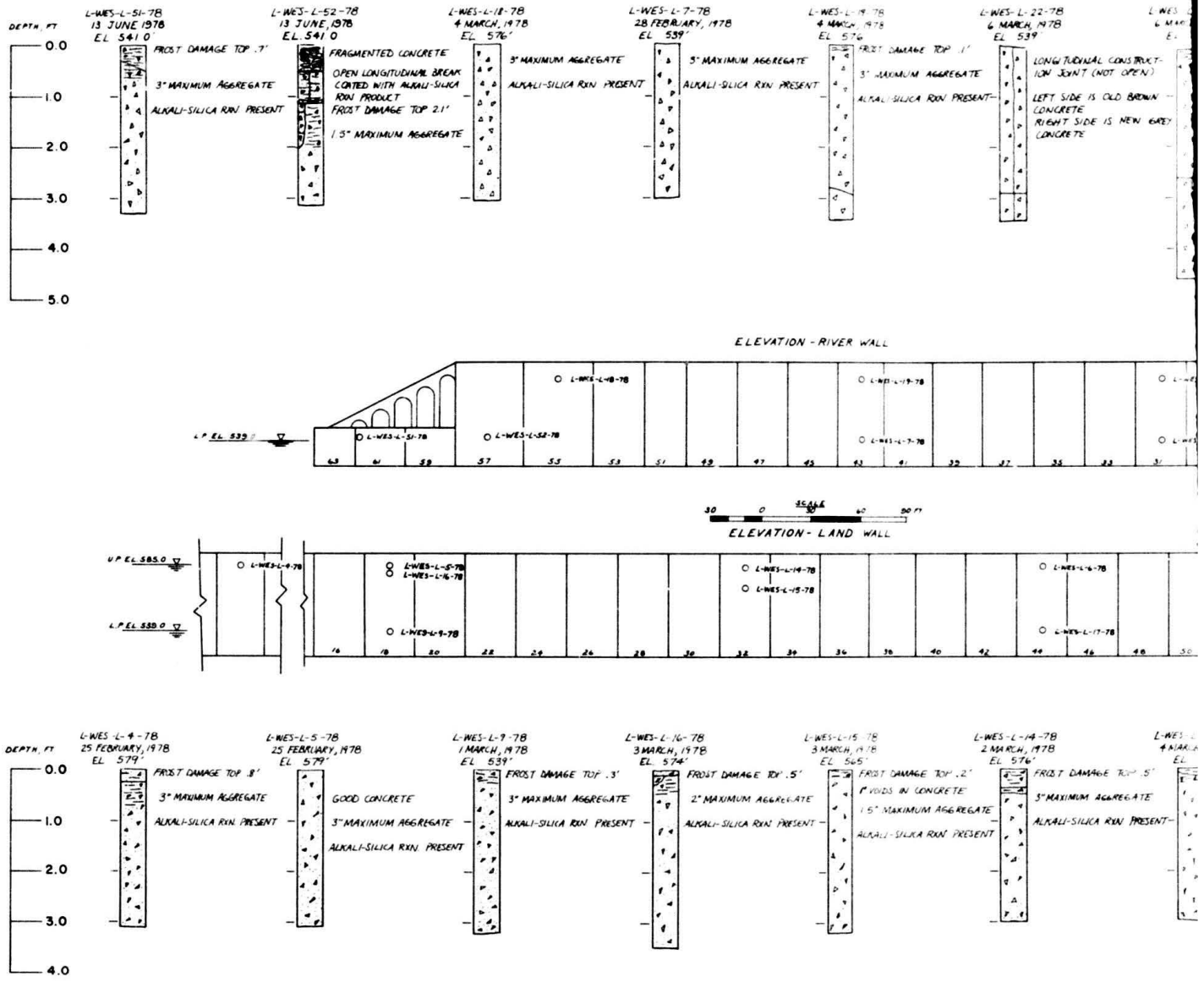
DEPTH, FT
0.0
1.0
2.0
3.0
4.0
5.0
L-WES-L-51-78
13 JUNE 1978
EL 541.0
FROST DAMAGE TOP .7'
3" MAXIMUM AGGREGATE
ALKALI-SILICA RXN PRESENT
L-WES-L-52-78
13 JUNE, 1978
EL 541.0
FRAGMENTED CONCRETE
OPEN LONGITUDINAL BREAK COATED WITH ALKALI-SILICA RXN PRODUCT
FROST DAMAGE TOP 2.1'
1.5" MAXIMUM AGGREGATE
L-WES-L-18-78
4 MARCH, 1978
EL 576'
3" MAXIMUM AGGREGATE
ALKALI-SILICA RXN PRESENT
L-WES-L-7-78
28 FEBRUARY, 1978
EL 539'
3" MAXIMUM AGGREGATE
ALKALI-SILICA RXN PRESENT
L-WES-L-19-78
4 MARCH, 1978
EL 576
FROST DAMAGE TOP .1'
3" MAXIMUM AGGREGATE
ALKALI-SILICA RXN PRESENT
L-WES-L-22-78
6 MARCH, 1978
EL 539
LONGITUDINAL CONSTRUCTION JOINT (NOT OPEN)
LEFT SIDE IS OLD BROWN CONCRETE
RIGHT SIDE IS NEW GREY CONCRETE
ELEVATION - RIVER WALL
L-WES-L-18-78
L-WES-L-19-78
L-WES-L-7-78
L-WES-L-51-78
L-WES-L-52-78
L P EL 539.0
63 61 59 57 55 53 51 49 47 45 43 41 39 37 35 33 31
SCALE
30 0 30 60 90 FT
ELEVATION - LAND WALL
U P EL 585.0
L P EL 580.0
L-WES-L-4-78
L-WES-L-5-78
L-WES-L-16-78
L-WES-L-9-78
L-WES-L-19-78
L-WES-L-15-78
L-WES-L-6-78
L-WES-L-17-78
16 18 20 22 24 26 28 30 32 34 36 38 40 42 44 46 48 50
DEPTH, FT
0.0
1.0
2.0
3.0
4.0
L-WES-L-4-78
25 FEBRUARY, 1978
EL 579'
FROST DAMAGE TOP .8'
3" MAXIMUM AGGREGATE
ALKALI-SILICA RXN PRESENT
L-WES-L-5-78
25 FEBRUARY, 1978
EL 579'
GOOD CONCRETE
3" MAXIMUM AGGREGATE
ALKALI-SILICA RXN PRESENT
L-WES-L-9-78
1 MARCH, 1978
EL 539'
FROST DAMAGE TOP .3'
3" MAXIMUM AGGREGATE
ALKALI-SILICA RXN PRESENT
L-WES-L-16-78
3 MARCH, 1978
EL 574'
FROST DAMAGE TOP .5'
2" MAXIMUM AGGREGATE
ALKALI-SILICA RXN PRESENT
L-WES-L-15-78
3 MARCH, 1978
EL 565'
FROST DAMAGE TOP .2'
1" VOIDS IN CONCRETE
1.5" MAXIMUM AGGREGATE
ALKALI-SILICA RXN PRESENT
L-WES-L-14-78
2 MARCH, 1978
EL 576'
FROST DAMAGE TOP .5'
3" MAXIMUM AGGREGATE
ALKALI-SILICA RXN PRESENT

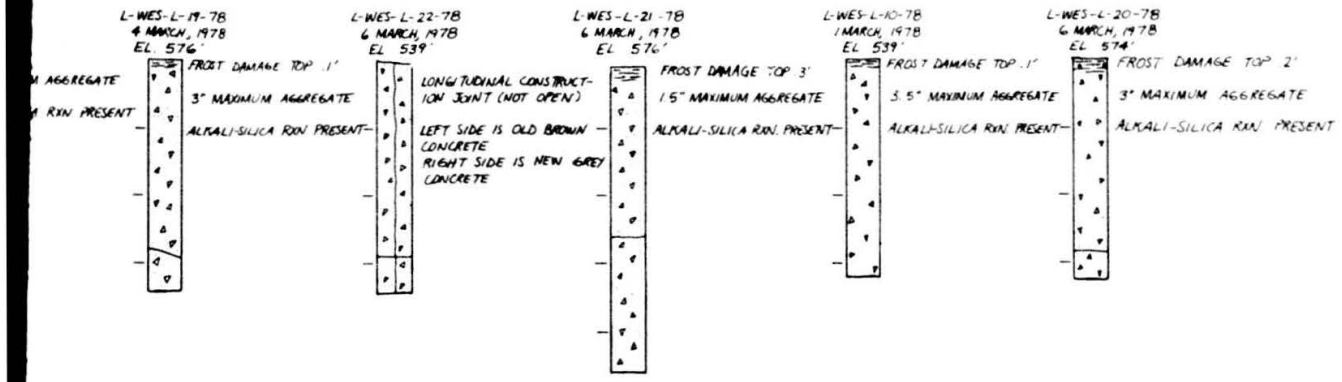

ELEVATION - RIVER WALL

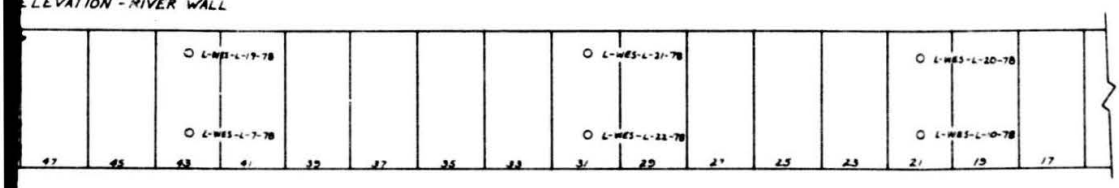

0 15 30 60 90 FT

ELEVATION - LAND WALL

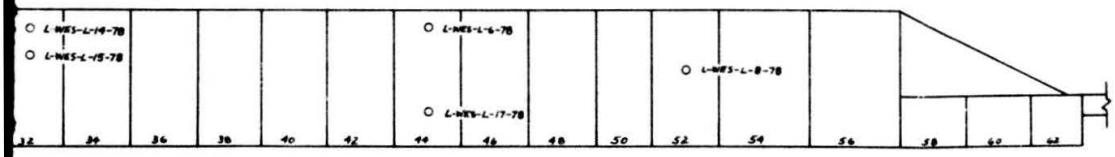

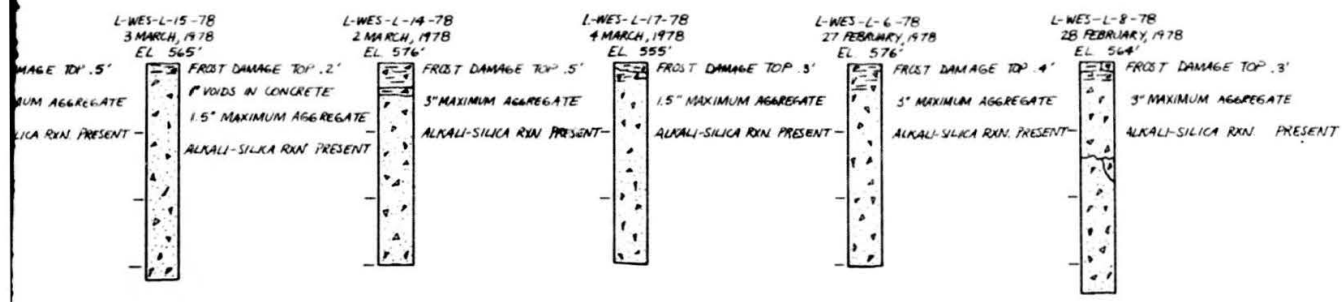

MAJOR REHABILITATION AND COMPLIANCE PHASES

LOCKPORT LOCK
ILLINOIS WATERWAY

CONCRETE CORE PROFILES
RIVER WALL AND LAND WALL

2

PLATE 19

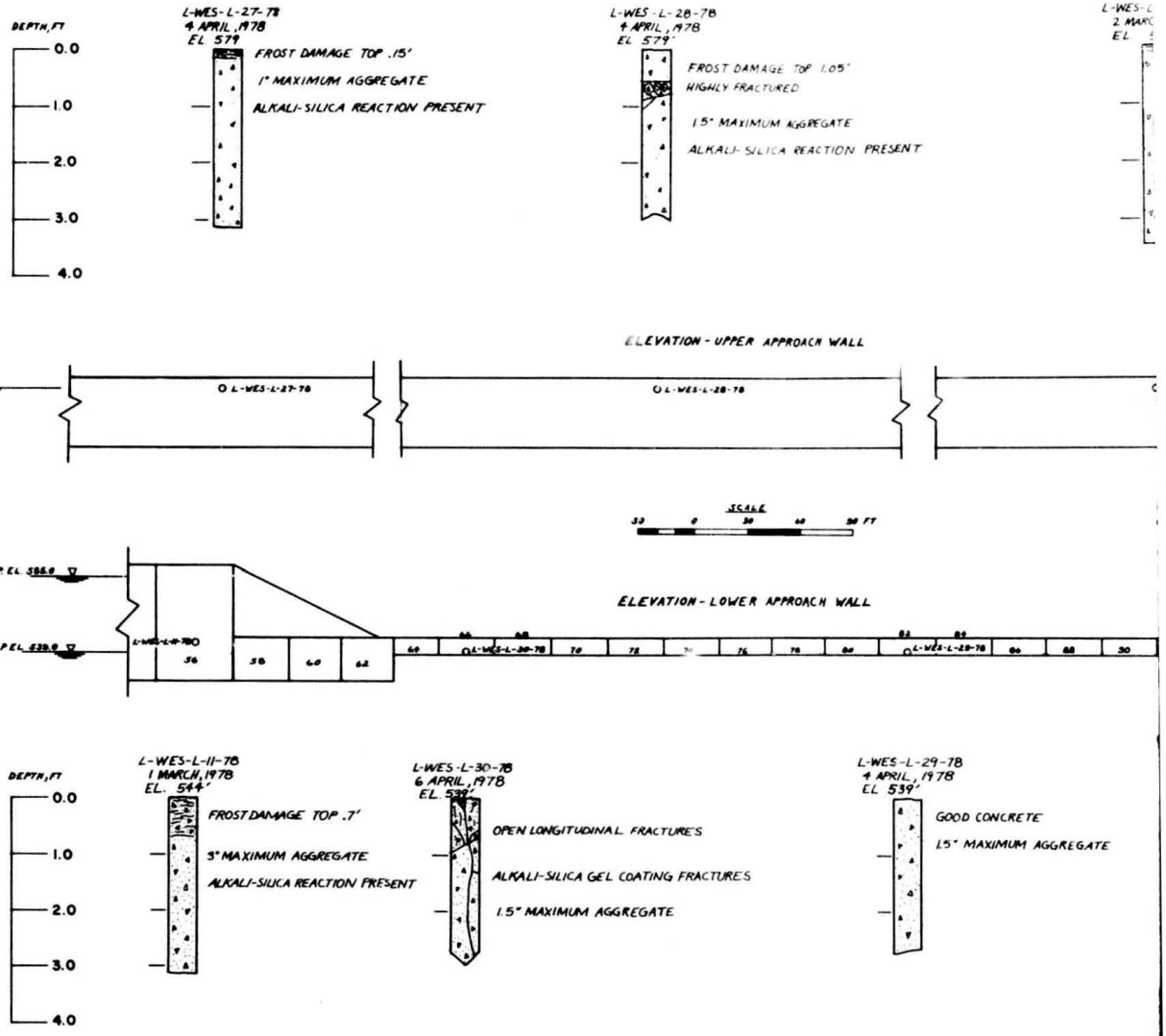
DEPTH, FT
0.0
1.0
2.0
3.0
4.0
L-WES-L-27-78
4 APRIL, 1978
EL 579
FROST DAMAGE TOP .15'
1" MAXIMUM AGGREGATE
ALKALI-SILICA REACTION PRESENT
L-WES-L-28-78
4 APRIL, 1978
EL 579'
FROST DAMAGE TOP 1.05'
HIGHLY FRACTURED
1.5" MAXIMUM AGGREGATE
ALKALI-SILICA REACTION PRESENT
ELEVATION - UPPER APPROACH WALL
U.P. EL. 586.0
L-WES-L-27-78
L-WES-L-28-78
SCALE
30 0 30 60 90 FT
U.P. EL. 586.0
L.P. EL. 539.0
ELEVATION - LOWER APPROACH WALL
L-WES-L-30-78
L-WES-L-29-78
DEPTH, FT
0.0
1.0
2.0
3.0
4.0
L-WES-L-11-78
1 MARCH, 1978
EL. 544'
FROST DAMAGE TOP .7'
3" MAXIMUM AGGREGATE
ALKALI-SILICA REACTION PRESENT
L-WES-L-30-78
6 APRIL, 1978
EL. 539'
OPEN LONGITUDINAL FRACTURES
ALKALI-SILICA GEL COATING FRACTURES
1.5" MAXIMUM AGGREGATE
L-WES-L-29-78
4 APRIL, 1978
EL 539'
GOOD CONCRETE
1.5" MAXIMUM AGGREGATE

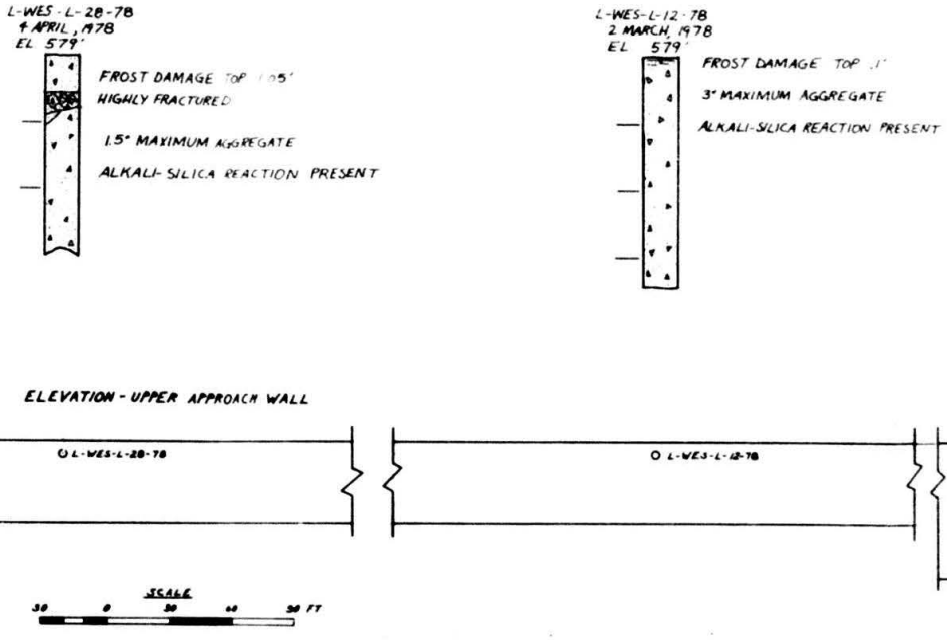

MAJOR REHABILITATION AND COMPLIANCE PHASES

LOCKPORT LOCK
ILLINOIS WATERWAY

CONCRETE CORE PROFILE
UPPER AND LOWER APPROACH WALLS

PLATE 20

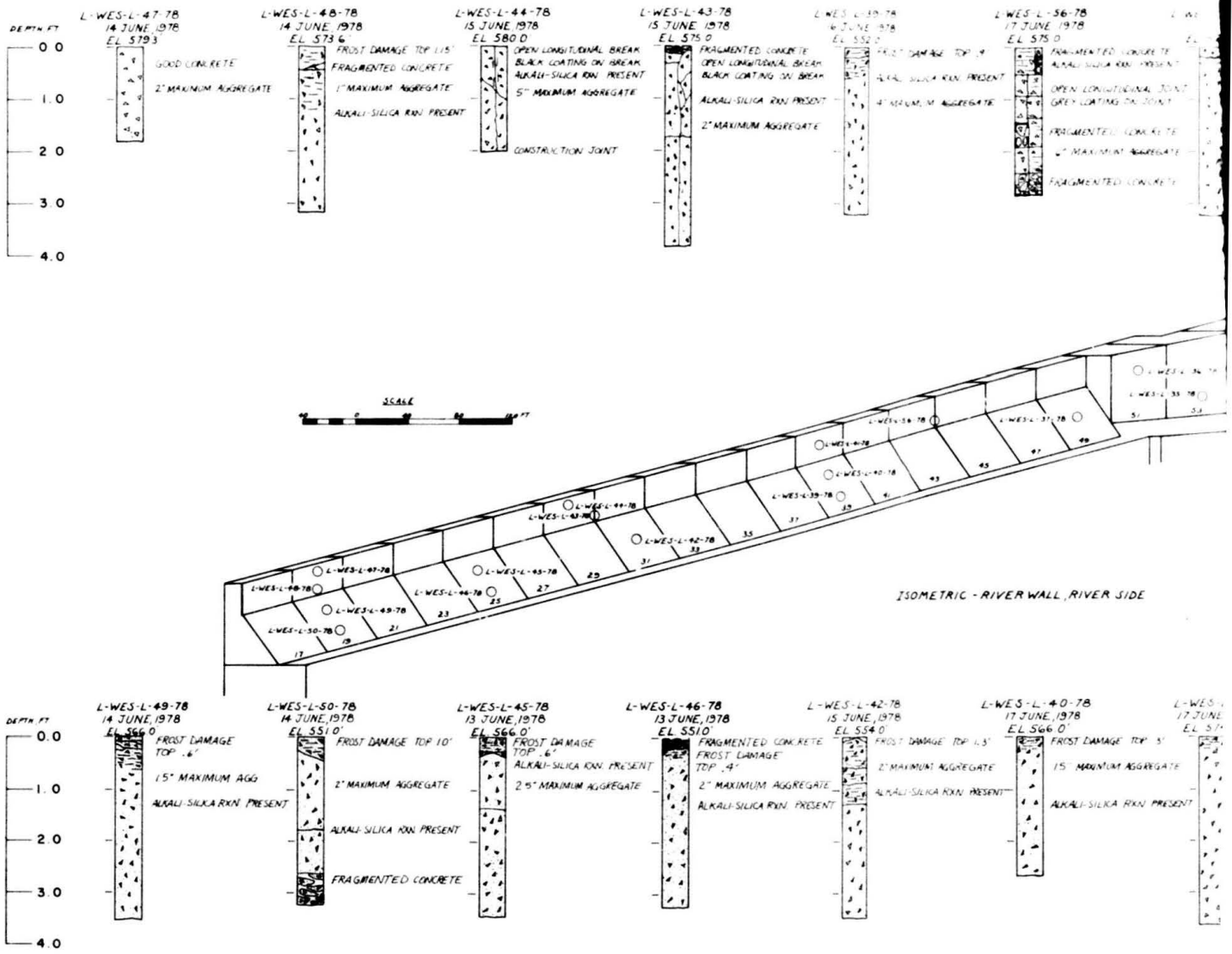
DEPTH FT
0.0
1.0
2.0
3.0
4.0
L-WES-L-47-78
14 JUNE, 1978
EL 579.3
GOOD CONCRETE
2" MAXIMUM AGGREGATE
L-WES-L-48-78
14 JUNE, 1978
EL 573.6
FROST DAMAGE TOP 1.5'
FRAGMENTED CONCRETE
1" MAXIMUM AGGREGATE
ALKALI-SILICA RXN PRESENT
L-WES-L-44-78
15 JUNE, 1978
EL 580.0
OPEN LONGITUDINAL BREAK
BLACK COATING ON BREAK
ALKALI-SILICA RXN PRESENT
5" MAXIMUM AGGREGATE
CONSTRUCTION JOINT
L-WES-L-43-78
15 JUNE, 1978
EL 575.0
FRAGMENTED CONCRETE
OPEN LONGITUDINAL BREAK
BLACK COATING ON BREAK
ALKALI-SILICA RXN PRESENT
2" MAXIMUM AGGREGATE
L-WES-L-39-78
16 JUNE, 1978
EL 552.2
FROST DAMAGE TOP 1.9'
ALKALI-SILICA RXN PRESENT
4" MAXIMUM AGGREGATE
L-WES-L-36-78
17 JUNE, 1978
EL 575.0
FRAGMENTED CONCRETE
ALKALI-SILICA RXN PRESENT
OPEN LONGITUDINAL JOINT
GREY COATING ON JOINT
FRAGMENTED CONCRETE
2" MAXIMUM AGGREGATE
FRAGMENTED CONCRETE
SCALE
0
50
100 FT
L-WES-L-47-78
L-WES-L-48-78
L-WES-L-49-78
L-WES-L-50-78
L-WES-L-45-78
L-WES-L-46-78
L-WES-L-42-78
L-WES-L-40-78
L-WES-L-39-78
L-WES-L-37-78
L-WES-L-36-78
L-WES-L-35-78
ISOMETRIC - RIVER WALL, RIVER SIDE
DEPTH FT
0.0
1.0
2.0
3.0
4.0
L-WES-L-49-78
14 JUNE, 1978
EL 566.0
FROST DAMAGE TOP .6'
15" MAXIMUM AGG
ALKALI-SILICA RXN PRESENT
L-WES-L-50-78
14 JUNE, 1978
EL 551.0
FROST DAMAGE TOP 1.0'
2" MAXIMUM AGGREGATE
ALKALI-SILICA RXN PRESENT
FRAGMENTED CONCRETE
L-WES-L-45-78
13 JUNE, 1978
EL 566.0'
FROST DAMAGE
TOP .6'
ALKALI-SILICA RXN PRESENT
2.5" MAXIMUM AGGREGATE
L-WES-L-46-78
13 JUNE, 1978
EL 551.0'
FRAGMENTED CONCRETE
FROST DAMAGE
TOP .4'
2" MAXIMUM AGGREGATE
ALKALI-SILICA RXN PRESENT
L-WES-L-42-78
15 JUNE, 1978
EL 554.0
FROST DAMAGE TOP 1.5'
2" MAXIMUM AGGREGATE
ALKALI-SILICA RXN PRESENT
L-WES-L-40-78
17 JUNE, 1978
EL 566.0'
FROST DAMAGE TOP .5'
1.5" MAXIMUM AGGREGATE
ALKALI-SILICA RXN PRESENT

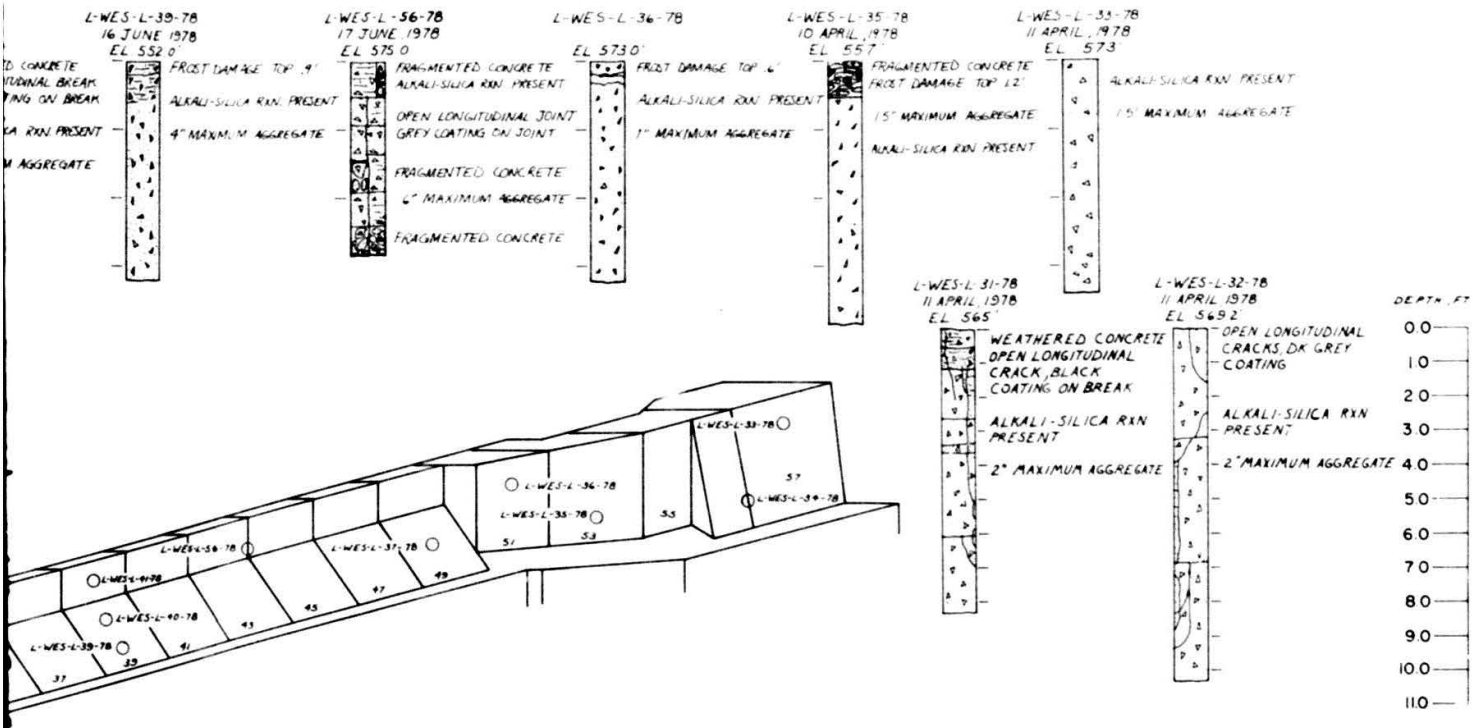

ISOMETRIC - RIVER WALL, RIVER SIDE

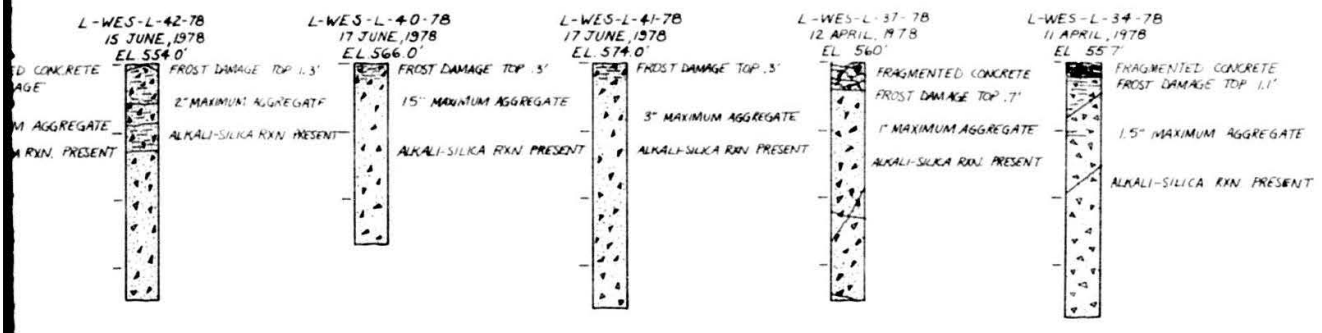

MAJOR REHABILITATION AND COMPLIANCE PHASES

LOCKPORT LOCK
ILLINOIS WATERWAY

CONCRETE CORE PROFILES
RIVER WALL, RIVER SIDE

2

PLATE 21

APPENDIX A

PHOTOGRAPHS OF EXPOSED CONCRETE SURFACES EXAMINED DURING SIGNIFICANT CRACK SURVEY

LOCKPORT LOCK, ILLINOIS WATERWAY

CHICAGO DISTRICT

Figure A1. Lockside face, cable gallery, river wall monolith 7, view 1

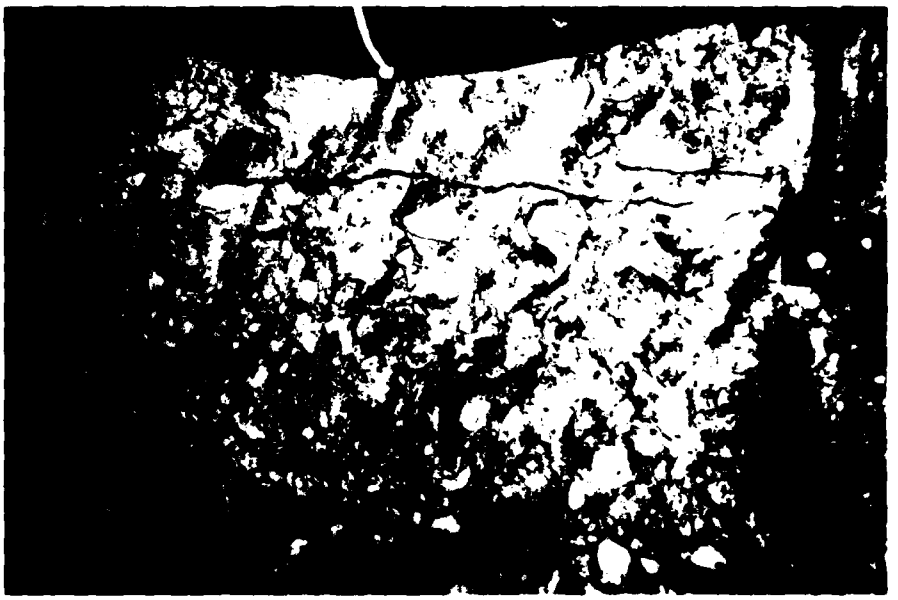

Figure A2. Lockside face, cable gallery, river wall monolith 7, view 2

Figure A3. Upstream face at lockside turn of river wall, cable gallery, monolith 11

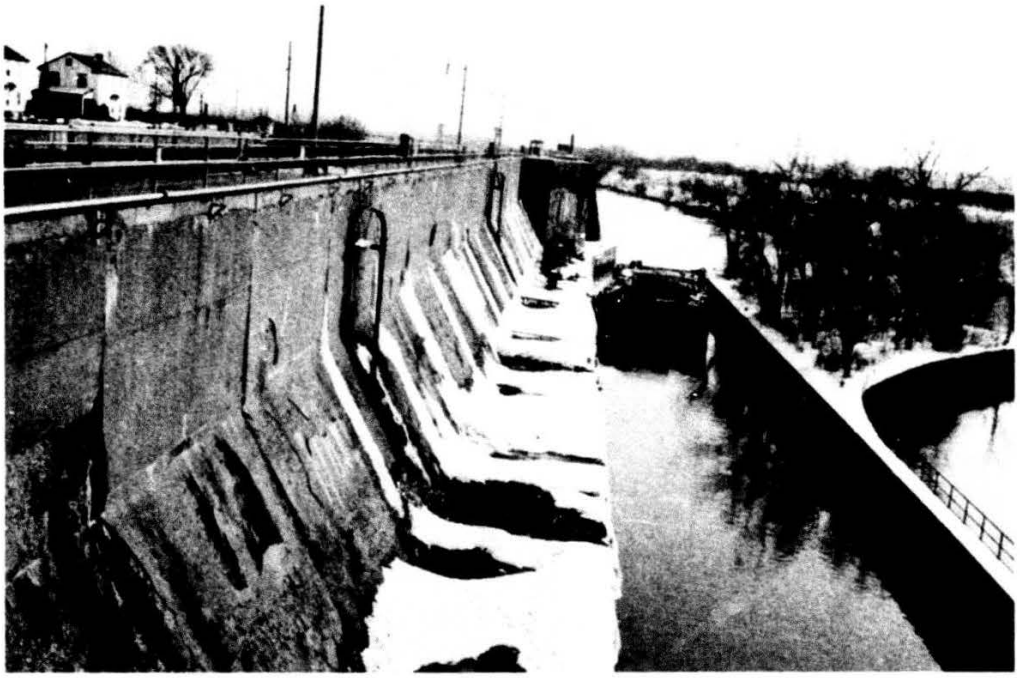

Figure A4. River face, river wall odd-numbered monoliths 17 through 49

Figure A5. River face, river wall monolith joint 17-19

Figure A6. River face, river wall monolith joint 19-21

Figure A7. River face, river wall monolith joint 21-23

Figure A8. River face, river wall monolith joint 23-25

Figure A9. River face, river wall monolith joint 25-47

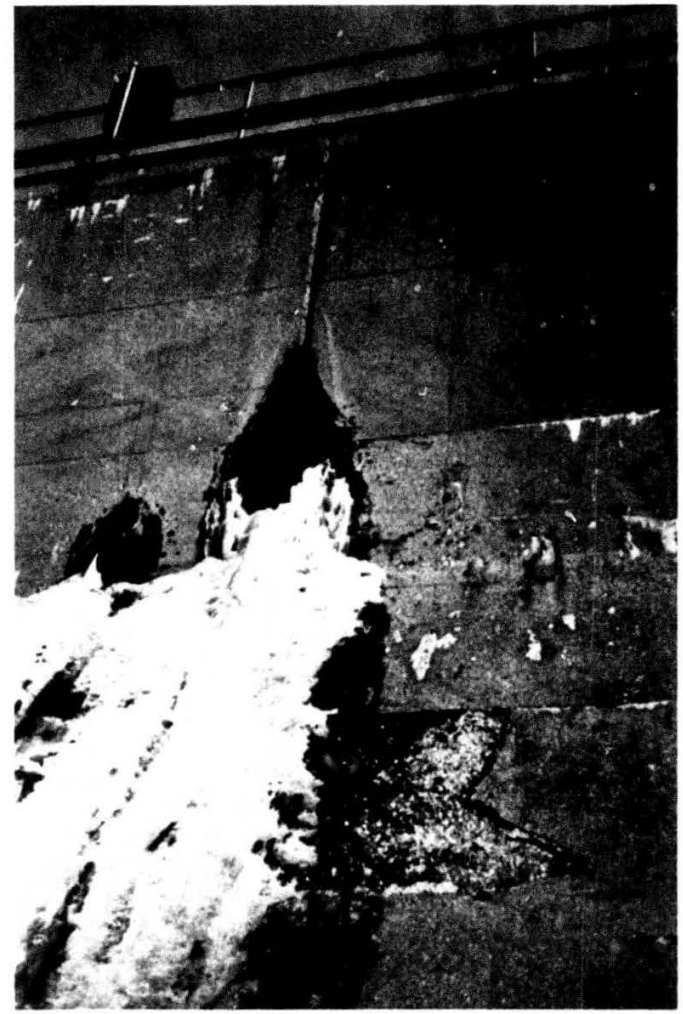

Figure A10. River face, river wall monolith joint 27-29

Figure A11. River face, river wall monolith joint 29-31

Figure A12. River face, river wall monolith joint 37-39

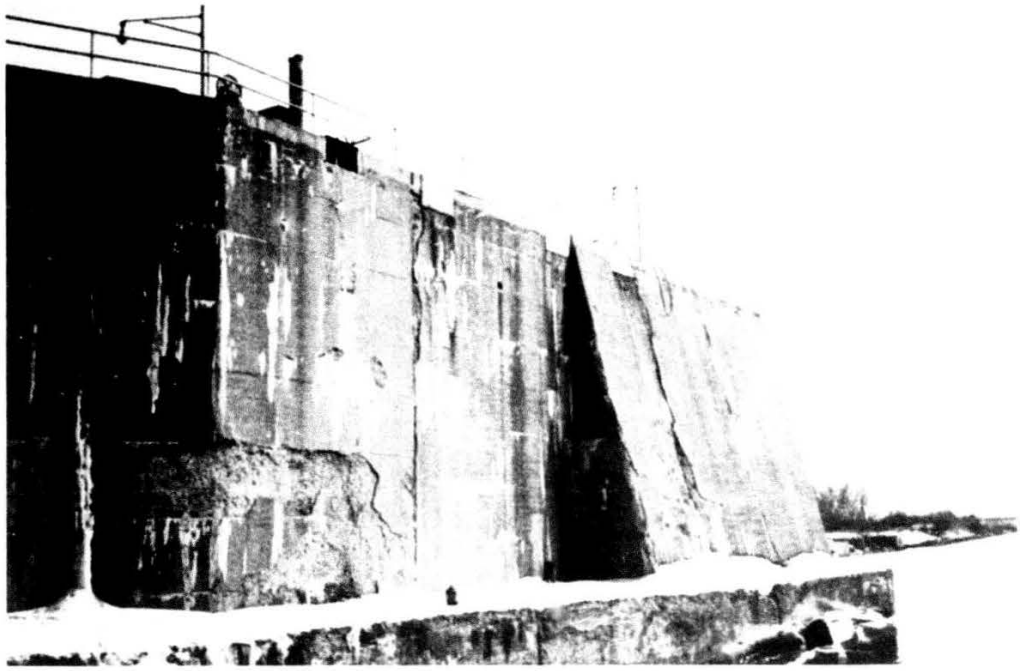

Figure A13. River face, river wall monoliths 53, 55, and 57

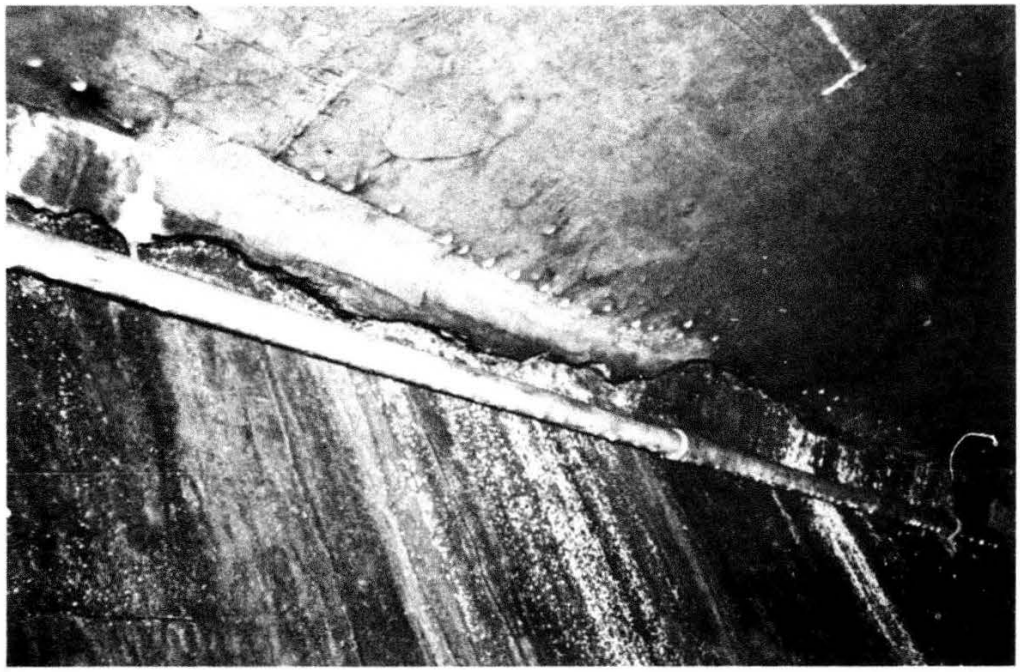

Figure A14. Corner crack, riverside, cable gallery river wall monolith 51

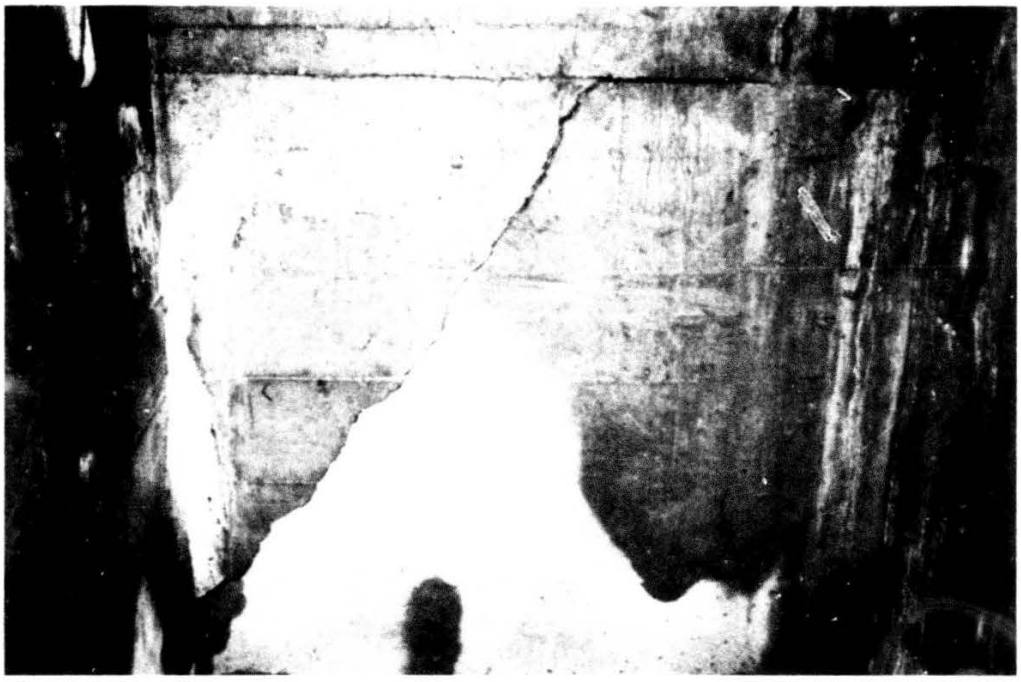

Figure A15. Downstream face, cable gallery river wall monolith 53

Figure A16. Lock face, river wall monoliths 51 and 53

Figure A17. Riverside face, river wall monolith 57

Figure A18. Downstream face, river wall monolith 57

Figure A19. Lock face, river wall monolith 57

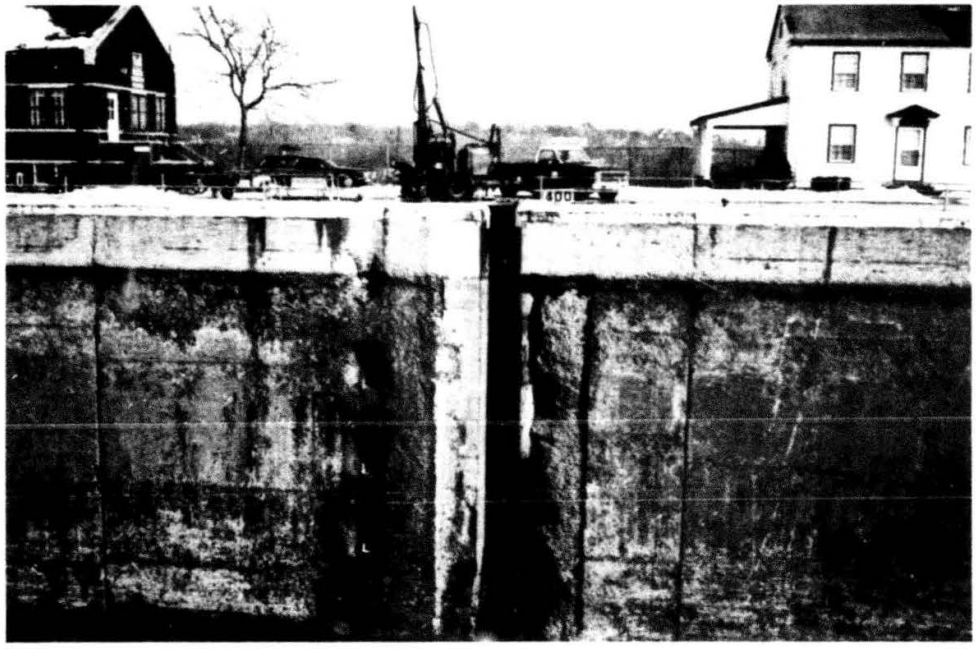

Figure A20. Lock face, land wall monoliths 34, 36, 38, and 40

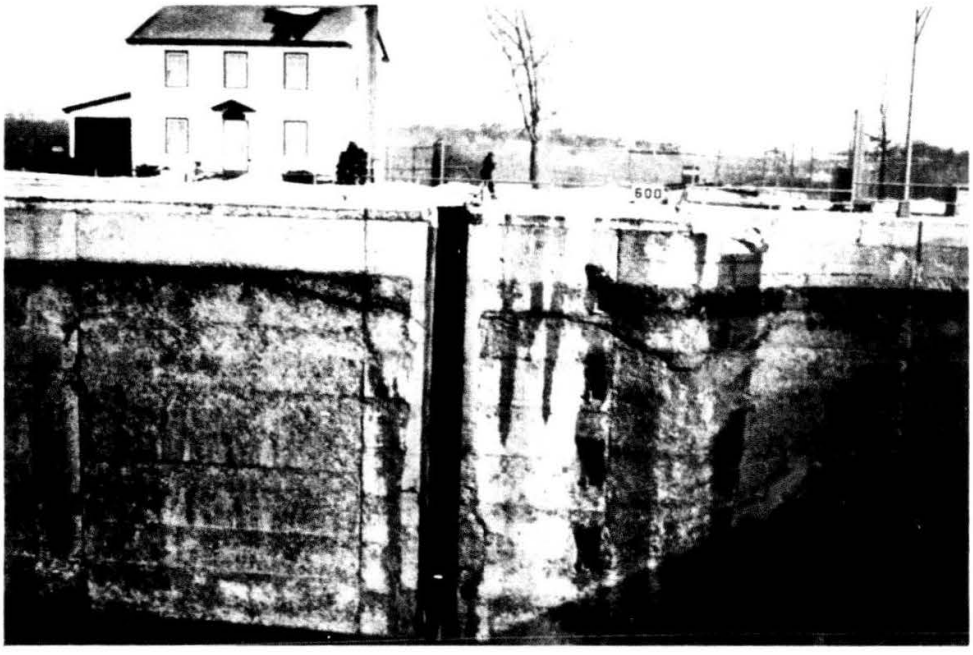

Figure A21. Lock face, land wall monoliths 48, 50, and 52

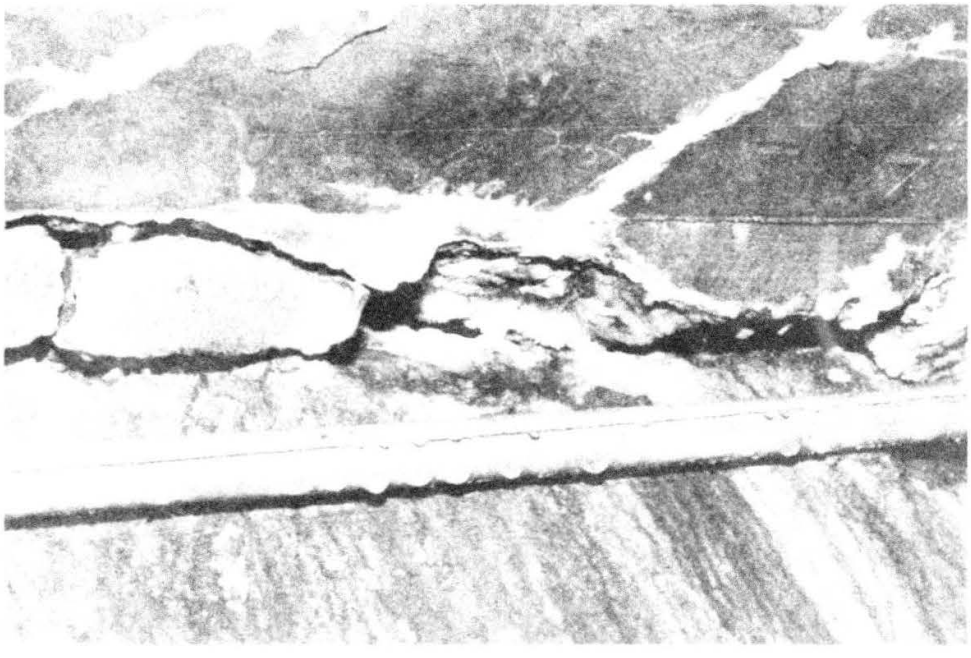

Figure A22. Corner crack, land side, cable gallery land wall monolith 52

APPENDIX B

PETROGRAPHIC EXAMINATION REPORT

LOCKPORT LOCK, ILLINOIS WATERWAY

CHICAGO DISTRICT

Corps of Engineers, USAE Waterways Experiment Station	Petrographic Report	Structures Laboratory P. O. Box 631 Vicksburg, Mississippi
Project Examination of Five Concrete Cores from Lockport Lock, Illinois Waterway		Date 24 July 1978 GSW

Samples

1. As part of the larger study of concrete and foundation rock from Lockport Lock for the U. S. Army Engineer District, Chicago, five concrete cores were furnished for petrographic examination. They represented concrete from the guide wall, river wall, and land wall of the lock. They had been chosen to include concrete typical of that in the best and the worst physical conditions. The cores are identified below:

Structures Laboratory Serial No.	Field Identification
CHI-14 CON-10	L-WES L-10-78, lower pool, monolith 21, elevation 537 ft at top of hole, horizontal 6-in. diameter core, 3.2 ft long; river wall sample, chamber side.
CHI-14 CON-11	L-WES L-11-78, 5 ft above lower pool, monolith 56, elevation 544.0 ft at top of hole, horizontal 6-in. diameter core, 3.1 ft long; guide wall sample near lower gates.
CHI-14 CON-14	L-WES L-14-78, 3 ft below upper pool, monolith 32, elevation 573.2 ft at top of hole, horizontal 6-in. diameter core, 3 ft long; land wall sample, chamber side.
CHI-14 CON-29	L-WES L-29-78, lower pool, monolith 82, elevation 539.0 ft at top of hole, horizontal 6-in. diameter core, 2.8 ft long; lower guide wall sample representing concrete in the best condition.
CHI-14 CON-31	L-WES L-31-78, 15.8 ft from the top of monolith 57, elevation 569.2 ft at top of hole, horizontal 6-in. diameter core, 8.3 ft long; river side of river wall near the lower gates; sample representing concrete in the worst condition.

The first three cores listed above were received 8 March 1978; the other two were received 24 April 1978.

Test procedure

2. The cores were examined and logs were prepared. The cores were then sawed along their long axes to allow a better view of the structure of the

concrete and the nature of the paste. The drilled and sawed surfaces were examined while the concrete was wet and while it was dry.

3. White reaction products found in voids and coating aggregates and their sockets were examined with a stereomicroscope. These reaction products were also examined as powder immersion mounts using a polarizing microscope.

4. Aggregate particles associated with the white reaction product were also examined as powder immersion mounts using a polarizing microscope and as powdered material by X-ray diffraction.

5. All X-ray diffraction patterns were made with an X-ray diffractometer using nickel-filtered copper radiation.

Results

6. The original vertical formed surface of all the cores had scaled off. Some of these surfaces were coated with algae. Four of the cores showed evidence of frost damage deeper than the surface scaling shown by core L-WES L-29-78 (Plate B2). Fracture of the concrete due to freezing and thawing was evident to a maximum depth of 0.6 ft in borings L-WES L-11-78 and L-WES L-14-78 (Plates B3 and B5). Frost action tends to develop parallel to subparallel cracks which are parallel to the advancing freezing isotherm ($\pm$ -2 C). These are usually parallel to the exposed surfaces of the concrete. This structure was built before air entrainment was required. The frost damage to concrete was principally caused by the lack of an adequate air-void system protecting the paste and also possibly to the presence of some nonfrost-resistant particles in the aggregate.

7. The coarse aggregate used in the production of this concrete was a natural gravel consisting mostly of dolomite with some chert and igneous rock particles. Some of these aggregate particles approached 3 in. in diameter, but most of the concrete appeared to have a maximum aggregate size of less than 2 in. The fine aggregate was a natural sand of mixed composition.

8. Examination showed the presence of alkali-silica gel lining the surfaces of old cracks and fractures, coating aggregates, and filling voids in four of the cores. This is indicated in Plates B1, B3, B4, and B5. The gel was white to translucent and usually showed some shrinkage cracks when dried. The presence of gel is proof that alkali-silica reaction has occurred in some and probably all of this concrete. It is difficult to sort out which damage is due to which mechanism in old concrete when frost damage and alkali-silica reaction have both occurred. However, in this case, the evidence suggests that frost damage caused the shallow near surface parallel cracking and the alkali-silica reaction is responsible for other cracking. On this basis other cracking is confined to the deeper vertical cracking in core L-WES L-31-78 (Plate B1) and to the extensive horizontal cracking along its length. Since such cracking was not apparent in the other cores even though most of them showed evidence of alkali-silica reaction the implication is that this reaction did not cause much damage to the concrete, and may have developed as a secondary consequence of the frost action rather than as damage that would have generated itself to an important extent. The nature of the cracking in this concrete is

like that described earlier for Starved Rock Lock and Dam* which is also located on the Illinois Waterway.

9. Some of the chert particles in the gravel contained chalcedony. This was one source of reactive aggregate. There may have been other reactive siliceous aggregate particles present but they were not identified. The carbonate particles consisted of dolomite with some quartz, potassium feldspar, and clay-mica. Some of these particles were rimmed which could indicate either alkali-carbonate rock reaction, or natural weathering that had occurred before their use as aggregate.

10. Clusters of ettringite needles were detected in voids in the concrete. It is a normal product of the hydration of portland-cement concrete but in excess it may be an indication of sulfate attack. This concrete is not believed to be in distress because of sulfate attack.

Summary

11. Examination of the five concrete cores indicated some frost damage to all. It ranged from only at the surface for core L-WES L-29-78 (Plate B2) to a maximum depth below the surface of about 0.6 ft for cores L-WES L-11-78 and L-WES L-14-78 (Plates B3 and B5). Evidence of alkali-silica reaction was found in four of the five cores and the reaction was probably present in the other one (L-WES L-29-78, Plate B2). This reaction appeared to have caused some cracking in core L-WES L-31-78 (Plate B1) only. Although some of the carbonate particles were rimmed and ettringite was plentiful in voids it was not believed that alkali-carbonate rock reaction or sulfate attack were indicated as causes of significant damage.

12. The examination did not show whether the potential for additional alkali-silica reaction was exhausted. Since the reaction can take a long time to complete, alkali-silica reaction should be considered as continuing throughout the existance of the lock. If the structure is repaired by the removal of fragile concrete and the addition of air-entrained concrete as repairs, thus keeping water from pentrating into the concrete, the structure should be stable in terms of the anticipated behavior of the concrete.

---

* Stowe, R. L., Pavlov, B., and Wong, G. S., "Concrete and Rock Tests, Major Rehabilitation, Starved Rock Lock and Dam, Illinois Waterway, Chicago District," U. S. Army Engineer Waterways Experiment Station, CE, Miscellaneous Paper, in press, May 1978.

Boring L-WES L-31-78 (CHI-14 CON-31)
Lockport Lock on the Illinois Waterway
Six-Inch Diameter Horizontal Concrete Core

Depth, ft

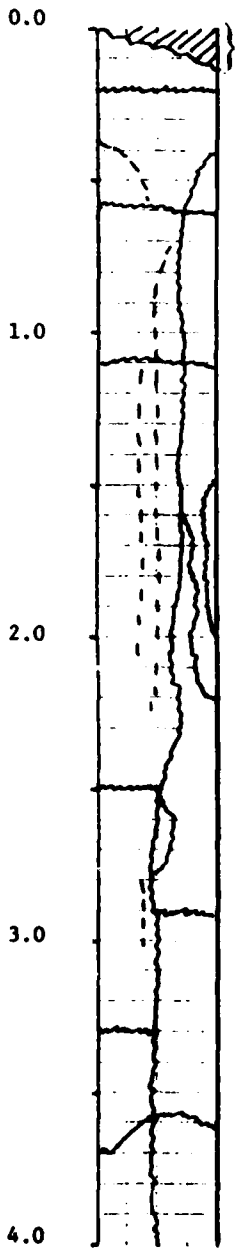

2-in. maximum size aggregate
Natural carbonate and siliceous aggregates
Good consolidation
No segregation
No entrained air
Some entrapped air

Longitudinal cracks exist from 0.4-ft to 4.9-ft depth. Cracks are open and have been coated with algae. Incipient longitudinal fractures were coated with alkali silica gel.

Preexisting cracks

Incipient fractures

Scale: 2 in. = 1 ft

Plate 1 (Continued)

Depth, ft

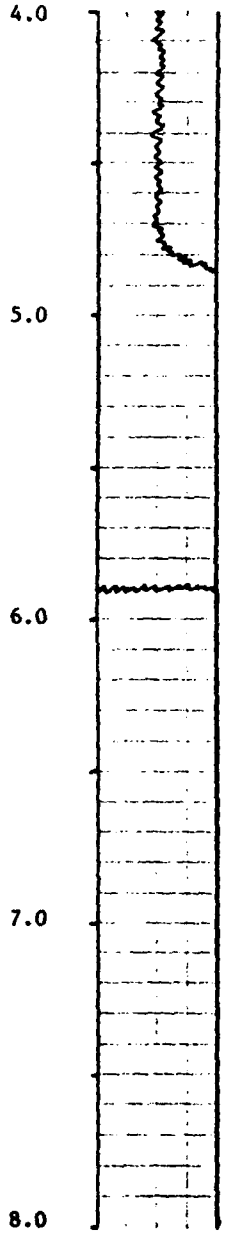

Concrete in good condition
to end of boring at
8.2 ft (not shown)

Boring L-WES L-29-78 (CHI-14 CON-29)
Lockport Lock on the Illinois Waterway
Six-Inch Diameter Horizontal Concrete Core

Depth, ft

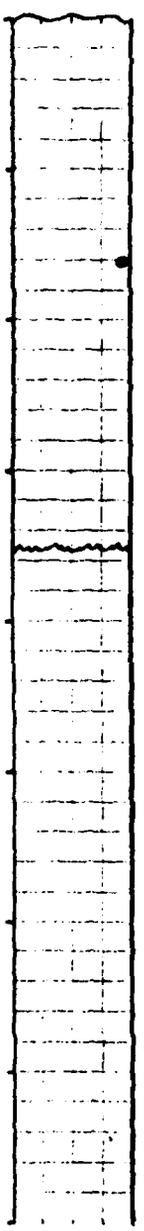

Scaled surface

0.75-in. steel rebar

End of boring

2-in. maximum size aggregate
Natural carbonate and siliceous aggregate
Good consolidation
No segregation
No entrained air
Some entrapped air
No alkali-silica gel was found
No apparent frost damage except scaling at top surface

Scale: 2 in. = 1 ft

Plate B2

Boring L-WES L-11-78 (CHI-14 CON-11)
Guide Wall, Lockport Lock on the Illinois Waterway
Six-Inch Diameter Horizontal Concrete Core

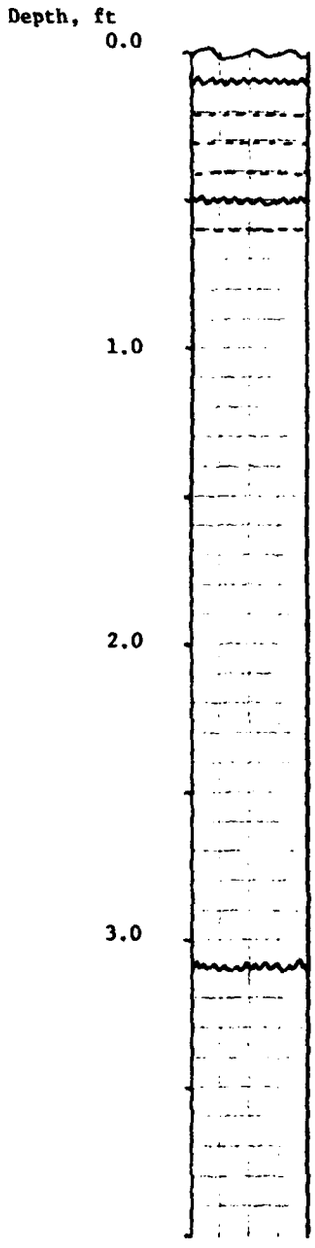

2-in. maximum size aggregate
Natural carbonate and siliceous aggregate
Good consolidation
No segregation
No entrained air
Some entrapped air
Some alkali-silica gel was found in voids and fractures near the top of the core
Clusters of needles of ettringite were found in voids throughout the length of core

Scale: 2 in. = 1 ft

Plate B3

Boring L-WES L-10-78 (CHI-14 CON-10)
River Wall, Lockport Lock on the Illinois Waterway
Six-Inch Diameter Horizontal Concrete Core

Depth, ft

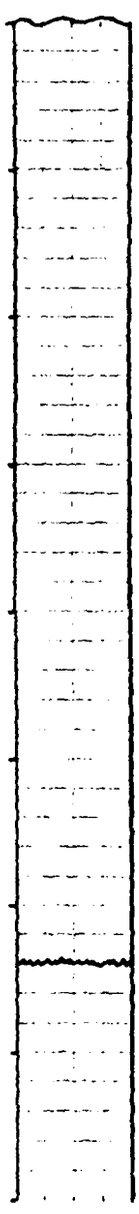

Scaled surface, algae coated

Maximum depth of frost damage

3-in. maximum size aggregate
Natural carbonate and siliceous aggregate
Good consolidation
No segregation
No entrained air
Some entrapped air
Some alkali-silica gel in voids near the top surface of core

End of boring

Scale: 2 in. = 1 ft

Plate B4

Boring L-WES L-14-78 (CHI-14 CON-14)
Land Wall, Lockport Lock on the Illinois Waterway
Six-Inch Diameter Horizontal Concrete Core

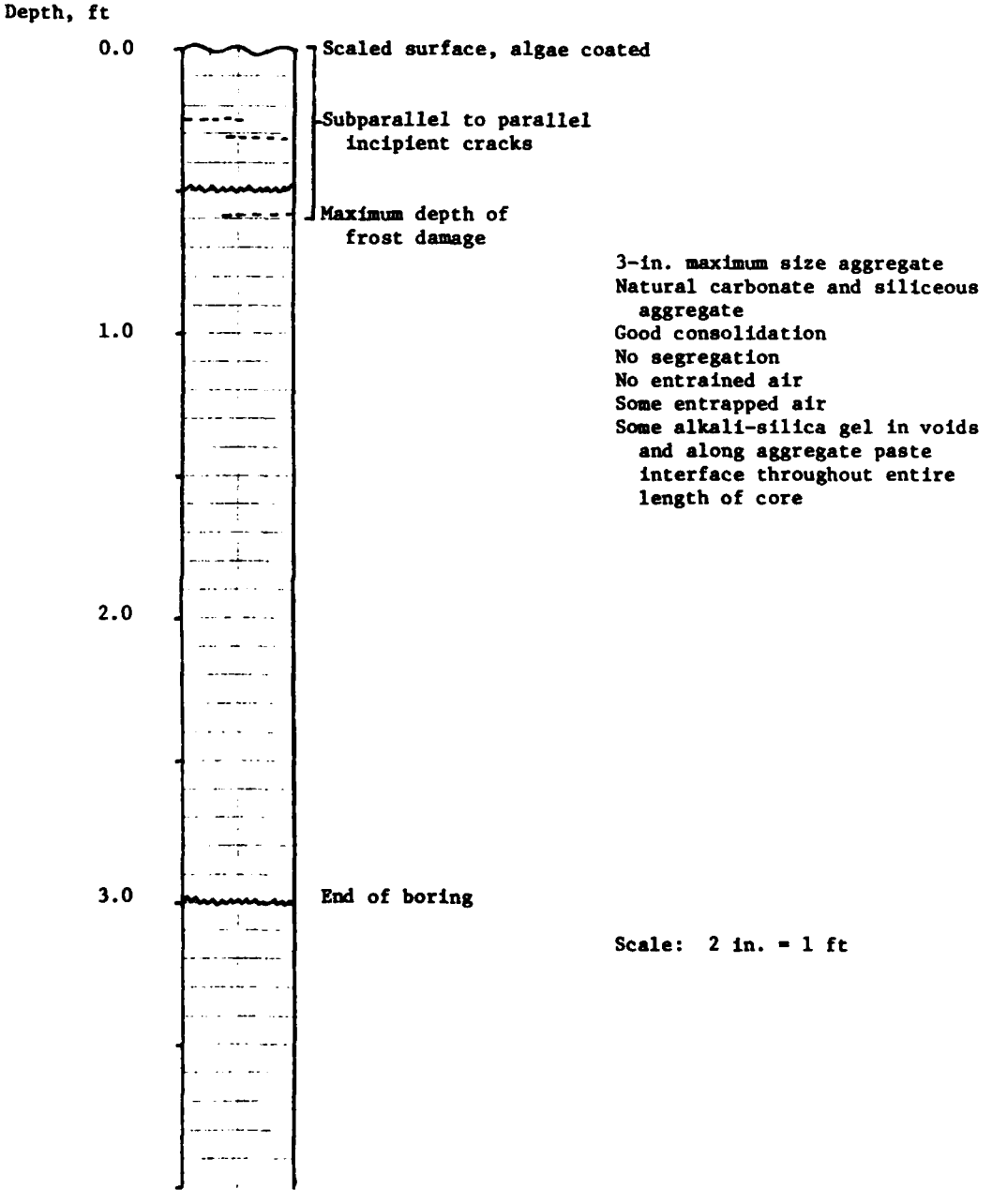

Plate B5

APPENDIX C

LETTERS FROM THE ILLINOIS STATE GEOLOGICAL SURVEY

August 22, 1978

ILLINOIS STATE GEOLOGICAL SURVEY
NATURAL RESOURCES BUILDING, URBANA ILLINOIS 61801 TELEPHONE 217 344-1481

Jack A. Simon, CHIEF

August 22, 1978

Ms. Barbara Pavlov
U.S. Army Corps of Engineers
Waterways Experiment Station
Structures Laboratory
Vicksburg, Mississippi 39180

Dear Ms. Pavlov:

Enclosed is a copy of my letter of May 16, 1973, to F. Kuehnel of the Chicago District, which we discussed in our telephone conversation of August 17. Also enclosed are copies of materials from our files related to the Corps investigations of Lockport.

The cross-section through the "700 series" holes has been revised to reflect our current stratigraphic terminology and interpretations. The interpretation of #700 should be considered tenuous as this core is very fractured and broken. It may be cut by faults which have displaced portions of it into an unusual stratigraphic order. Since we rely on certain key-beds which are not recognizable in this core, any conclusions retain a significant probability of error. Cores #700 and 702 were given to us by the Corps and are available for examination if you wish to see them. Copies of our brief descriptions of all four (4) of these cores are enclosed.

Core #CLP-519 is also in the Illinois State Geological Survey core collection (C11483). A geological description of it is enclosed. A copy of a portion of the topographic map showing the location of these borings is also enclosed.

Very truly yours,

Michael L. Sargent

Michael L. Sargent
Assistant Geologist
Stratigraphy and Areal
Geology Section

Enclosure

May 16, 1973

Mr. Frank Kuehnel, Geologist
U. S. Army Corps of Engineers
219 S. Dearborn Street
Chicago, IL 60406

Dear Frank:

Enclosed please find copies of a location map, a cross-section of the cored bore holes, and very brief core descriptions with our geological formation tops.

As displayed by the cross-section, there appears to be a significant structure between several of the borings. With the Brandon Bridge Member in three of the cores, there is no doubt in my mind about those correlations. The fourth boring provides a much greater challenge. Chips of that core were dissolved in acid to test for diagnostic fossils. One sample of the upper part of that core yielded fossils which suggest that part is Niagaran in age. This supported our previous interpretation of these strata based on their lithology. Absolute proof or dismissal of this interpretation would require an additional 20'-25' of core from #CLP 700. Based on the thickness of the Markgraf Member in the other borings, this much additional core should reach the top of the very characteristic Brandon Bridge Member.

Dr. Herbert Glass ran X-ray diffraction analyses of clay encountered in two of the bore holes. The sample from approximately 50' of #CLP 702 was high illite with some kaolinite and a little mixed layer clay containing layers of illite and montmorillonite. The other sample from approximately 87' of #CLP 701 was well layered (bedded) but was very similar mineralogically to the above sample with the addition of a little chlorite.

On the basis of many years of analyzing all types of clay materials, it is Dr. Glass' opinion that these clays are of Pennsylvanian age. They were probably deposited in solution expanded joints and fractures during a period of erosion which occurred at that time. Dr. H. B. Willman, Emeritus, Head of the Stratigraphy and Areal Geology Section of the Survey, independently suggested the same origin. He has observed similar clay pipes in many quarries in Silurian rocks of the Will-Cook Counties area. Although an attempt was

made to find conodont fossils which would tell the age of the clay fillings, no fossils could be found. Attempts to further disaggregate the sample without destroying these diagnostic fossils are in progress and I will inform you at a later date of any positive results.

Sincerely,

Michael L. Sargent
Assistant Geologist
Stratigraphy and Areal
Geology Section

Enclosures

Copy to W. C. Smith

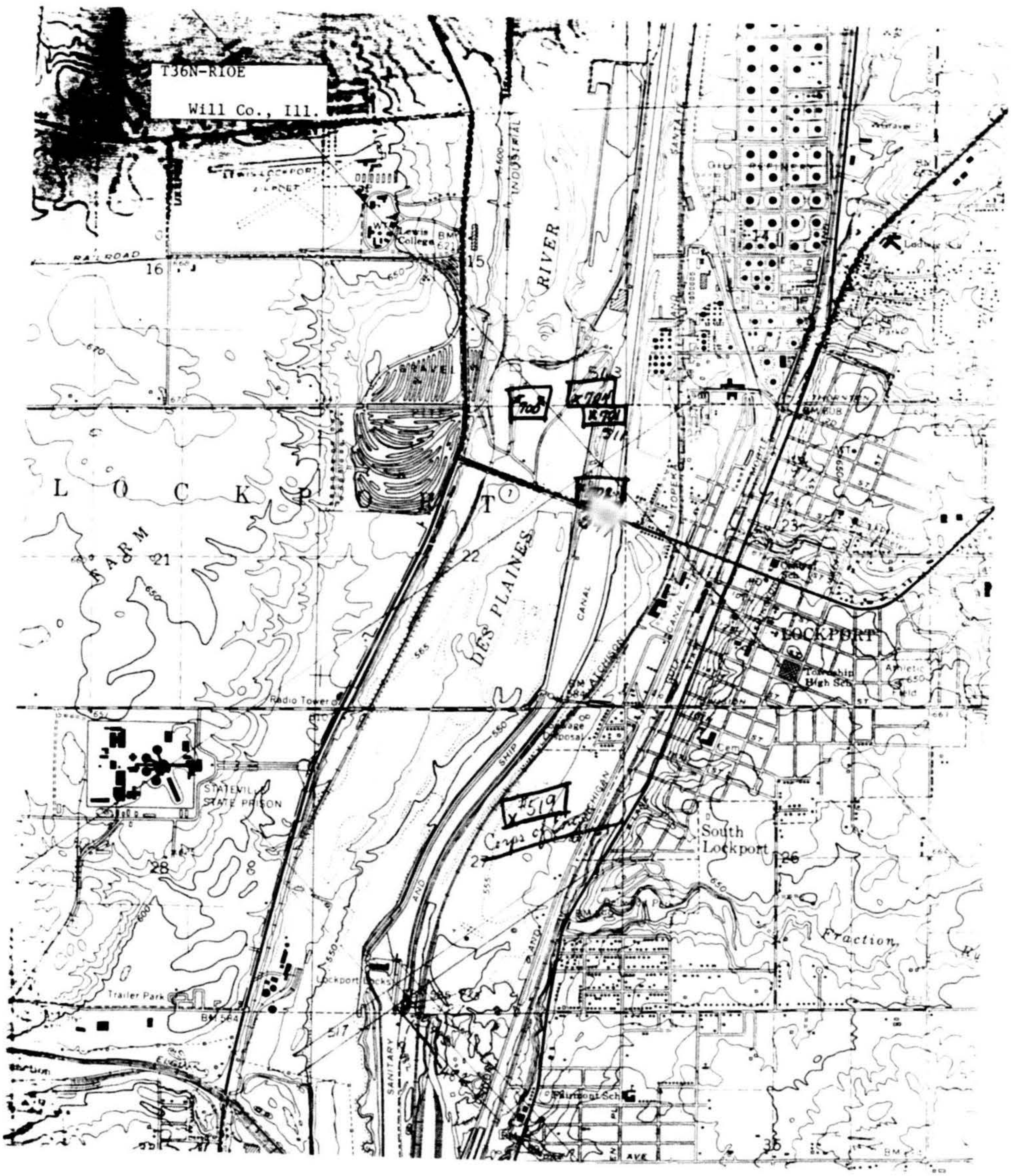
T36N-R10E
Will Co., Ill.
LOCKPORT
L O C K P O R T
DES PLAINES
RIVER
CANAL
SHIP
SANITARY
AND
STATEVILLE
STATE PRISON
South
Lockport
Lewis
College
GRAVEL
PITS
Radio Tower
Trailer Park
Township
High Sch
Athletic
Field
Fraction
#519
#708
#704
#701
15
16
21
22
23
26
27
28
35

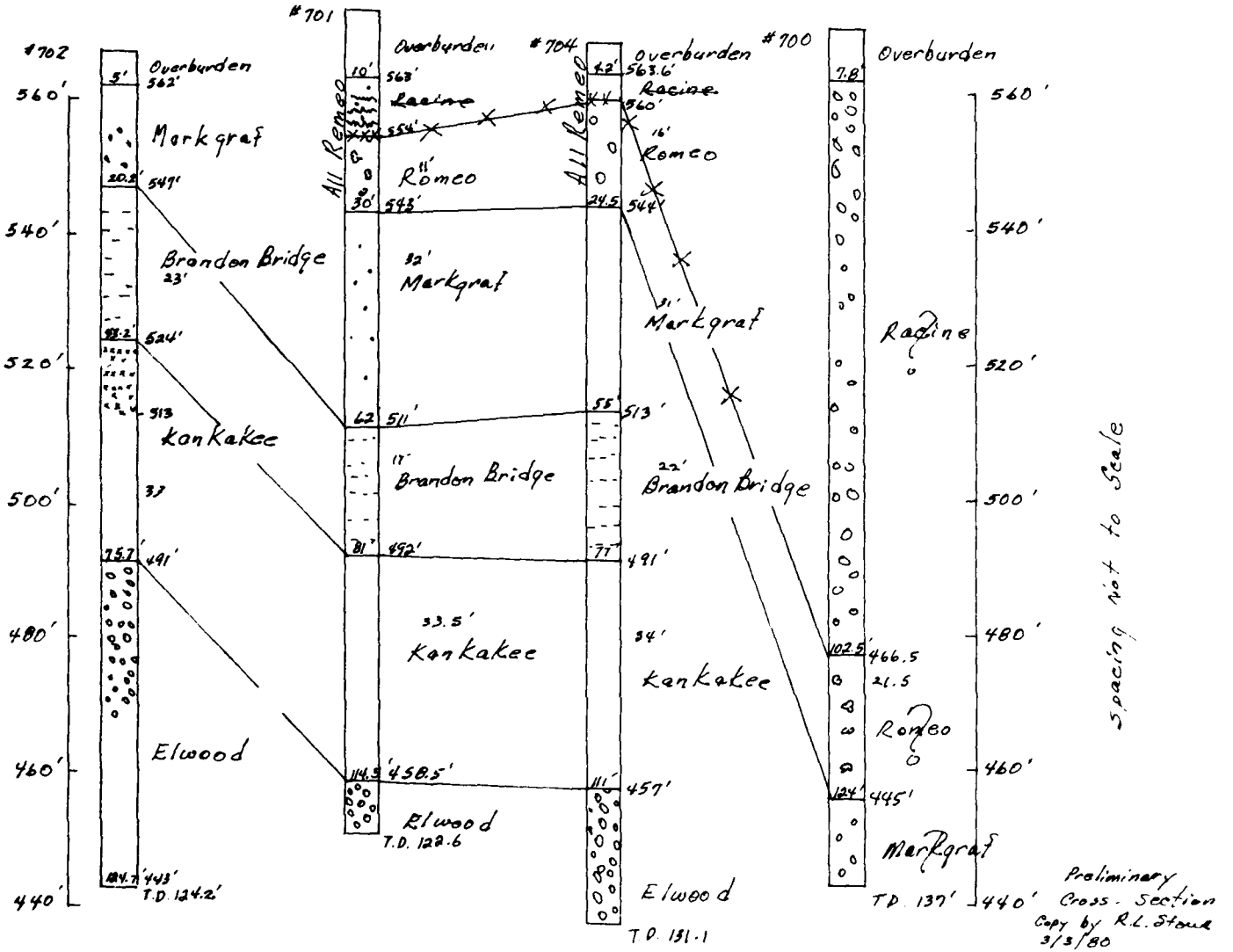
#702
#701
#704
#700
Overburden
Markgraf
Brandon Bridge
Kankakee
Elwood
Racine
Romeo
All Remeo
T.D. 124.2'
T.D. 122.6
T.D. 131.1
TD 137'
560'
540'
520'
500'
480'
460'
440'
Spacing not to Scale
Preliminary
Cross-Section
Copy by R.L. Stone
3/3/80

In accordance with letter from DAEN-RDC, DAEN-ASI dated 22 July 1977, Subject: Facsimile Catalog Cards for Laboratory Technical Publications, a facsimile catalog card in Library of Congress MARC format is reproduced below.

Stowe, Richard L
Concrete and rock tests, major rehabilitation and compliance, Lockport Lock, Illinois Waterway, Chicago District / by Richard L. Stowe ... [et al.]. Vicksburg, Miss. : U. S. Waterways Experiment Station ; Springfield, Va. : available from National Technical Information Service, 1980.
83, [42] p., [24] leaves of plates : ill. ; 27 cm. (Miscellaneous paper - U. S. Army Engineer Waterways Experiment Station ; SL-80-4)
Prepared for U. S. Army Engineer District, Chicago, Chicago, Illinois.
References: p. 83.

1. Concrete tests. 2. Cracks. 3. Illinois Waterway. 4. Lockport Lock. 5. Lock walls. 6. Rock tests (Laboratory). 7. Sinkholes. 8. Ultrasonic velocity. I. United States. Army. Corps of Engineers. Chicago District. II. Series: United States. Waterways Experiment Station, Vicksburg, Miss. Miscellaneous paper ; SL-80-4.
TA7.W34m no.SL-80-4